



**An electrochemical sensor for efavirenz based on electrode modification
with silver-gold bimetallic nanoparticles functionalised nanoclay**

by

Sizwe Ngcobo (Student number. 215138023)

Master of Technology (Cape Peninsula University of technology)

**Dissertation submitted in fulfilment of the requirements of Master applied
sciences degree (Chemistry)**

In Faculty of Applied sciences (Chemistry Dept.)

Cape Peninsula University of Technology

Supervisor: Prof M C Matoetoe

Co-Supervisor: Dr KL Maqashu

Date: March 2022

Declaration

I, **Sizwe Ngcobo**, declare that the content contained in this dissertation represent my own authentic and independent work. This dissertation has not been submitted for academic assessment for any qualification at any institution. In addition, the dissertation expresses my own articulation of the work and not that of the presiding institution (CPUT).

Signed..........

Date.....03/03/2022.....

Abstract

This study synthesized Ag and Au NPs through chemical reduction method, whilst Ag-Au was synthesized through co-reduction method where sodium citrate was used a reducing agent for both monometallic and bimetallic synthesis. Corresponding metallic nanoclay composites, Ag-PGV, Au-PGV and Ag-Au-PGV bentonite were all synthesised through similar synthesis methodology as metallic NPs as metallic NPs were reduced unto PGV nanoclay bentonite.

The metallic NPs and their nanoclay composites were optically characterized through Fourier-transformation infrared spectroscopy (FT-IR), UV/Visible spectroscopy (UV/Vis), Scanning electron microscopy (SEM) and X-ray diffraction (XRD). However, characterization using UV/Visible spectroscopy was conducted for metallic NPs and not composites due to colloidal nature of composites. Ag and Au monometallic exhibited 436 nm and 512 nm specific characteristic wavelengths whilst Ag-Au bimetallic NPs exhibited characteristic wavelengths of 414 nm and 516 nm for Ag and Au, respectively. FT-IR mainly depicted COO^- functional groups which confirmed successful capping of metallic NPs and nanoclay composites.

XRD exhibited diffraction planes which are related to 2θ values both Ag and Au metals, and both were largely depicted in diffraction planes of Ag-Au bimetallic NPs. As confirmation of successful functionalization of PGV bentonite clay, similar diffraction planes were observed in Au-PGV, Ag-PGV and Ag-Au-PGV bentonite composites, respectively. SEM depicted nanoclay composites average particle size as significantly bigger than that of metallic NPs, the shape of particles of metallic NPs were resembled in their clay composites, which confirmed functionalization of bentonite clay.

The evaluation of electrochemical properties of metallic NPs and clay composited were obtained through use of Cyclic voltammetry (CV). Transducers were fabricated through drop-coating of metallic NPs and clay composites sensing films method .CV showed that bentonite nanoclay is largely insulated by silicates but exhibited small electroactivity of Fe. The electroactivity of Ag and Au monometallic, Ag-Au bimetallic NPs appeared similar, whilst

clay composites depicted similar peak potentials as those observed for monometallic and bimetallic NPs.

A study of electrochemical properties of metallic NPs and their clay composites carried using 0,1 HCl as supporting electrolyte obtained through electrochemical parameters from both Randles-sevcik and Laviron's methods depicted parameters such as surface coverages(Γ), electron-transfer rate constants (K_s), electron-coefficient($n\alpha$) and diffusion coefficients(D). Ag-Au-PGV was deduced as superior sensing film as it exhibited, 2,16 Γ , 1,76 K_s , 0,07 $n\alpha$ 2,29 x 10⁻⁸ cm²/s parameters, which were superior to other sensing films.

Consequently, Ag-Au-PGV composite as best modifier was used as platform with addition of human serum albumin (HSA) in detection of EFV using DPV, which was the best detection technique. Experimental and detection parameters optimization were deduced and drop-casting method was deduced as best modifier method whilst 1M PBS as supporting electrolyte. Optimized detection parameters which included, step-potential, pulse amplitude, and initial potential were determined to be 0,015V/s, 0,085Vs⁻¹ and 1,15V.

Varying of step-potential was used to determine the kinetic parameters of electrooxidation of EFV. Through Randles-Sevcik and Laviron equations, kinetic parameters were determined to be 1,11 K_s , 0,2 α and 2,76 x 10⁻⁹ cm²/s in electrocatalytic reaction with Ag-Au-PGV/HSA platform. The electrocatalytic reaction mechanism produced a single electron-transfer between platform interface and EFV. The calibration curve exhibited EFV Limit of detection (LOD), Limit of quantitation (LOQ) and Sensitivity of 0,13 uM, 0,4uM and 2,53 x 10⁻⁹ uA uM⁻¹ cm⁻². Interferences studies of EFV demonstrated plausible selectivity of platform, as 83% and 94% EFV content were recovered in sample matrix containing glucose, ascorbic acid and sodium chloride, whilst reproducibility and repeatability of detection of EFV standard were statistically plausible with RSD values of 4,90% and 3,21%, respectively.

Real sample applicability of a platform evaluated from EFV spiking urine samples produced EFV recoveries of 94% and 115% , respectively. EFV mass concentration experimentally obtained from commercial capsules averaged to 192.02 mg. This were comparable to 200 mg EFV concentration specified by commercial manufacturer of EFV capsules, whilst stability of the Ag-Au-PGV/HAS platform demonstrated performance deterioration rate of 10% after 3 days for spiked EFV samples whilst 20% for EFV pharmaceutical capsule.

Acknowledgements

I thank God Almighty for continued Grace and gift of life, without Him its not possible that I would be where I am today.

I would also want to pass many thanks to my supervisor, Prof Matoetoe and Dr Silwana for their continued academic support and advise. Their expertise and experience within this scientific field proved valuable to my academic progress, and for that I am extremely grateful. In addition, I would like to thank my electrochemistry club colleagues for words of encouragement and motivation that we shared amongst each other, but above all academic assistance that I received from each and every one of them.

To my National Research Foundation (NRF) I appreciate the financial assistance that I received it was vital and assisted me to get by on day-to-day basis, but above all the opportunity to learn and trusting me with chance to undertake this scientific project. To Cape Peninsula University of Technology (CPUT) institution, I appreciate the vital assistance of facilities and instrumentation that ensured that work was being done with little to no hassles. I thank both the foundation and institution for that from the bottom of my heart. Long may it continue.

Last but not least, my family and close friends that were concerned about my life and academic life. They uplifted me whenever I need motivational boost, every single one of you offered that albeit in different ways. I appreciated and grateful for those efforts, much love.

Honourable mention to my late grandmother Philisiwe Zondi. This success is mine, but you deserve a credit for assuring me that I would get to the other side of the tunnel a better person, much appreciated, Nondaba Gagashe Kamancinza.

Dedication

This is dedicated to myself, my partner, acquaintances, friends and the Ngcobo family at large. I would not have been able to achieve what I have achieved without their continued support, which came in various ways.

Special thanks to God Almighty for giving me strength and comfort when tough got going and I felt emotionally and mentally fatigued to continue on this turbulent yet educational journey that I embarked but I withstood all and came out the other side stronger and wiser

Research output

1. Conferences

South African nanotechnology initiative (SANI), Cape Peninsula University of Technology (CPUT), Wits University, South African(Virtual). 8 October 2022.

2. Publications

S Ngcobo, M.C Matoetoe, B Silwana and K Maqashu. Bentonite nanoclay Opto-electrochemical properties improvement through bimetallic Silver -Gold nanoparticle. 2022. *Journal of Nanotechnology*. Hindawi

Table of Contents

Declaration.....	2
Abstract.....	3
Acknowledgements.....	5
Dedication.....	6
Research output.....	7
1. Conferences.....	7
2. Publications.....	7
List of Figures.....	11
List of Tables.....	12
Abbreviations.....	13
Chapter 1: Study overview.....	14
1.1.2 Introduction.....	17
1.1.3 Delineation.....	18
1.1.4 Research problem.....	18
1.1.5 Study objectives.....	19
Specified outlined objectives of the study.....	19
1.1.6 Methodology.....	20
1.1.7 Outcomes.....	20
1.1.8 The outline of chapters.....	20
1.2 References.....	21
Chapter 2: Literature review.....	26
2.1 Introduction.....	26
2.2 Antiretrovirals.....	26
2.3 Efavirenz.....	27
2.4 Detection and quantification methods of EFV.....	30

2.4.1	Current techniques	30
2.4.2	Electroanalytical techniques	33
2.4.4	The electrochemical effect of nanoparticles on detection methods/techniques.	41
2.4.5	Nanoclay modified sensors	42
2.6	Reference	44
Chapter 3: Synthesis and Characterisation		48
Chapter 3 summary		48
3.1	Introduction	48
3.2	Synthesis of AuNPs and AgNPs via chemical method reduction method.....	50
3.3	Characterization nanoparticles	53
3.4	Experimental methods	56
3.4.1	Reagents	56
3.4.2	Synthesis of Ag and Au NPs	56
3.4.3	Synthesis of Ag-Au bimetallic NPs	57
3.4.4	Preparation of Ag-Au bimetallic functionalized PGV-bentonite nanoclay	57
3.4.5	Preparation of modified GCE.....	57
3.4.6	Electrochemical characterization	58
3.4.7	Infrared spectroscopy & UV/Vis spectroscopy characterization	58
3.4.8	X-ray diffraction characterization (XRD).....	59
3.4.9	Scanning electron microscope (SEM).....	59
3.5	Results and Discussion	59
3.5.1	UV/Vis spectroscopy.....	60
3.5.2	Infrared spectroscopy	61
3.5.3	X-ray diffraction (XRD).....	64
3.5.4	Scanning electron microscope (SEM).....	65
3.5.5	Electrochemical studies.....	66
3.6	Conclusion	83

3.7 References.....	84
Chapter 4: Efavirenz method development.....	90
Chapter 4: Summary.....	90
4.1 Development and application of an electrochemical Efavirenz sensor.....	90
4.2 Experimental.....	93
4.2.1 Material, reagents, and instruments.....	93
4.2.2 GC and GC electrode modified preparation.....	94
4.2.3 Optimization of experimental conditions methodology.....	94
4.2.4 Preparation EFV working standards for calibration curve.....	95
4.2.5 Method validation methodology	95
4.2.6 Determination of EFV in pharmaceutical capsules methodology.....	96
4.3 Results and discussion	96
4.3.1 Electrochemical identification of Efavirenz at bare GCE and GCE/Ag-Au/PGV bentonite/HSA.....	96

List of Figures

Figure 1-1: Chemical structure of efavirenz.....	14
Figure 2-1:Summary of ARVs based on their classes and their respective action mechanisms (De clercq,1998 and Rivera,2020)	27
Figure 2-2:A demonstration of one of EFV synthesis pathways	28
Figure 2-3:Inhibitory depiction diagram of EFV against HIV-1 (H -stands for HIV-1).....	29
Figure 2-4:Depiction of electrochemistry operating within an electrochemical technique.....	34
Figure 2-5:A chart of most prominently studied and most used electroanalytical techniques of analytical scientific tools	35
Figure 2-6:Typical components of an electrochemical sensor and their typical functions	37
Figure 2-7:An illustration showing the impact of BMNPs in comparison to monometallic NPs systems.....	40
Figure 2-8:A functionalization of typical bentonite clay with bimetallic NPs	44
Figure 3-1: Diagram depicting prominent synthesis methodologies of monometallic and bimetallic NPs ((Rajput, 2015, Feng et.al, 2014).....	49
Figure 4-1:EFV electrochemical identification of 200 uM EFV on bare GCE (A and B) and Ag-Au-PGV/HSA platform at 30 mvs and differential pulse voltammetry in 0,5M PBS pH 7.2 supporting electrolyte.....	96

List of Tables

Table 2-1 : A depiction of some results from current methods that have been used.	32
Table 3-1:Characteristic peak wavelengths ascribed to respective characteristic functional groups.....	63
Table 3-2:Electrochemical properties exhibited by NPs.....	67
Table 3-3:Electrochemical properties exhibited by NPs and PGV bentonite based on Nernstian theory on electron-transfer process.....	71
Table 3-4:An exhibition of dimensionless parameter(Λ) and standard rate(K_0) for all NPs and PGV bentonite composites based on Nicholson theory on electron-transfer process.....	73
Table 3-5:Presentation of obtained Randles Sevcick properties for all NPs and PGV composites.....	79
Table 3-6:Electron transfer-rate constant and electron-transfer coefficient obtained through Shain Nicholson and Laviron's equation and plot for all NPs and PGV composites.....	82
Table 4-1:Electrochemical properties obtained from Randles Sevcick plots and Laviron equation for 200 μ M EFV	103
Table 4-2:Characteristics and parameters of EFV calibration plot using DPV at GCE/Ag-Au-PGV-HSA platform.....	104
Table 4-3:Summary of studies depicting sensitivities of electrochemical sensors used for detection of various ARVs and pharmaceuticals in various media.	105
Table 4-4:Summary of EFV recoveries observed under the influence of each interferent. .	106
Table 4-5:Summary of EFV recoveries obtained from two different concentrations of urine samples.	107

Abbreviations

ARV	Antiretroviral
CV	Cyclic voltammetry
DFA	Food and Drug Administration
DNA	Deoxyribonucleic acid
DPV	Differential pulse voltammetry
dsDNA	Double stranded DNA
EFV	Efavirenz
HIV	Human immunodeficiency virus
NNRTI	Non-nucleoside reverse transcriptase inhibitor
NRTI	Nucleoside reverse transcriptase inhibitor
RT	Reverse transcriptase
TB	Tuberculosis
SWV	Square wave voltammetry
PIs	Protease inhibitors
CV	Cyclic voltammetry
DDTC	Diethyldithiocarbamate
FT-IR	Fourier transformation infrared spectroscopy
UV-Vis	Ultra-violet visible spectroscopy
XRD	X-ray diffraction
TEM	Thermal electron microscopy
SEM	Scanning electron microscopy

Chapter 1: Study overview

1.1 Chapter summary

This chapter's main objectives are focused on the analysis and discussion of the primary research problem mainly its root cause and the consequent effects brought by it. The chapter thus describes the pathway on how the research proposes to resolve the core issues presented by the research. Meanwhile, the background section precisely ascertains the chemical, physical and historical description of the analyte at the core problem of the research. The rest of the chapter outlines specific objectives of the study and related proposed solution mechanisms and methodologies.

1.1.1 Background

Efavirenz (EFV) is an anti-retroviral drug that belongs to *Sustiva* family of drugs (Matthews *et al*, 2001). It was developed by Du Pont Pharma under the previous name of Codename DMP 266 in the mid-80's and was later approved by United states in 1998 followed by acquisition of the European distribution licence obtained in May 1999 (Matthews *et al*, 2001). Its usage is known to reduce the amount of the HIV-1 virus in the body effectively as well as slowing down the damage incurred in the immune system of the infected.

EFV is chemically described as (4*S*)-6-chloro-4-(2-cyclopropylethynyl)-4-(trifluoromethyl)-1*H*-3,1-benzoxazin-2-one with an empirical formula of $C_{14}H_9ClF_3NO_3$ (PubChem,2020). The Figure 1 below is a depiction of S-enantiomer of EFV which is said to be the pure form of the compound.

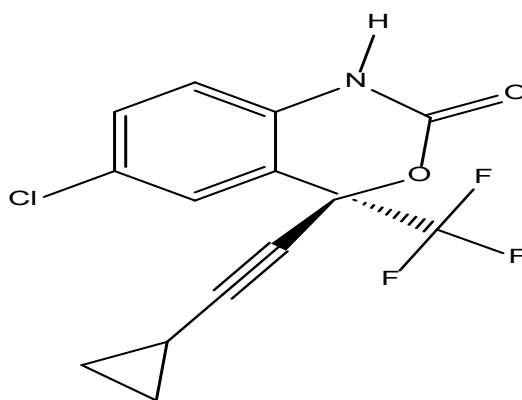


Figure 1-1: Chemical structure of efavirenz

EFV belongs to non-nucleoside transcriptase inhibitors (NNRTIs) drugs, whose mode of action to inhibit HIV is by binding near reverse transcriptase site, resulting in replication within the cells thus inhibiting a polymerase activity. Hence, it is only effective in inhibiting HIV-1 from transcribing or replicating and thus changing its RNA to DNA, which enables it to replicate through blood cells and not eradication of HIV-1 (Apostalovo *e.tal*, 2015). EFV is one of the preferred NNRTIs, commonly used as the first line of regimens which usually include Emtricitabine and Tenofovir. This combination has been in existence at least from early 2000's and is commonly referred to as high active antiretroviral therapy (HAART). HAART packages are today manufactured and distributed across Africa, Sub-Saharan region being the area with the highest distribution HAART packages (Apostalovo *e.tal*, 2015).

Prescribed HAART has EFV reported concentration of 600 mg/L, which is almost twice the concentration of the other components because it is the most active ingredient within the combination. One of the reasons contributing to this fact is primarily due to EFV high insolubility. EFV is reportedly highly soluble in alcoholic and organic media like ethanol and dimethyl formamide (DMF) whilst being sparingly insoluble in other few aqueous buffers. Hence, to compensate for this shortcoming EFV must be supplied in higher concentration than other regimens to effect maximum therapeutic impact. This however comes with an adversity which brings about EFV toxicity in Antiretroviral therapy (ART) patients. The high concentrations, which are largely insoluble, become a great metabolism challenge, as it was reported that about 20% of sub-Saharan Africans are genetically slow metabolisers, which puts them at high risk of EFV toxicity compared to other ethnic groups from various parts of the world (Castro *et.al*, 2011).

Apart from this complication, there has been other reported adverse effects of EFV strongly linked with its concentration in ART and these include psychosis, psychiatric effects, and ataxia. The patients' weight has been identified as possible contributing for above side effects (Eley. B and Whilmhurst. J,2018). Hence, clinicians have reported that a person who weighs under 30 kg should receive ART that contain EFV concentrations which are less than 600 mg which is the standard prescription.

Moreover, high EFV concentrations have been reported to induce drug-drug interactions within patients who are under administration of other therapies simultaneously with HAART. This occurrence is seen among HIV-1 patients who are on antidepressants and those who have

histoplasmosis which is an infection that is common among HIV-1 disseminated patients (Eley B and Whilmhurst J,2018).

However, another underlying issue to all the problems associated with EFV could attribute to the contamination of water with traces of EFV (Weerakon *et.al*,2019). HAART are produced and imported in large amounts, but a fair amount remains unused until they are deemed to have expired then get exposed using various disposal methods. This in turn contaminates water supply with high EFV concentrations for various communities who primarily receive partially purified water from municipality water (Weerakon *etal*,2019).

This is a substantive argument or suggestion because vast majority of the ART patients are reported intoxicated with EFV through over-dosing which has little to no traceability (Woldemedhin *et.al*,2012). This has, in many cases created a situation whereby patients have received a HAART package with different combinational regimens with a hope of mitigating the toxicity caused by EFV over-dosing (Woldemedhin *et.al*,2012).

Hence, there have been various techniques to use to help minimize EFV toxicity by monitoring the concentrations of EFV in various media. These include high performance liquid chromatography (HPLC) and high-performance thin layer liquid chromatography (HPTLC) (Phale *et.al*, 2009). These techniques have produced satisfactory results with EFV analysis but because of costly operations are rarely recommended (Phale *et.al*,2009). Similarly, spectroscopic techniques are one of the best methods that are usable to help monitor EFV concentrations in various media mainly because of sensitivity and rapidity however due to the limited affordability they are inaccessible for general and public use (Deepan *et.al*, 2015).

This has led to the surge of the use of electroanalytical tools in recent times governed by cyclic voltammetry, differential pulse voltammetry and square wave voltammetry techniques through sensor fabrication as an alternative method for EFV concentrations monitoring system. This has been achieved mainly through the utilization of various types of nanoparticles, particularly metallic nanoparticles as they have been mostly used as one of the main source of materials with which sensors can be fabricated from to perform different types of functions.

The types of nanoparticles used include metallic nanoparticles, bimetallic nanoparticles, and quantum dots etc. Some of these nanomaterials exhibit high toxicity hence have limited application in various fields. However, the use of electrochemical means through fabrication of sensor is viable for quantitative and qualitative analysis of EFV concentrations this is because nanoparticles, particularly metallic nanoparticles often exhibit excellent

electrochemical properties hence offer greater interaction with EFV electrochemically. Additionally, they are easy to use, rapid, sensitive, and accessible compared to chromatographic and spectroscopic technique.

1.1.2 Introduction

The EFV drug molecule contains one chiral-centre and the absolute configuration of the molecule is S. Although a few analytical methods reported in literature for determination efavirenz and its related substances in drug substance and in a capsule formulation have cited that only R-enantiomeric form of EFV is obtainable in large amounts though S-enantiomer is the absolute form of EFV(Silvestri *et.al*,2016).

The bioavailability of EFV has made it one of the significantly engaging antiretroviral in discussions pertaining to HIV-1 inhibitory mechanisms. EFV has shown relatively fast onset action time which ranges between 3-5 hours and effective protean binding of 99% which is the inhibitory action imposed on HIV-1 from further replicating (Kumar *et.al*,2016).

Meanwhile, the pharmacokinetics of EFV are equally satisfactory with an estimated 50% rate of absorption when taken after high-fat meal and even greater rate absorption when taken with lighter meals or during fasting period (Kumar *et.al*,2016). However, clinically proven and unconfirmed adverse effects of EFV have rendered it being analysed and studied for unimpressive reasons culminating from reported toxicity, adverse reactions, and drug-drug interactions.

The combinational symptoms effected by these adverse effects include but not limited to euphoria, depersonalization, confusion, vomiting, diarrhoea, delusions, headaches and more. However, the more traceable issue of them all is the issue of EFV overdosing which directly and indirectly linked to the already underlined EFV adversities (Silvestri *et.al*,2016).

Furthermore, there has been concerns of neural tube defect due to EFV exposure during conception and first trimester. However, the risk of neural tube defect associated with EFV appears to be like that in the general population therefore, EFV should be continued in women who become pregnant while receiving an EFV-containing regimen for viral suppression. There has been a re-demonstration that the safety of efavirenz in pregnancy, with the occurrence of only one case of skeletal dysplasia in an efavirenz-exposed infant among 395 women with first-trimester exposure to EFV-based ART (Silvestri *et.al*,2016).

The culmination of these adverse EFV has necessitated scientific intervention and several techniques and method have been exhausted ranging from chromatographic and spectroscopic methods. However, these have notable reported shortcomings hence electroanalytical tools have recently gained advantage. And thus, this study proposes an efficient, stable, and affordable electrochemical sensor that can be used to monitor EFV in HAART formulation and river samples. This will also involve understanding of the interaction between EFV drugs and the sensor which will be fabricated from synthesis of silver-gold bimetallic nanoparticles functionalized on the nanoclay. It will be tested as a possible solution for the issues currently associated with the inexplicable overdosing and immunity of EFV among patients.

1.1.3 Delineation

The problem at the core of the research revolves precisely around an anti-retroviral drug, EFV analysis and detection in water, pharmaceutical commercial drugs and biological samples. The toxicity levels displayed by patients as a result of its various ways of misuse and disposal methods is not undertaken. The study reviews the critical analysis of scientific techniques and methods that have been applied in the past, and thus proposes a scientific tool and methodology advancing on current and past methods. The chronology and structural outline of the proposed solution is depicted by sections below.

1.1.4 Research problem

ART that contains EFV are commonly used in south Africa and predominantly Sub-Saharan Africa. However, in recent times the ART has come short in terms of effectively inhibiting HV-1 transcription in patients.

It has been and still is difficult to know all the causes leading up to the problem currently experienced. However, one of the causes is strongly associated with poor disposing method of ART medication by ART manufacturers and health facilities. ART manufacturers and health facilities dispose non-conforming, expired, and excess drugs into landfills. Naturally, these drugs dissolve underground and make their way into groundwater.

Groundwater form most parts of streams in Africa, and thus these streams become infected with traces of EFV. Most streams are utilised by municipalities through recycling systems to produce water for communities, and municipalities use water purification methods which are not designed to remove some impurities, including EFV hence people inadvertently consume

substantial variable amounts of EFV and thus overdose and also mix up with scheduled intakes of ART for patients. This fact may lead to EFV immunity and overdose problems which effectively renders ART ineffective and perhaps toxic to ART patients.

Therefore, this potential crisis has necessitated that an alternative be used by governments/municipalities to eradicate EFV and other related impurities from contaminating portable water. This paper is thus proposing a nanoclay functionalized bimetallic electrochemical sensor as a tool which could be used to assess and monitor water before it is supplied to various communities where the interaction of EFV with the surface of the electrode will be studied using cyclic and differential pulse voltammetry.

1.1.5 Study objectives

The primary objective of the dissertation is to repurpose bentonite clay through surface functionalization with Ag-Au bimetallic NPs to fabricate sensory platform and study its electrocatalytic properties that aid in detection studies of antiretroviral such as EFV. The second part of the objective is to determine the optimum working conditions and parameters to enhance its sensitivity and electroactivity in determination of EFV. The work that each of the following chapters is set to achieve is outlined below.

Specified outlined objectives of the study

- Synthesis of stable bimetallic silver-gold montmorillonite supported nanoparticles from cost effective precursors (AgNO_3 and HAuCl_4) and functionalization via chemical reduction/co-reduction.
- Characterization of bimetallic nanoparticles (MMT-functionalized), Ag-Au bimetallic NPs, monometallic NPs, nanoclay and EFV using UV-visible spectroscopy, Infrared spectroscopy.
- To study the electrochemical properties of the of silver-gold montmorillonite composites, silver-gold bimetallic NPs and monometallic NPs.
- To fabricate the electrochemical sensor for EFV analysis by modification of the glassy electrode with sensing film that depicted highest electrochemical efficiency.

- To Optimise fabrication of the electrochemical sensor and determine the optimum detection conditions for EVF. This will be followed by determination of analytical parameters.
- To validate the sensor through interference studies, recovery studies using spiking of different matrixes

1.1.6 Methodology

Synthesis of Ag, Au and Ag-AuNPs through chemical reduction/co-reduction method and respective bentonite composites. These will be subsequently characterized spectroscopically, morphologically, and electrochemically. Henceforth, using drop-casting/drop coating method, a sensor will be fabricated from most electrochemical sensing material. Optimization of experimental, analytical parameters and conditions of electrochemical sensor will be carried out. Using optimum conditions and parameters, method validation studies will be conducted through interference, recovery, and stability studies, followed by subsequent analytical application of the sensor on commercial real sample.

1.1.7 Outcomes

- To provide data on Efavirenz
- A new alternative method of analysis of EFV containing ART
- The alternative technique that could be used in ART monitoring laboratories
- The findings will be published in journals
- The Government and non-government organizations could benefit by getting information from the research.

1.1.8 The outline of chapters

- **Chapter one** discusses the essential background of the dissertation and explore more on the rationale and problem statement of the dissertation and proposes methods that will aid in addressing the problem identified.

- **Chapter two** discusses the literature review on various similar drugs but with more focus of the drug of interest. It interrogates on various forms of analytical tools that have been used in the past to attempt to address similar problems. It underlines the deficiencies of these tools thus proposes and articulates an analytical alternative tool.
- **Chapter three** mainly discusses the synthesis of metallic NPs and their clay composites. Thereafter, the optical, morphological, and electrochemical characterization of synthesized metallic NPs and clay composites with aim to ascertain their optical, morphological and electrochemical properties using Fourier-Transformation Infrared spectroscopy (FT-IR), UV/Visible spectroscopy (UV/Vis), Scanning electron microscopy (SEM) and X-ray diffraction (XRD).
- **Chapter four** outlines the fabrication and application of Ag-Au-PGV/HSA sensing platform for detection of EFV. Optimization studies were done to ascertain optimum working conditions for electrocatalytic reaction of EFV and using optimized conditions EFV recovery studies were done.
- **Chapter five** concluded on a summary on the main findings particularly from chapter 3 and chapter 4 and outlined possible recommendation for future work from this current work.

1.2 References

Alabbad, S and Adil S.F .2014. *Gold & silver nanoparticles supported on manganese oxide: Synthesis, characterization, and catalytic studies for selective oxidation of benzyl alcohol*. Arabian journal of chemistry. Vol 7(1192-1198).

Apostolova N , Funes A and A Alvarez. 2015. *Efavirenz and the CNS: what we already know and questions that need to be answered*. Journal of antimicrobial chemotherapy. Vol 2693-2708(70).

Arvizo. R and Bhattacharya. R. 2010. *Gold nanoparticles: Opportunities and Challenges in Nanomedicine*. ResearchGate. Vol 7(6). 753-763.

Bozal, B., Uslu, B., Ozkan, S.A. 2011. A review of electroanalytical techniques for determination of anti-HIV drugs. *International Journal of Electrochemistry*, doi: 4061/2011/343947.

Castro A, de Souza N and A. Rey. 2011. *Determination of efavirenz in diluted alkaline electrolyte by cathodic adsorptive stripping voltammetry at the mercury film electrode*. Journal of Brazilian chemical society. Vol 22(9).

D. Chen and S. Wang. 2006. *Protective agent-free synthesis of Ni–Ag core–shell nanoparticles*. ResearchGate. Vol 100(3).468-471.

Chouhan, N. 2018. Silver Nanoparticles: Synthesis, Characterization and Applications. 10.5772/intechopen.75611.

Comer, J and Corner, I. 1967. *Applications of Thin-Layer Chromatography in Pharmaceutical Analyses*. Journal of pharmaceutical science. Vol 54(4).413-436.

Dogan-Topal, B, Uslu, B., Ozkan, S.A. 2009. Voltammetric studies on the HIV-1 inhibitory drug Efavirenz: The interaction between dsDNA and drug using electrochemical DNA biosensor and adsorptive stripping voltammetric determination on disposable pencil graphite electrode. *Journal of Biosensors and Bioelectronics*, 24, 2358-2364.

Eley B and Whilmhurst J. 2018. *Neuropsychiatric adverse effects of efavirenz*. The neurology of HIV infection. 152(99-116).

Garrido C, Simpson C and Dahl N. 2015. *Gold nanoparticles to improve HIV drug delivery*. Future Medicinal Chemistry. 1097-1107(9).

G. Gangahara, U. Maheshwarib and S. Guptac. 2014. ‘Application of nanomaterials for the removal of pollutants from effluent streams.’ *Nanoscience Asia*. Vol. (2). 140-150.

Gupta. K, Dubey. S and Malik K. 2017. *Application of modern electroanalytical techniques: Recent trend in pharmaceutical and drug analysis*. International journal of pharmaceutical sciences and research. Vol 2. 2450-2458.

S. Gurunathand, Z. Lui, W. Shen and X. Zhang. 2016. ‘Silver Nanoparticles: Synthesis, Characterization, Properties, Applications, and Therapeutic Approaches’. *International journal of molecular sciences*. 17(9). 1534.

Hassan Y. 2012. *Electroanalytical Methods in Pharmaceutical Analysis and Their Validation*. Springer link. 811(75).

H. Rao, Y. Liu, J. Zhong. 2017. 'Gold nanoparticle/Chitosan, S co-doped multiwalled carbon nanotubes sensor: Fabrication, characterization, and electrochemical detection of nitrite'. *ACS sustainable chemical engineering*. (5)10926-10939.

Hoetelmans, R.M.W. 1999. Quantitative determination of Efavirenz (DMP 266), a novel non-nucleoside reverse transcriptase inhibitor, in human plasma using isocratic reversed-phase high-performance liquid chromatography with ultraviolet detection. *Journal of Chromatography B*, .734, 55-61.

Julian C.H, Jolanta K. 1999. *Crystal structure of the HIV-1 integrase catalytic core and C-terminal domains: A model for viral DNA binding*. Proceedings of the national academy of sciences of the united states of America. 97(15).

J. Wang. 2013. 'Template electrodeposition of catalytic nanomotors'. *Faraday discussions*. Vol 164. 9.

Kumar P and Lakshmi Y.2017.*An Oral Formulation of Efavirenz-Loaded Lactoferrin Nanoparticles with Improved Biodistribution and Pharmacokinetic Profile*. HIV medicine. Vol 18(7).452-462.

Kumar S and Rao R. 2009. Development of Rapid UV Spectrophotometric Method for the Estimation of Efavirenz in Formulations. *E-Journal of chemistry*. 7(3).856-860.

Kumar S and Wu F. 2012. *One-pot Synthesis of Dopamine Dithiocarbamate Functionalized Gold Nanoparticles for Quantitative Analysis of Small Molecules and Phosphopeptides in SALDI- And MALDI-MS*. National library of medicine. Vol 137(7).38-1629.

Laura Abis. 2018. *Gold and Gold-Palladium Catalysts Synthesized by a Modified Sol-Immobilisation Method for Thermal and Plasmonic Glycerol Oxidation*. Cardiff Catalysis institute.

Lu. H, Tian. B and Wang. T. 2017. *Montmorillonite-Supported Fe/Ni Bimetallic Nanoparticles for Removal of Cr (VI) from Wastewater*. *Chemical engineering transactions*. 50-1.

- Matthews Z , Woolf J and Mazenko R. 2001. *Determination of efavirenz, a selective non-nucleoside reverse transcriptase inhibitor, in human plasma using HPLC with post-column photochemical derivatization and fluorescence detection* .Journal of pharmaceutical and biomedical analysis. Vol 925-934.
- Mekewi M.A, Darwish A.S and M.S Amin. 2016. *Copper nanoparticles supported onto montmorillonite clays as efficient catalyst for methylene blue dye degradation*. Egyptian journal of petroleum. Vol 25(2). 269-279.
- Mishra S, Thiruppathi R and Ganapathy M. 2016.*Nanoparticle Functionalization and Its Potentials for Molecular Imaging*. Advance science. Vol4(3).
- Mout R, Moyano D and Rana S. 2012. *Surface functionalization of nanoparticles for nanomedicine*. Chem soc rev. Vol 41(7).2549-2544.
- Nasrabadi M, Abbasi M and Davaran S. 2014. *Bimetallic nanoparticles: Preparation, properties, and biomedical applications*. Artificial Cells, Nanomedicine, and Biotechnology. Vol 376-380(44:1).
- Palfreeman, A., Youle, M. & Farthing, C. (1988). *Drugs in HIV and AIDS*. Wiley, Chichester.
- Phale. M and N Shah. 2009. Quantitative Estimation of Efavirenz by High Performance Thin Layer Chromatography. Department of pharmaceutical analysis. Vol 1(4).
- Reddy, N., Padmavathi, Y., Mounika, P., & Anjali, A. 2015. *FTIR spectroscopy for estimation of efavirenz in raw material and tablet dosage form*. International Current Pharmaceutical Journal, 4(6), 390-395.
- Sarasa-Nacenta, M., Lopez-Pua, Y., Lopez-Cortes, L.F., Mallolas, J., Gatell, J.M., Carne, Y. 2001.*Determination of Efavirenz in ARV by thermogravimetric analysis detection*. *Journal of thermogravimetry B*, 763, 53-59.
- Silvestri R and Famiglini V. 2016. *Focus on Chirality of HIV-1 Non-Nucleoside Reverse Transcriptase Inhibitors*. MDPI. 21(2). 221
- Thapliyal, N Chimunze T and Karpoormath R. 2016. *Research progress in electroanalytical techniques for determination of antimalarial drugs in pharmaceutical and biological samples*. Royal society of chemistry. 62(57580-57602).

Thapliyal N, Osman N and Patel H. 2015. *NiO–ZrO₂ nanocomposite modified electrode for the sensitive and selective determination of efavirenz, an anti-HIV drug*. Royal society of chemistry. 50(40057-40064).

Veldkamp, A.I., Van Heeswijk, R.P.G., Meenhorst, P.L., Mulder, J.W., Lange, J.M.A., Beijnen, J.H.,

Weerakoon. D and Lim.E. 2019. *Fate of environmental pollutants*. Water environment pollutants 91(10).

Woldemedhin .B and Tajure N . 2012. *The Reason for Regimen Change Among HIV/AIDS Patients Initiated on First Line Highly Active Antiretroviral Therapy in Southern Ethiopia*. North American journal of medical sciences. Vol 4(1). 19-23.

Chapter 2: Literature review

2.1 Introduction

This chapter discusses the various known ARVs and their various detection methods ranging from traditional analytical methods to electroanalytical methods. Although the focus is on EFV, the chapter discusses the successful application and shortcomings of all techniques reported mainly on most ARVs. Furthermore, the effect of electrochemical sensing using nanomaterials modifications such as monometallic, bimetallic and their functionalized composites and other types of sensors as alternate detection methodologies are critically discussed focusing mainly on their drug applications as well as their shortcomings are also reviewed.

2.2 Antiretrovirals

Antiretrovirals (ARVs) are one of the most produced drugs in the world but even more so in Africa, particularly sub-Saharan Africa (Ford *et.al*,2011). One of the main reasons for this very large scale of ARVs is because of antiretroviral treatment program (ART) which is currently distributed in huge amounts in sub-Saharan Africa for Human immune virus/Acquired immune deficiency syndrome(HIV/AIDS) treatment but precisely HIV-1 (Attaran *et.al*,2001).

HIV-1 is mainly an intracellular parasite that is wholly dependent on a host living cell for replication. Thus, the conventional idea and approach to eradicate or minimise its effect is to continuously produce ARVs equipped to effectively inhibit the HIV-1 replication process at a rate that meets or is greater than the demand (Attaran. A *et.al*,2001). However, due to HIV-1 gene modification that occurs naturally with time which is the case for most other viruses. ART administration thus experiences limitations because of HIV-1 changes in RNA codons and this equally demands continuous modification in ARVs to counteract these changes (Imai *et.al*,2011). Furthermore, to this day there has been at least 25 ARVs that have been produced and approved for treatment of HIV-1 in particular but extended to AIDS according to different categories (Imai *et.al*,2011). These categories are primarily comprised of six classes of ARVs (Refer to the figure 2-1).

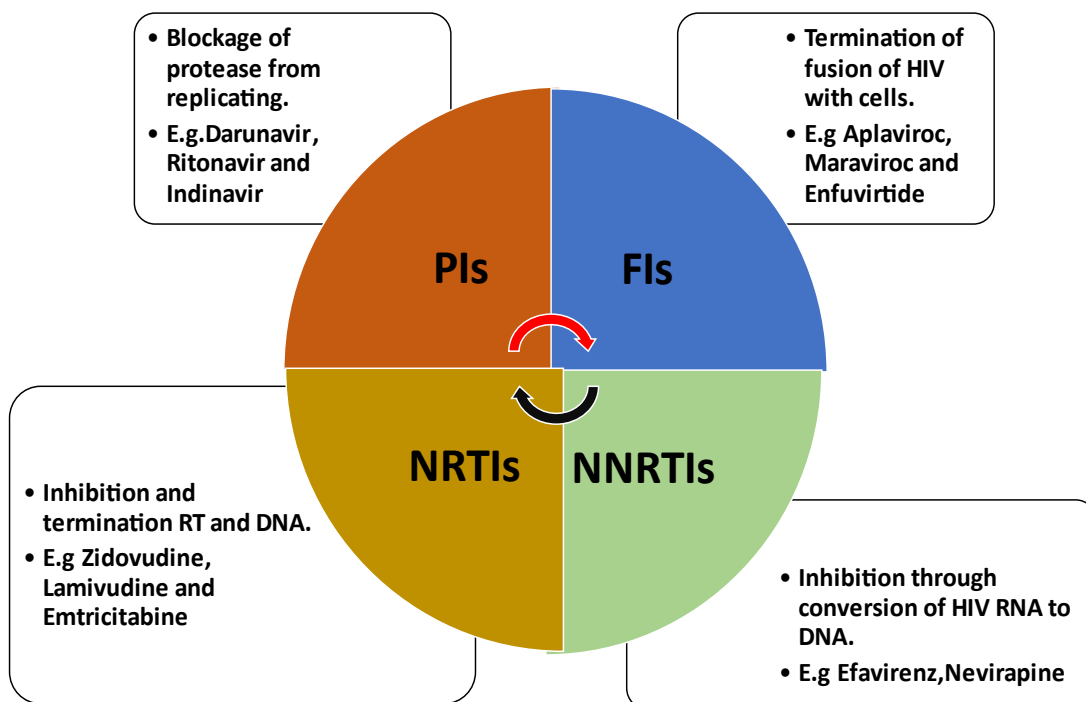


Figure 2-1: Summary of ARVs based on their classes and their respective action mechanisms (De clerq,1998 and Rivera,2020)

These classes of different ARVs are all used and have been used in different parts of the world. However, NNRTIs and NRTIs have been the most produced and used ARVs in Africa but mostly in sub-Saharan Africa. NNRTIs are chemically distinct from nucleosides and, unlike the NRTIs, do not require intracellular metabolism for activity. In general, NNRTIs are a group of small hydrophobic compounds with diverse structures that specifically inhibit HIV-1 reverse transcription (RT), but not HIV-2 RT (De Clercq,1998). In addition, NNRTIs ARVs ART can be taken with or without food intake which is advantageous compared to other ARVs from different classes.

2.3 Efavirenz

Efavirenz (EFV) as an ARV has been very effective as first line regimen compared to other various ARVs particularly NNRTIs which are currently the most used ARVs in Africa. EFV has been proven to reduce HIV-1 viral load to below 400 copies/ml within six months in 60 to 80% of people who have not previously taken any HIV treatments (Yimer, *et.al*,2015). The effectiveness of the drug as first in line regimen in HIV-1 ART is highly recommendable

particularly in sub-Saharan Africa. EFV in combinational therapy has had more success than other combinational therapies led by other ARVs in recent years. This is backed by EFV impressive bioavailability which is almost 50% without food and reaches maximum absorbed concentration within 4 hours after being administered.

EFV does not occur naturally, thus is a synthetic drug that is synthesized from organic materials. One of the few synthetic routes that can be used to synthesize EFV using 4-chloroaniline as starting material proceeded by seven other chemical steps to yield EFV of excellent chemical and optical purity. The reaction is said to asymmetrically produce overall yield of 62%, refer to figure 2-2 below (Zhao *et.al*,1998).

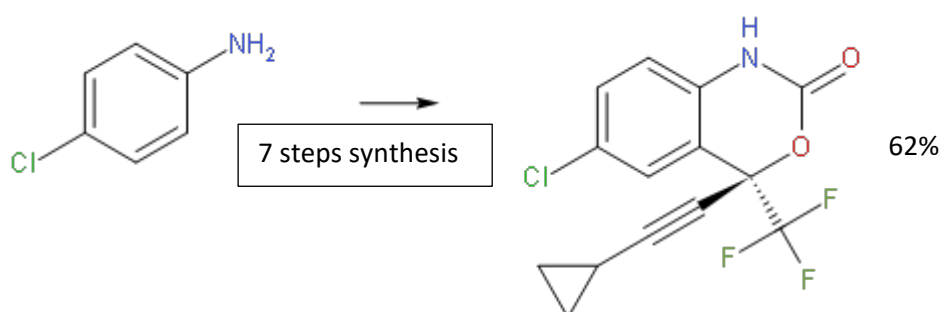


Figure 2-2:A demonstration of one of EFV synthesis pathways

The success of EFV against HIV-1 is due to its potent action mechanism compared to other ARVs. HIV-1 without EFV binds to the RT (Reverse transcriptase) active sites, thus it is able to replicate itself as depicted by the diagram below. However, in the presence of EFV, this action is exceedingly minimal (Zhao *et.al*,1998). This is because EFV binds to the RT active site unopposed before HIV-1 is able to, hence HIV-1 does not have an effective interaction with RT active site because EFV barrier that has been created. EFV is thus able to tame the HIV-1 potency and hinders its ability to replicate itself within the living cell as illustrated by the diagram below. Numerous studies have recommended EFV because of its ability to inhibit the HIV-1 replication power better than most NNRTIs. As it seen below that the rate of replication was reduced by almost 50% (Braz *et.al*,2010)

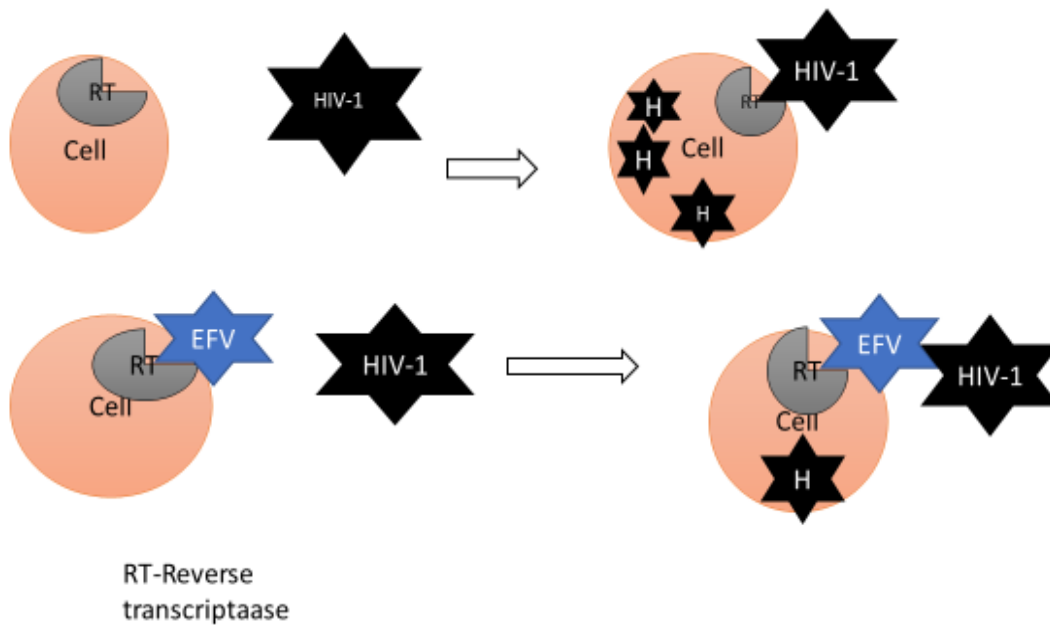


Figure 2-3: Inhibitory depiction diagram of EFV against HIV-1 (**H**-stands for HIV-1)

EFV has a poor solubility. Therefore, aqueous solutions-must be combined with regimes of impressive solubility in combinational therapy to improve the overall solubility of EFV within ART (Ozdemir *et.al*,2018). It also has pKa value of 10 which indicates that it is highly alkaline in nature which further explains its low degree of dissociation in aqueous media like water. This chemical property of EFV is advantageous because it is safer to consume orally as it does not increase acidity in the stomach but rather increases basicity which induces neutrality and that creates ideal conditions for optimum EFV metabolism. This property of EFV one of the most significant properties that has made it better suitable for ART administration ahead of other competing ARVs.

EFV generally occur in the environment through various aqueous systems which include rivers, effluent water, ground water, dams and even surface water. However, prominently ARVs are found in rivers which makes big part of municipal water. EFV find its way into various streams through disposals from clinics and health facilities. The disposed and dissolved ART traces occur in wastewater that is primarily recycled and redistributed for consumption to various communities (Ncube *et.al*,2018). Small concentrations of EFV is removed during wastewater purification, however larger concentrations remain undetected in water that is ultimately produced as drinking water which may cause ART resistance toward patients (Ncube *et.al*,2018).

A scientific intervention is necessary, and studies have been conducted using different techniques with some success. But in recent years, scientific community has been seeking an efficient alternative because of current and previous limitation experienced with certain analytical techniques. Hence, this study is aimed at providing an alternative electroanalytical tool that will help to scientifically monitor, detect, and quantify the EFV environmental traces in water particularly and other biological samples like urine and serum with great sensitivity, and rapidity and at relatively low cost.

2.4 Detection and quantification methods of EFV

The need for detection and quantification methods of EFV and other ARVs is of great importance for both environmental and biological reasons, which are critical for human survival, thus to reduce ART-containing EFV quantities occurring through over-dosing amongst most HIV-1 patients which is a biological crisis needs scientific intervention. As such, some of these efforts have been made through use of traditional analytical detection methods, which have had success in recent years, however as the issues associated with EFV and other ARVs have scaled up, these methods have started to have limited success. Moreover, attempts in developing new analytical techniques to remedy the health issues brought by ART through influx of these drugs in various parts the environment has not ceased. Although in various parts of the world, particularly in sub-Saharan Africa traditional techniques are still very much in use but ART health issues deem these current methods inadequate due to drug complexities and inadequate sensitivity exhibited by these techniques.

2.4.1 Current techniques

Chromatographic and spectrometric techniques are two of the most popular techniques that have been traditionally used to detect and quantify EFV and other related ARVs in various types of samples for decades (Schoeman *et.al*,2015). These techniques are still currently used and have been successfully applied in analysis of pharmaceuticals such as EFV, and other organic analytes with satisfactory levels of sensitivity and selectivity.

Various studies have reported the use of High-performance liquid chromatography (HPLC) in the analysis of EFV and other ARVs (Schuman *et.al*,2005) as can be seen in table 1-1. These HPLC methods are used to determine ARVs are validated and used by pharmaceutical industries. As such, there has been reported success with these techniques in drug applications, more so that there have been improvements in some of these methods as some have been made to have compatibility to perform simultaneous determinations of ARVs and other drugs alike (Else, *et.al*,2010).

According to a recent study, HPLC was used to simultaneously detect and quantify a total of six ARV which included Efavirenz, Nevirapine, Zidovudine and Tenovir. The advantage of this is believed to be one of the solutions to the problem currently faced with HIV HAART product counterfeiting as the technique showed excellent selectivity during the sample matrix analysis and confirmed the types and quantify of drugs which are present.

Other studies reported satisfactory results done by various forms of HPLC methods in terms of limit of quantitation (LOQ) and limit of detection (LOD) but these ranges are only applicable and excellent in context of pharmaceutical formulations but not traces of analytes as that generally requires even greater sensitivity which would give lower LOD and LOQ. Hence, HPLC methods have limited applicability, often expensive operation to use and not time-consuming

On the other hand, the application of spectrometric techniques has not been applied as regularly as chromatographic over the years. Fourier transformation infrared spectroscopy (FT-IR) has been seldom used in ARVs and other related analytes because it does not have excellent capacity to carry out quantitative analysis but rather is adequate for qualitative analysis.

Tandem mass spectrometry modification with liquid chromatography (LC-MS-MS) is one of fewest techniques that have been devised through combinational analytical instrumentation to improve detection of various analytes but particularly pharmaceuticals such as EFV. This method is reported to have shown much desired precision, sensitivity, selectivity, and reproducibility. However, despite this success it is relatively inaccessible for general application because often hybrid methods require expertise. Hence, the reason it is used as an alternative method to existing ones in clinical studies done by forensic scientific investigators and other clinicians for comparative studies (Phung, *et.al*,2018). Meanwhile, other limitations often said about this method include use of large sample and time-consuming sample preparations and actual analysis.

Table 1-1 : A depiction of some results from current methods that have been used.

Technique	Detection	Sample	LOD ^a /LOQ ^b /LLOQ ^c	References
Spectroscopic	LC-MS/MS	Human hair	EFV-0.05ng/mg(LLOQ) Lopinavir-0.05 ng/mg(LLOQ) Ritonavir-0.01 ng/mg(LLOQ)	Huang.Y <i>et.al</i> , 2008
	LC-MS/MS	Dam water	0,09 ng. L ⁻¹ (LOD) 0,2 ng. L ⁻¹ (LOQ)	Rimayi <i>et.al</i> ,2018
	UV/Vis	Tablets	-----	Deepan. T <i>et.al</i> , 2015.
	FT-IR	Pharmaceutical formulations	0.993g/ml (LOD) 148.84 g/ml (LOQ)	Reddy. <i>et.al</i> ,2015
Chromatographic	HPLC UV-DAD	Pharmaceutical formulations Prepared standards	EFV-0.38 ug/ml(LOQ) ZDV-1.48ug/ml (LOQ) NVP- FTC-	Jocelyn. <i>et.al</i> , 2019
	HPLC	Human plasma	0.2 uM (LOQ)	Veldkamp. <i>et.al</i> ,1998
	HPTLC	Bulk drug formulation and capsule	0,7ug(LOD) and 1ug per spot(LOQ)	Phale. <i>et.al</i> ,2009

Consequently, with the reported success of both chromatographic and spectroscopic methods. These methods are not viable to eradicate ART crisis particularly in sub-Saharan Africa because of limitations that were previously outlined (refer to chapter 1) and the economic state of this African region. Hence, new viable methods designed to particularly benefit potential users like Africans and other group of people hard-hit by HIV-1 and inadequacy of drug detection systems /methods have had to be devised, methods that are particularly rapid in terms of data acquisition, require little sample and highly sensitive of which such properties are not offered by traditional current methods.

,

2.4.2 Electroanalytical techniques

Electroanalytical methods have gained a lot of traction in recent years particularly with drug analysis and few other relevant analytes. The electroanalytical technique subject is an umbrella to methods that include voltammetry, polarography and even sensors of various kinds. These have different but excellent properties and features that makes them ideal alternative to traditional methods, and these are broadly eluded to in chapter 1. In addition, these methods are one of few methods that can facilitate the electrochemical studies of drugs, from which the reactivity of drugs amongst other properties can be obtained. Hence, particularly for most pharmaceuticals' studies and determinations, the electroanalytical techniques are best equipped compared analytical traditional tools.

This is possible because of electrochemistry which is used as a tool that can be employed in the analysis of molecules/analyte that exhibit electrochemical behavioural properties by polarographic and voltametric electrochemical techniques. The two main pathways electrochemical indications through which these techniques are oxidation and reduction. This involves a loss or gain of an electron from that electroactive specie, thus for detection of the analyte to occur it generally has to follow a particular electrochemical mechanism, which is indicative of loss and gain of electrons reversibly or either of them irreversibly or even quasi-reversibly (Refer to figure 2-4 below).

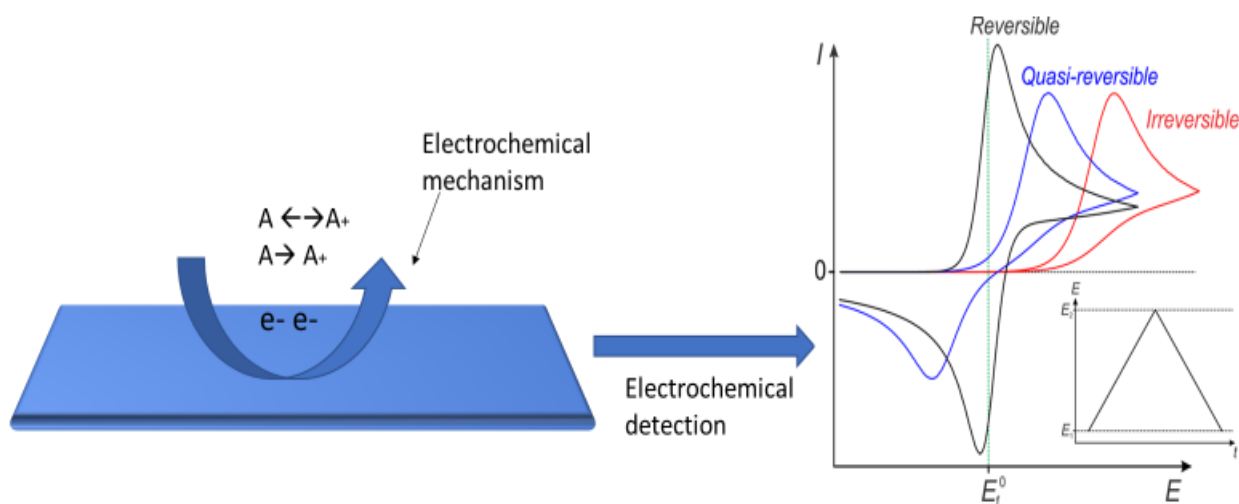


Figure 2-4: Depiction of electrochemistry operating within an electrochemical technique

Voltammetry and polarography are two of the most used in drug analysis and in recent years ARVs. These methods have predominantly been reliant on the use of electrochemistry to study electrochemical behaviour of various drugs including ARVs. The use of electrochemistry allows them to carry out qualitative and quantitative analysis of all oxidizable analytes. Most ARVs have few electrochemical properties that allows them to be analysable with these methods, EFV does undergo oxidation because of NH-group which gets deprotonated. This property can be used by these methods to exhibit oxidation potential of EFV and how it can change if the medium amongst other several parameters are changed. The exhibited oxidation potential is distinct to every oxidizable substance and is obtained through extraction of standard state potential from the curve meanwhile quantitative information is obtained by relating current to the concentration of analyte in the bulk solution (Elgrishi, *et.al*,2018).

There have been several studies that have reported the use of these electroanalytical techniques in analysis of ARVs and other drugs. The diagram below exhibits a few prominent electroanalytical techniques that the studies have reported most detection and determination of drugs studies from.

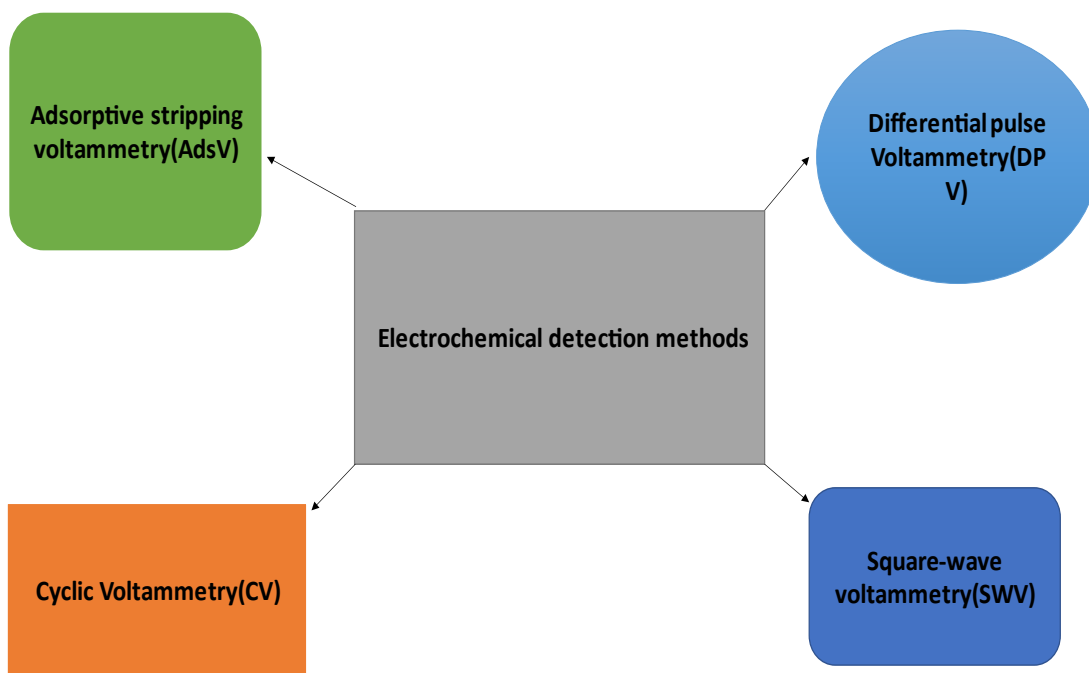


Figure 2-5:A chart of most prominently studied and most used electroanalytical techniques of analytical scientific tools

These techniques are considerably sensitive of electroanalytical tools or methods compared to traditional methods. In addition, the wider applicability and versatility of stripping techniques which include anodic, cathodic and adsorptive. These techniques have an independent capacity of carry out multi-metal determination in one solution with adequate sensitivity. Meanwhile, cathodic stripping particularly brings an advantage of detecting insoluble salts, and thus it is justifiable that they have gained more interest in drug analysis especially with trace determinations. In addition, DPV and SWV are two of the most sensitive voltametric techniques, for instance, SWV suppressed background currents much more effectively than CV and for this reason, analyte concentrations on the nanomolar scale can be registered utilizing SWV over CV or LSV. Meanwhile, DPV also pulse voltammetry like SWV where a current is sampled within a pulse, although this makes the technique accurate and sensitive the background currents are not as equally removed as with SWV, thus DPV is slightly less sensitivity between the two. In addition, other reasons are broadly discussed in chapter 1. However, these methods as a class have limitations and shortcomings that are also discussed in chapter 1, and these have led to traction around sensors as tools that meet the challenges previously and currently faced with these methods.

2.4.3 Types of sensors and relevant components

Furthermore, are a part under electroanalytical techniques that have more potential and have also shown greater potential of maximizing the capacity of these methods. Sensors can be classified depending on the type of signal output they produce as information report about an analyte be it quantitative or qualitative data. The signal output or energy transfer can be electromagnetic, thermal, electrochemical, or even mechanical. In addition, some literatures suggest that sensors can somewhat convey a chemical transducing mechanism which is often seen with enzymic, DNA and molecules detection sensors (Araujo *et.al*,2007). Furthermore, electrochemical sensors among them is voltammetric and potentiometric devices that are based on chemically sensitized field effect transistor and potentiometric solid electrolyte gas sensors. Electrical sensors include those with metal oxide and organic semiconductors as well as electrolytic conductivity sensors. Mass sensitive sensors include piezoelectric devices and those based on surface coustic waves. Magnetic sensors mainly based on paramagnetic gas properties. Thermometric sensors based on the measurement of the heat effect of a specific chemical reaction or adsorption involving the analyte. Other sensors are based on emission or absorption of radiation (Araujo *et.al*,2007).

These types of sensors all have been used in different studies, but biosensors and electrochemical sensors are the two most types of sensors that have been used in ARVs and other drug analysis. As it was discussed in chapter 1, sensors offer excellent sensitivity and selectivity because they are often used for specific analyte detection and that is further enhanced by varying certain conditions.

Hence, there are few studies that have reported the analysis of ARVs using a sensor, but particularly electrochemical sensor. This has seen success as some of these studies produced satisfactory results in terms of LOD of ARVs in sample matrix, but most studies have produced unsatisfactory levels LOD and LOQ because the sensor clogs in analysis involving complex sample matrix (Jiang *et.al*,2020). These have been highlighted as the main shortcomings of some electrochemical sensors most importantly those with unmodified surfaces (See a demonstration below).

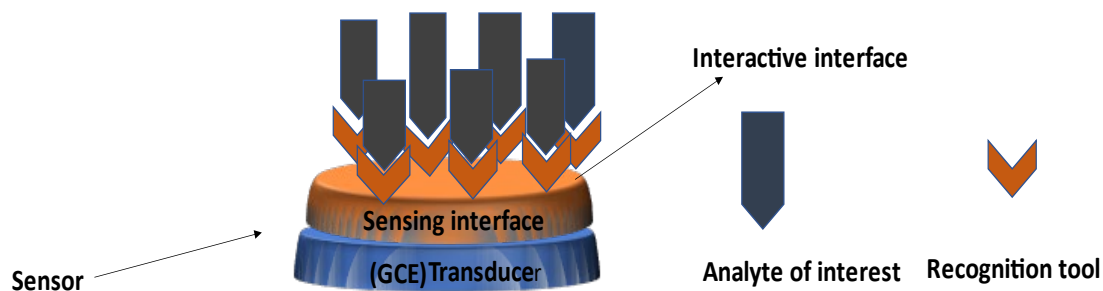


Figure 2-6: Typical components of an electrochemical sensor and their typical functions

This is a typical depiction of a sensor, particularly an electrochemical sensor and over the years electrochemical sensors have been the most used type of sensors and has the most overall growth in interest and application of all types of existing sensors. This is because electrochemical have a better and wider range of applicability, selectivity, and sensitivity.

Typically, an electrochemical sensor consists of few components which include, sensing interface sometimes known as a receptor and is supported by a transducer which is often the sensor itself. These are the main component of a typical transducer or sensor, but the most important of them all is a receptor or sensing interface. This is because the receptor is the recognizing tool that often works through contact or adsorption with the analyte hence it is a bridge of communication between the transducer and the analyte (Jimenez *et.al*,2012).

Generally, for example, the electrochemical sensor is glassy carbon electrode (GCE) which is a typically a voltametric/ampereometric type of a sensor. These types of sensors are said to mainly interact with analytes electrochemically and thereby obtain an electrical signal which is either converted into potential or current through a process called signal transduction. The signal transduction function is primarily performed by transducers, and there are several types of transducers today amongst which include temperature transducer, pressure transducer, piezoelectric transducer and many more.

These transducers operate similar in principle but use different pathways to deliver data, as such with electrochemical transducers like GCE, the transduction process is mostly governed through conversion of chemical (concentration) or electro-chemical (redox) to electronic energy, which is true only to chemical sensors like the electrochemical sensor demonstrated in figure 2-6.

The recognition tool of various transducers or sensors is often dependent on the type of analysis, analyte of interest and a base transducer. The receptors are classified based on types of stimuli or a react upon specific interaction with a certain analyte under a specific environment, and the primary role of these are to qualitative and/or quantitative interact with target analyte, however the interaction varies with type of receptor. Hence, there are different types of receptors amongst which include mainly chemoreceptors, thermoreceptors, mechanoreceptors and photoreceptors. However, in recent years because of fast advancing developments, these traditional types of receptors have seen less in terms of application because of introduction of like nanomaterials and modified chemoreceptors which are mainly comprised of organic molecules and biological molecules like proteins. There are many reasons for these advancements but one of them is to improve the interaction with target-analytes which in turn optimize the sensitivity of the transducer, and another one is to improve selectivity and widen the range of applicability of transducers to a few more types of analyte than just to only one specific analyte.

Moreover, as there have been developments in nanomaterial industries and how they can be maximized in terms of capacity and properties in order to enhance the determination of drugs. Metallic nanomaterials have gained more interest than most types in recent years but particularly the bimetallic nanomaterials. Metallic nanoparticle (NPs) can be synthesized and modified with various chemical functional groups which allow them to be conjugated with antibodies, ligands, and drugs of interest and thus opening a wide range of potential applications in biotechnology, magnetic separation, and preconcentration of target analytes, targeted drug delivery, and vehicles for gene and drug delivery and more importantly diagnostic imaging (Jong *et.al*,2008).

Monometallic NPs are one of the few first type of nanoparticles that can be easily synthesized and applied in various chemical analysis and often consist of only one metal. The particle sizes of monometallic NPs are often dependent on a typical metal noble or alkali used and synthesis pathways. These factors play a pivotal role in the fundamental performance of the monometallic NPs. Furthermore, generally monometallic NPs have been used as a catalysts and coating material for various sensors used in different scientific applications. Other applications of monometallic NP include electronics, optics and microbial agents for microorganisms like *Escherichia coli*.

Two of the commonest and mostly used monometallic NPs have been silver (Ag) and gold (Au) and these two have been applied as monometallic NPs and in a bimetallic NPs system because of their excellent biocompatibility, optical properties, high surface area to volume ratio. But what has been very useful and important, is the conductivity, thermal stability, and catalytic activity of these metals, which all are critically important for enhancement of electrochemical sensor (Kumar *et.al*,2018). Some studies have reported the used Ag-NPs in detection of an ARV, Tenofovir. Ag-NPs was used to functionalize benzalkonium chloride particles which in turn vastly enhanced the conductivity and catalytic properties of the electrochemical sensor. The effect of the functionalized were observed with considerable decrease in LOD. Moreover, the voltammetric oxidation pathway of tenofovir was also investigated (Dogan-Topal *et.al*,2018).

In contrast, the application of Au-NPs in drug analysis particularly ARVs has been mainly with drug delivery systems which is part of the biomedical applications. A recent study reported the use of Au-NPs together with immunochromatographic assay as a semi-quantitative measure of monitory HIV-inhibitor concentrations in the patients, and the method was reportedly successfully. It was suggested that the method could be used as a tool of monitoring PI, NRTIs and NNRTIs levels of although more clinical studies had to be carried for method validation (Garrido *et.al*,2015).

The reported success that monometallic NPs has had in the analysis of other ARVs, is down to mainly electrochemical properties. ARVs, particularly EFV are oxidisable in certain media. Hence, an electrochemical sensor modified with AgNPs or any other relevant metal is adequately compatible to improve interaction between the sensor and EFV because mainly of conductivity and catalytic power between EFV and surface of a sensor. Thus, with metallic NPs surface area would be enhanced which would exceedingly improve sensitivity towards EFV. Moreover, the use of both Ag NPs and Au-NPs with other non-metallic substances of different nature, does improve some properties of these metallic NPs. However, it has been reported that the challenge or shortcoming of that, is that the shape and size of formed NPs of Ag or Au changes and that affects the efficacy of the NPs. The effect is less potent if the incorporation of NPs is involving two metals of complementary characteristics (Garrido *et.al*,2015).

As results this has sparked interest in bimetallic NPs systems whereby metals are incorporated with each other to improve certain properties whilst maintaining minimal negative effect within

properties that are supplementary. Bimetallic NPs (BMNPs) systems are generally better than monometallic mainly because of exceedingly enhanced surface area to volume ratio, catalytic power, conductivity, and stability (Sergeev *et.al*,2014). The diagram below demonstrates the physical difference between a surface of sensor that has been functionalized with only one monometallic NPs whilst the other with two, thus a bimetallic system. It also underlines the effect in terms of surface area, catalytic effect all which affect the electrochemical interaction with EFV thus a difference in signal absorption output.

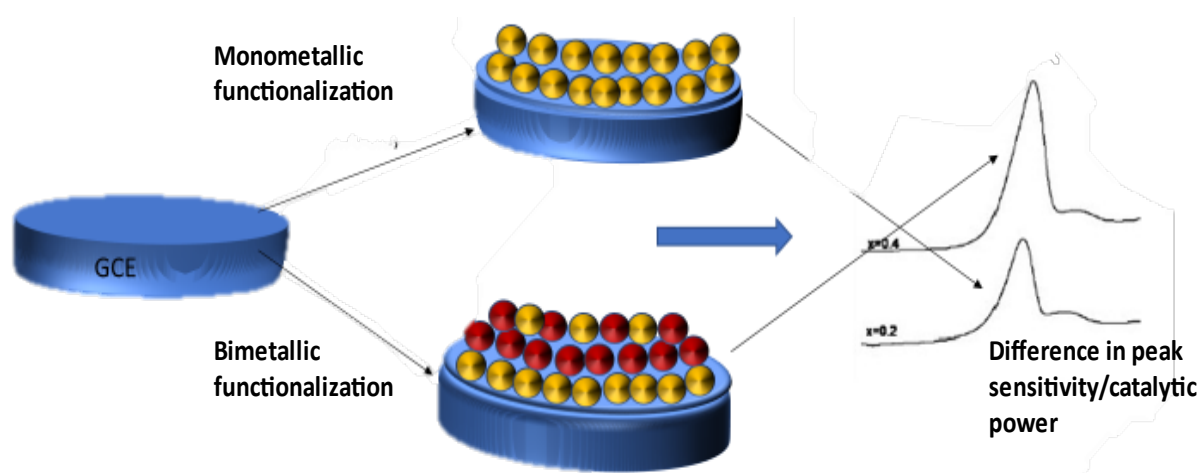


Figure 2-7: An illustration showing the impact of BMNPs in comparison to monometallic NPs systems

Contrary to monometallic NPs, BMNPs constituting metals and their sizes determine the properties of the system. The study of the BMNPs has not been long in existence as only recently have researchers analysed their preparation and characterization in much detail. The preparation techniques of BMNPs are mainly core-shell, alloys, and contact aggregate. The subsequent catalytic power of the BMNPs is said to be different and that is heavily affected by preparation methodologies. The applications of BMNPs have a wider range compared to monometallic NPs because of improved properties. These applications include electrocatalysis, imaging, biomedical devices, and nanomedicine. It is worth mentioning that monometallic NPs do carry some of these applications but BMNPs carry them to greater effect.

2.4.4 The electrochemical effect of nanoparticles on detection methods/techniques

The effect of different types of nanoparticles on different techniques but particularly electrochemical techniques and methods is mainly on the sensitivity through overall detection limits and limits of quantitation of techniques and methods alike. In addition, the effect brought by an introduction of nanoparticles is sometimes dependent on the type of nanoparticles used. For examples, monometallic and BMNPs generally improve various electrochemical techniques and method through electron-transfer rate constant and electron transfer coefficient as the introduction of highly conductive metal ions brings excessive conductivity within the system, which enhances the electrochemical interaction with target electroactive analyte because of excessive of electron movement in the system. In addition, parameters like electron-transfer coefficient and transfer rate constant decrease and increase respectively, as the energy barrier between analyte and detecting material decreases and speed of electrochemical interaction between analyte and detecting interface increases as a results of fluent electron movement.

Similarly, the overall sensitivity of electrochemical techniques in catalysis is vastly improved by the BMNPs specifically compared to monometallic NPs because the BMNPs offers exceedingly more electroactive sites upon which catalytic reactions are able to occur electrochemically. This effect increases the overall capacity of a particular electrochemical technique in conduction of electrochemical catalysis. Similarly, with non-metallic NPs although they possess significantly inferior electroactive sites and properties alike, as they predominantly operate and interact through adsorption with target analyte although materials like metal oxides exhibit a degree of electrochemical interaction.

Furthermore, as these typical non- pure metallic nanomaterials use adsorption as primary mode of interaction with target analyte, surface area is generally the prime factor that improves the overall detection capacity of the technique and method alike because these nanomaterials are typically large molecules. Moreover, compared to organic molecules and proteins, metal oxides offer enhance the sensitivity of the technique through both surface area a significant degree of electron transfer coefficient and electron-transfer rate constant, which are significantly low compared to pure some metallic and BMNPs. However, the electrochemical hybrid effect exhibited by metal oxides affect the electrochemical methods and techniques more than organic and protein materials in terms of overall detection sensitivity.

Furthermore, recent studies have shown that BMNPs system have an even better existing dimension, where organic or inorganic materials can be supported into BMNPs producing BMNPs nanocomposite. Generally, BMNPs nanocomposite consist of a mixture of at least three or more distinct components whose properties generate a new material with multifaceted properties. Thus, such developments have had impact in treating diseases like cancer, and detection of some vitamins amongst many other applications. The range of applications for BMNPs nanocomposite is wider than that of BMNPs because of greater enhancements of BMNPs nanocomposite in terms of properties. In addition, because of that these types of nanocomposite, according to few studies are a preferred alternative used for most drug detection analysis including some ARVs where these nanocomposites are used as components of conductive biosensors or electrochemical sensors.

However, with all the outlined advantages of a BMNPs and BMNPs nanocomposites systems over monometallic NPs system. These systems have been associated with cases of instability that exist between the two types of monometallic NPs. This has been seen or observed mainly through degradation of one of the metallic NPs within a BMNPs system which occurs because of oxidation. This effect causes the BMNPs to chemically disintegrates, which generates high levels of agglomeration within BMNPs (Sergeev *et.al*,2014).

Hence, this limitation of BMNPs has led to many scientific interventions amongst which include the use of nanoclay as a possible and alternative solution. According to various studies, some nanoclay have excellent chemical and physical properties that have proved to be beneficial particularly for BMNPs systems.

2.4.5 Nanoclay modified sensors

Nanoclay such as bentonite, which predominantly exists as montmorillonite (MMT) forms large part of the nanoclay and has been the most common and the best studied nanoclay, which has been used in polymer nanocomposites for almost three decades. Indeed, bentonite clays are being used for widespread applications. They are used as thickener in paints, and additive in ceramics. They are also employed in food, pharmaceutical and cosmetics. In medicine, they are used for treatment of various ailments including pains, wound healing, bacterial infections, and stomach ulcers (Murray,2006). Bentonites are being applied as adsorbents, catalysts, and modified electrode materials due to their relatively high surface area, good ion-exchange

capacity, and adsorption capacity. They also provide a good and stable support for immobilization of biomolecules and electrocatalysts. Sodium bentonite which has a layer thickness of 1 nm possesses good intercalation, swelling, and ion-exchange features. It has attracted remarkable attention in electrochemical sensing particularly for the detection of cations. The other attracting feature which inspires applications of bentonite-based materials in different fields is related to their benign and environment friendly nature. They are being employed in modification of electrodes for electrochemical sensing (Patil et.al,2019).

Hence, analytical methods based on nanoclay electrochemical sensing have gained noteworthy consideration of researchers predominantly due to their high sensitivity, simplicity, and relatively low cost. However, some nanoclay modified electrodes experience unwanted species and impurities from aqueous solutions tend to accumulate on the surface of the nanoclay modified electrodes owing to their hydrophilic nature (Patil et.al,2019). This problem is further complicated when dealing with electroactive matrices, the nanoclay modified electrodes are easily poisoned or fouled due to the accumulation of interferents on the surface. Hence, sometimes these sensors tend to show poor sensitivity and selectivity toward target analytes and cannot differentiate between the analytes with closely related oxidation potentials.

Consequently, such sensors have been further chemically modified with conductive substrate or electroactive materials, films, or coatings. The modified electrodes are fabricated to enhance the sensitivity of detection which is not possible otherwise. In recent years, BMNPs have been amongst the mostly used type of conductive substrates in further functionalization of nanoclay sensors and have served as electrocatalysts and lead to enhanced electron transfer kinetics.

Furthermore, the importance of nanoclay functionalization through the use of BMNP system is crucial in many ways, but the main significance and enhancements that BMNP system offer to nanoclays such as bentonite are improved surface area of the system, which brings about an improved catalytic effect, improved conductivity contributed by a supporting metal ions which aids with the electrochemical properties of the system and lastly nanoclays such as bentonite offers a preventative measure with degradation of BMNPs system through oxidation by instilling stability within the system. ZnO and AgNPs have been used in the past to modify various types of nanoclay based sensors. According to some sources, the use of both these types of NPs brings about excellent combinational effect in terms of excellent catalytic effect, conductivity and surface area, which introduces more catalytic sites, and these are brought by

AgNPs and ZnO NPs as individual NPs to even greater effect as composites (Saddiqi *et.al*,2018). The demonstration of this is depicted by the diagram below.

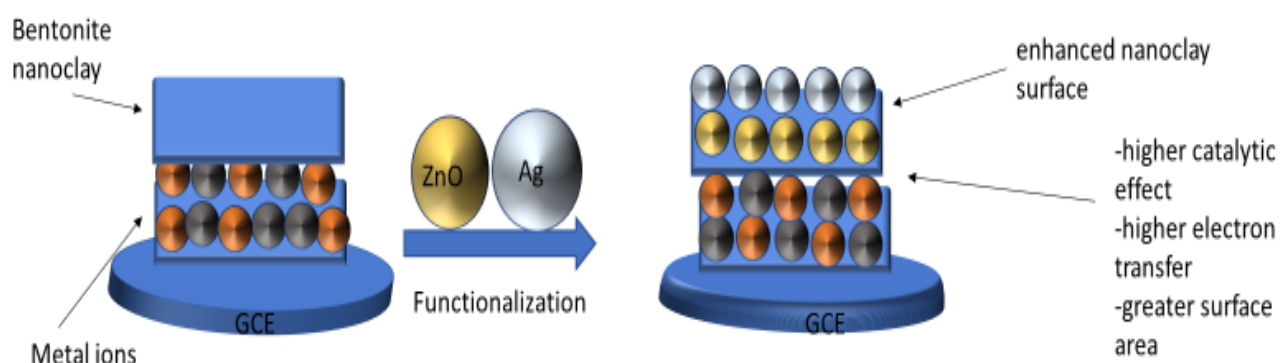


Figure 2-8:A functionalization of typical bentonite clay with bimetallic NPs

The effect that is done by the functionalization of nanoclays does not only provide stability and longevity within sensing material but improves the electrochemical properties of nanoclays themselves. The enhancements are beneficial in various drug analyses including that of ARVs because of its electrochemical properties, ARV drugs have a greater potential to interact with such systems as the electron-transfer would be greater because of an increased in electroactive surface area through BMNPS introduction into MMT surface. This would increase the detection of target analytes and other electroactive drug in terms of sensitivity and electrochemical interaction between sensing surface and analyte of interest

2.6 Reference

Araujo. A and Montenegro.M.2007. *Optical Sensors and Biosensors Based on Sol-Gel Films. Researchgate.Vol.23*

Arvand.M, Pourhabib.A and Giahi.M. 2017. *Square wave voltammetric quantification of folic acid, uric acid and ascorbic acid in biological matrix. Journal pharmaceutical analysis.Vol.7(2).110-117.*

Attaran. A, Sachs. J and Farmer. P .2001. *Community-based approaches to HIV treatment in resource-poor settings. The lancet. Vol (358).404-409.*

Declercq. E, Schols. D and Moore. J.1998. *AMD3100, a small molecule inhibitor of HIV-1 entry via the CXCR4 co-receptor*. Nature medicine. Vol (4).72-77.

Delia M Rivera, MD Assistant Professor, Department of Pediatrics, Division of Infectious Disease and Immunology, University of Miami Leonard M Miller School of Medicine

De jong.H and Borm.P.2008. *Drug delivery and nanoparticles: Applications and hazards*. International journal of nanomedicine. Vol.3(2).133-149.

Dogan-Topal.B and Okzan. S.2018. *An Electrochemical Sensor Based on Silver Nanoparticles-Benzalkonium Chloride for the Voltammetric*. Determination of Antiviral Drug Tenofovir. An international journal devoted to electroanalysis, sensors and bioelectronic devices.Vol.30(5). 943-954.

Elgrishi. N, McCarthy.D and Dempsey.L.2017. *A Practical Beginner's Guide to Cyclic Voltammetry*. Journal of chemical education. Vol (95).197-206.

Else.L,Watson.V and Tjia.J.2010. *Validation of a rapid and sensitive high-performance liquid chromatography–tandem mass spectrometry (HPLC–MS/MS) assay for the simultaneous determination of existing and new antiretroviral compounds*. Journal of chromatography B.Vol.878(19).1455-1465.

Garrido.C , Simpson.C and Bresse.J. 2015. *Gold nanoparticles to improve HIV drug delivery*. Future medicinal chemistry. Vol.7(9).1097-1107.

Imai. K and Ochiai. K. 2011. *Role of histone modification on transcriptional regulation and HIV-1 gene expression: possible mechanisms of periodontal diseases in AIDS progression*. Journal of oral science. Vol (53). 1-13.

Jiang.C, He.Y and Lui.Y.2020. *Recent advances in sensors for electrochemical analysis of nitrate in food and environmental matrices*.Vol.145(16). 5400-5413.

Jimenez.D, Diaz.G and Blanco-Lopez.C.2012. *Chapter 1 - Molecularly Imprinted Electrochemical Sensors: Past, Present, and Future*. Molecularly imprinted sensors. pp1-34.

Jocelyn. M, Augustin. M and Tresor.M .2019. Development and validation of HPLC methods for simultaneous analysis of 6 antiretrovirals in pharmaceutical formulations. Journal of analytical and pharmaceutical research.Vol.8(2).

- Katti.D and Katti.S.2017. *Chapter 10 - Predictive Methodologies for Design of Bone Tissue Engineering Scaffolds*. Materials for bone disorders. Pp453-492.
- Knez.Z and Leitgeb.M. 2020. *Development of Chitosan Functionalized Magnetic Nanoparticles with Bioactive Compounds*. Nanomaterials.Vol.10(10).1913.
- Kumar.K, Venkatesh. N and Kuila. A.2018. *Metallic Nanoparticle: A Review*. Journal of scientific and technical research. Vol.4(2).
- Leandro. C and Moreira.J. 2010. *Determination of Zidovudine in Pharmaceuticals by Differential Pulse Voltammetry*. Journal of analytical letters. Vol.43(12).1951-1957.
- Matthews.C, Woolf.E and Mazenko.R.2002. *Determination of efavirenz, a selective non-nucleoside reverse transcriptase inhibitor, in human plasma using HPLC with post-column photochemical derivatization and fluorescence detection*. Journal of pharmaceutical and biomedical analysis. Vol.28(5).925-934.
- Murray, H.H., 2006. Bentonite applications. *Developments in Clay Science*, 2, pp.111-130.
- Ncube.S and Madikizela.L.2018. *Environmental fate and ecotoxicological effects of antiretrovirals: A current global status and future perspectives*. Water research. 231-247.
- Ourari.A, Tennah.F and Ruiz-Rosas,R. 2017. *Bentonite Modified Carbon Paste Electrode as a Selective Electrochemical Sensor for the Detection of Cadmium and Lead in Aqueous Solution*. International journal of electrochemical science. Vol.13.
- Ozdemir. A, Sanli.S and Sanli. N.2018. *A New Method for Determination of Efavirenz and pKa by Using LC-UV*. International Journal of Pharmaceutical Research & Allied Sciences.Vol.7(4). 120-126.
- Patil, M.M., Shetti, N.P., Malode, S.J., Nayak, D.S. and Chakklabbi, T.R., 2019. Electroanalysis of paracetamol at nanoclay modified graphite electrode. *Materials Today: Proceedings*, 18, pp.986-993.
- Phale. M and N Shah. 2009. Quantitative Estimation of Efavirenz by High Performance Thin Layer Chromatography. Department of pharmaceutical analysis. Vol 1(4).
- Phung.N, Okochi.K and Louie.A.2018. *Development and validation of an assay to analyze atazanavir in human hair via liquid chromatography/tandem mass spectrometry*. Mass communication in spectrometry. Vol.32(5).431-441.

Reddy, N., Padmavathi, Y., Mounika, P., & Anjali, A. 2015. *FTIR spectroscopy for estimation of efavirenz in raw material and tablet dosage form*. International Current Pharmaceutical Journal, 4(6), 390-395.

Schuman, M., Schneider, S., Omes, C., Wennig, R., Fundira, L., Tayari, J.C. and Arendt, V., 2005. HPLC analysis of generic antiretroviral drugs purchased in Rwanda. *Bull Soc Sci Med Grand Duche Luxemb*, 3, pp.317-325.

Sergeev.M ,Busev.S and Revina. A.2014. *Catalytic properties of monometallic and bimetallic palladium and rhodium nanoparticles obtained in reverse micellar systems*. Nanotechnology reviews.Vol.3(5). 2191-9097.

Siddiqi, K.S., ur Rahman, A. and Husen, A., 2018. Properties of zinc oxide nanoparticles and their activity against microbes. *Nanoscale research letters*, 13(1), pp.1-13.

Thapliyal, N Chimunze T and Karpoormath R. 2016. *Research progress in electroanalytical techniques for determination of antimalarial drugs in pharmaceutical and biological samples*. Royal society of chemistry. 62(57580-57602).

Zhang.F, Li.L and Luo.L. 2012. *Electrochemical oxidation and determination of antiretroviral drug nevirapine based on uracil-modified carbon paste electrode*. Researchgate.Vol.43(3)

Zhao. D, Reamer.R and Silverman.S .1998. Practical Asymmetric Synthesis of Efavirenz (DMP 266), an HIV-1 Reverse Transcriptase Inhibitor. ACS publications. Vol (63). 8536–8543.

Zheng. H, Zupeng.Y and Chen.J.2019. *Highly selective and stable glucose biosensor based on incorporation of platinum nanoparticles into polyaniline-montmorillonite hybrid composites*. Microchemical journal. Vol.152(104266)

Chapter 3: Synthesis and Characterisation

Chapter 3 summary

This chapter discusses the synthesis and characterisation of Silver (Ag), Gold (Au), Silver-Gold (Ag-Au) NPs and their subsequent nanoclay composites. All outlined metallic NPs were synthesised using chemical reduction and co-reduction method, respectively. Meanwhile, nanoclay composites were synthesised through functionalization of PGV bentonite via chemical reduction seeded growth method.

The metallic NPs and clay composites were all optically characterized using FT-IR, whilst UV/Vis spectroscopy carried out only metallic NPs characterization. Morphological and electrochemical characterization was performed on both metallic NPs and their respective clay composites.

3.1 Introduction

The synthesis of metallic nanoparticles (NPs) follows more than one route. The pathways followed in the synthesis of NPs is generally deterministic of factors such as particle distribution, morphology and sizes of particles formed. Over the years, there has been various metallic NPs synthesis methods that have been applied according to different purposes, which are depicted by figure 3-1.

Typically, the galvanic replacement approach has been employed to prepare heterostructures that would otherwise be challenging to synthesize by other means. Usually, one metallic NPs precursor is slowly introduced into a growth solution of another metallic NPs in a specific ratio depending on concentration and covalency of ions. In contrast, the seeding growth technique has been shown to be exceptional when it comes to controlling the size of NPs. In this technique, small metal NPs are first prepared and served as seeds (nucleation sites) which are mixed with a growth solution to synthesize larger particles. In addition, chemical reduction because of its overall superiority in terms of particle size and distribution has seen enhancing developments originating from traditional chemical reduction like galvanic replacement and seeded growth.

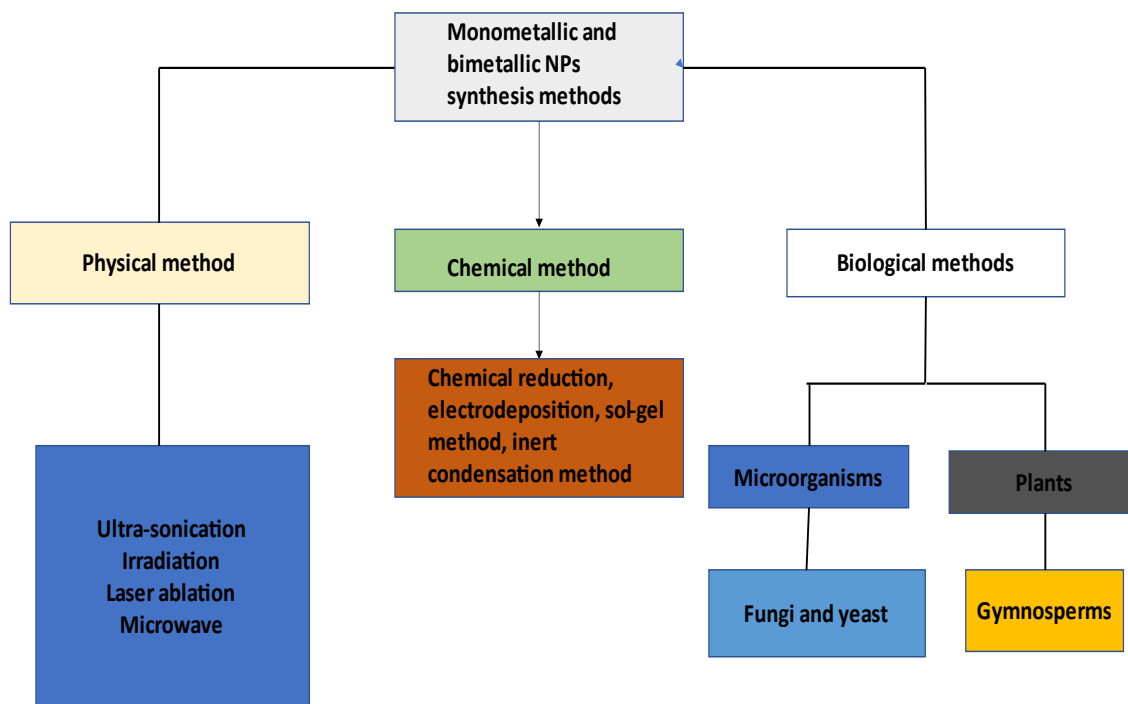


Figure 3-1: Diagram depicting prominent synthesis methodologies of monometallic and bimetallic NPs ((Rajput, 2015, Feng et.al, 2014).

The advantages associated with these methods include, controlled sized particle distribution, cost effective, while the disadvantages are particle sizes dependence to temperature, pH, and synthesis can be relatively time consuming. However, because of accessibility, affordability and typical optimum particle size and distribution achieved by these methods, they remain one of the most used in various application of nanoscience or nanotechnology.

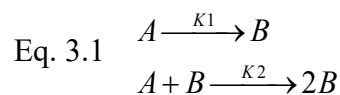
Consequently, monometallic NPs such as AgNPs and AuNPs have been synthesized by various techniques including wet chemical method, sol-gel method, hydrothermal synthesis method, chemical vapour deposition, precipitation method, laser vaporization condensation method and spray-pyrolysis method (Gangadhara et al. ,2014, Polte *et.al* ,2010). Most of these techniques were not extensively used on a large scale, but wet chemical synthesis has been widely used due to its simplicity (Awad et.al,2016).

Chemical methods often use water or organic solvents to prepare the Ag, Au and other metallic NPs alike. This process usually employs three main components, metal precursors, reducing agents, and capping agents (Rodriguez-Gonzalez *et.al*,2020). In this study Ag NPs synthesis method involved a Ag metal precursor, two stages reduction, which are nucleation then subsequent growth. The advantages of physical methods are speed, radiation used as reducing agents, and no hazardous chemicals are involved, but the downsides are low yield and high energy consumption, solvent contamination, and lack of uniform distribution (Lukoweic *et.al*,2020).

3.2 Synthesis of AuNPs and AgNPs via chemical reduction method

Chemical reduction method for the synthesis of Ag, Au and Ag-Au NPs is one of the cheapest and simplistic synthesis methods. This method has been used for many years, and recently chemists have been optimizing variables within the method to achieve highly stable NPs. This method predominantly uses reducing agents like ascorbic acid, sodium citrate and sodium borohydride to convert ions into atoms thus forming NPs of satisfactory shape and average size distribution (Nasrullah *et.al*,2020).

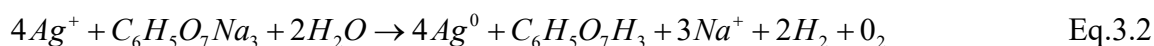
Factors affecting formation of these NPs that needs optimization include, but not limited to temperature, concentration of precursors and reducing agents and type thereof. Temperature, which is time dependent, has said to be vital for nucleation stage of NPs, and for optimum and faster nucleation of NPs. The temperature of the solution is boiled to 60°C. Size of metallic NPs like AgNPs and AuNPs increases slightly from 70 to 80 °C while it decreases sharply from 80 to 90 °C. It could be concluded that the decrease of size at high temperature is result from the sharply increased k_2 instead of the decreased k_2 (Huang *et.al*,2020). The mechanism that the formation of metallic NPs, particularly AgNPs and AuNPs follow is depicted below.



Where K_1 is a constant due to nucleation formation of metallic NPs, and K_2 is a constant due to autocatalytic surface growth of the NPs but the two averages to nucleation and growth, respectively. **A** represents the precursor metal ion whilst **B** is the growing metal nanocluster (Okzar *et.al*,2019).

Furthermore, other papers suggest that the optimum formation of AgNPs and AuNPs is greatest within temperature range of 17-32°C (48nm) because of fusion of particles, whilst temperatures above it cause a slight decrease to 45 nm. The effect of time on the formation of NPs is mostly dependent on the temperature, higher temperatures often lead to faster formation of NPs but not necessarily the shape and sizes of the NPs (Huang *et.al*,2020).

Synthesized NPs properties are affected by concentration of precursors reducing agents during synthesis. Literature reports that the increase in the concentration of reducing agent, metal precursor and particle sizes tend to increase proportionally (Sibiya *et.al*,2014). As the concentration of a particular reducing agent increases, colour changes are observed, which is characteristic of the surface plasmon resonance (SPR) (Lui *et.al*,2018). The colour of metal NPs such as AgNPs depends on the shape and size of the nanoparticles and the dielectric constant of the surrounding medium. According to a recent study, only electrons with free electrons, especially Au, Ag, Cu and the alkali metals, possess plasmon resonance in the visible spectrum, which gives rise to such colours. It should be noted that higher concentrations of stabilizing agent could also cover up the nanoparticles, thus reducing the dispersity of the nanoparticles in solution, which could be indicated by the formation of larger sizes of NPs (Huang *et.al*,2020). The equation 1 and 2 below typically demonstrates the reduction process of Ag and Au ions into Ag and Au colloidal particles in solution through use of typical trisodium citrate reducing agent, which is the commonest reducing agent utilised due to its reducing power, affordability, and non-toxicity. It is reported that trisodium citrate is a significantly better reducing agent than most agents owing to three citrate ions which offer a significantly superior electron exchange to ions in solution, subsequently forming atoms or nanoparticles (Huang *et.al*, 2020)



Note, from the equations that the role of reducing agents is to donate electrons to ions forming atoms. Therefore, the type of reducing agent is also vital for optimum formation of NPs as well as for size distribution of particles formed. Generally, the nucleophilic molecules have the greatest tendency to donate electrons compared to electrophilic molecules which have a high electron affinity. Consequently, reducing agents that are nucleophilic in nature would tend to aid with formation of better NPs in terms of size, shape and distribution NPs. Some studies

reported a small and uniform sized NPs synthesized by increasing pH of the reaction mixture. The nearly spherical AgNPs were converted to spherical AgNP by altering pH. When increasing the pH values will result in the formation of larger nanoparticles but with more accurate crystallite sizes (Iravani *et.al*,2014).

Metallic NPs have since gone through modifications, primarily to improve their already existing properties but particularly electrochemical properties (Guerrini,2018). Thus, bimetallic NPs have been used to enhance properties such as better rate of catalysis and due to improved surface area, catalytic power and conductivity from enhanced overall electrochemical properties. Some applications of bimetallic NPs, include uses as antimicrobial agent in the field of biomedical sciences, and in photothermal cancer therapy and in electrochemical catalysis.

In the synthesis of bimetallic NPs, at least two metal sources must be used, (eg Ag^+ and Au^{3+}). Their presence during the reduction process generally determines the typical nature of formed bimetallic NPs. As such, alloyed NPs are generally formed in a synthesis process that introduces both metal sources simultaneously, thus forming an alloy of statistical content between two metal ions (Guerrini, 2018). A method that generally produce this formation is chemical co-reduction method.

In contrast, another bimetallic NPs prominent method that is used is sequential reduction method sometimes referred to a seeded growth method belonging to a class of colloidal synthesis techniques for metallic NPs (Iravani,2016). This method generally produces a bimetallic nanocluster that is typically core-shell, where metal sources are not introduced simultaneously but in step intervals causing one to be reduced first whilst the other is reduced unto the reduced atoms of the other one when it is introduced on the next interval. The resulting core atoms are generally from a nobler metal of the two, although the reverse analogy is reported to be possible provided a working condition are suitable (Iravani, 2016).

Other synthesis methodologies of bimetallic NPs include incipient wetness impregnation of the support with solution of metal precursors. Although this method is simple to execute, the resulting clusters vary widely both in composition and particle size distribution, which generally affect their catalytic performance (Landry *et.al*, 2016). On the other hand, synthesis of bimetallic NPs with zeolites has been showed to produce highly dispersed uniform clusters. However, the use of zeolites affects significant levels of steric hindrance. Hence, the colloidal

synthesis methods for bimetallic NPs remain simple and reproducible compared to the forementioned synthesis techniques (Landry *et.al*,2016).

Bimetallic NPs have since undergone various modifications for different applications from imaging to nanomedicine and heterogenous catalysis (Garrido-Ramirez *et.al*,2016). Nanoclay functionalization with bimetallic NPs is one of the few recent advancements that has been made and currently growing at a rapid rate.

Nanoclays have been used as sensing films for various chemical analysis but the results have been of low sensitivity due to the insufficient reactivity and robustness of the nanoclay films as several components of nanoclay are reported to be silicates which are relatively chemically and electrochemically inert under normal conditions (Mohsen *et.al*,2021). Thus, their functionalization with metallic NPs, particularly bimetallic NPs systems that possess excellent catalytic power and electrochemical reactivity which enhances sensitivity has gained more than significant traction from various research scope but particularly in nanoscience.

The synthesis methods generally used to form the composites from clay functionalization are limited to seeded growth or sometimes galvanic replacement approach. Seeded growth method adds an array layer of reduced metallic ions unto the surface of the clay, while galvanic replacement uses the advantage of the heat to dislodge metal ions within the clay replacing them with the desired ones (Raji,2016). These methods have been used frequently due to simplicity and plausible reproducibility and size distribution and shapes of particle formed.

The application of the synthesised metal clay composites has been reported to have wider range than bimetallic NPs due to their increased surface coverage of composites. They are effectively utilised in organic pollutants in wastewater remediation and as sensing films in fabrication of various kinds of electrochemical sensors (Stankovic *et.al*, 2015).

3.3 Characterization nanoparticles

The characterization of noble metallic NPs such as Ag, Au ,their bimetallic NPs and composites properties may include but not limited to catalytic, conductivity, electrical, magnetism, absorption that are carried through various types of techniques and instrumentation. (Sharma *et.al*,2019). This study used spectroscopic and voltammetry techniques to characterize NPs

synthesize, and absorption capacity of metallic NPs synthesised was carried out using UV/Vis spectroscopy because, they are excitable upon being irradiated with light. This method of characterization has been employed effectively for years (Dzimitrowicz *et.al*,2019).

The UV/Vis spectroscopy is an easily available technique for characterization of noble metal nanoparticles. This technique is widely used for determination of size and shape of metal nanoparticles. The tuning of optical properties of noble metal nanoparticles under various stimuli can be studied using UV/Vis spectroscopic method (Nedyalkov *et.al*,2018). UV/Vis spectroscopy can also be used to monitor the kinetics of formation of monometallic and bimetallic NPs. Growth of metal nanoparticles in polymeric network or growth of polymeric network around metal nanoparticle core can be studied using UV/Vis spectroscopy. This technique can also be used for investigation of various applications of hybrid materials in catalysis, photonics, and sensing (Begum *et.al*,2018). Although UV/Vis spectroscopy has a very high limit of detection, which is a disadvantage it does characterization of metal ions competently.

Infrared (IR) spectroscopy provides highly discriminatory information due to the excitation of inherently specific fundamental vibrational transitions characteristic of molecular species. Nanoparticles of diverse nature have been characterized and their synthesis confirmed using different spectroscopic techniques in the infrared range (Ke *et.al*,2019). Nanoparticles with inherent infrared absorptions or functional groups present at their surface may thus be directly characterized via infrared spectroscopy. Furthermore, different ligands attached to nanoparticles may readily be identified according to their vibrational signatures in a rapid, precise, and non-destructive way. Thus, verification of protective groups and confirmation that the desired material is synthesised can be made.

FT-IR spectroscopy was successfully applied in this study in the characterization of Au and Ag metallic NPs. However, as effective as it was, it is generally not recommended as has relatively high detection limit and the exciting power is inadequate for metallic excitation (El Nagggar *et.al*, 2018). Other disadvantages that hinder spectroscopic techniques as means of characterizing analytes is the fact that it is an expensive instrumentation.

Voltammetric techniques such as cyclic voltammetry (CV) and differential pulse voltammetry (DPV) are used to carry out electrochemical property studies of both metallic and bimetallic NPS. The study used properties such as peak potential and peak current as means of deducing the electrochemical behaviour of the metallic NPs and composites formed, which were largely

qualitative studies conducted mainly using CV as the peak potential exhibited qualitative data as all potentials at which these NPs and composite are active were unique to one another. In contrast, peak currents exhibited quantitative property, as it deduced the concentration mainly of the diffusing ions which resulted in diffusion current. This property is deduced by both CV and DPV, however DPV was used to conduct quantitation of ions due to greater sensitivity.

Furthermore, the DPV technique presents advantages, such as avoiding the use of digestion or enhancing steps and requiring a simplified procedure since all the steps are performed in the same solution. In consequence, it is usually quicker than other non-direct methods (Scholz, 2015). Since a direct electron transfer needs to be produced between the electrode surface and the nanoparticles, they have to be at a very close distance to enable electron channelling. This fact has led to more studies more hence there has been vast developments in the synthesis of many bimetallic NPs of various types (Scholz,2015). This study hence employs, cyclic voltammetry (CV to characterize Au and Ag monometallic properties NPs).

CV was further applied for kinetic studies of NPs and composites through mainly Randles Sevcik equation, although other equations such as lavirons equations have been successfully applied by various studies in the past. According to randles secvik equation as is used in studies concerning effect of scan rate on peak currents and diffusion of active electrochemical species (Ferrari,2018). These deductions helped deduce some parameters for NPs and composites which included active surface area of active species and number of electrons involved in the electrochemical reaction.

$$I_p = \left(\frac{n^2 \times F^2}{4RT}\right) \times \Gamma(v.A) \quad \text{Eq. 3.4}$$

Where, i_p is the peak current, n refers to number of electrons involved whilst v and A are the scan rate and surface area of working electrode, respectively used to determined electroactive surface (Γ). Meanwhile, the lavirons is also an equation that is used to determine different variables, such as transfer rate constant, transfer coefficient as well as number of electrons (Ferrari,2018). Apart from such, it has been used to study effects of scan rates on peak potentials in electrochemical detection active species. As such, electrochemical detection of NPs has been achieved by the direct oxidation or reduction of an electroactive component of the NP, typically a metal component of the NP (Lui *et.al*, 2016).

The morphological studies of monometallic, bimetallic, and metallic composites are carried through use of X-ray diffraction, scanning electron microscopy (SEM). These techniques aid

with provision of data on typical formation of crystals of NPs composition, their particle sizes, inner structure of crystals and surface information (Li et.al,2018). X-ray diffraction largely highlights crystallinity of the crystals formed. Some of these techniques do provide a degree of quantitative data, as often seen with Energy Dispersive X-ray (EDX) capacity to exhibit both qualitative and quantitative data particularly on metallic NPS (Thapliyal *et.al*,2016).

The metal nanoclay composites are also characterized with various methods ranging from spectroscopic, voltametric to confirm that the desired material is synthesised and to ascertain changes in structure, morphology, optical and electrical properties because of the modification.

This chapter is on synthesis, characterization of the Ag, Au monometallic NPs, Ag-Au bimetallic NPs and their nanoclay composites. As such, it provides the insight on the synthesis methodologies that was followed in the study and all characterization techniques that were used to conduct quantitative and qualitative verification studies of the compositional facets on the synthesised materials.

3.4 Experimental methods

3.4.1 Reagents

AgNO₃(Silver Nitrate) (Aldrich,99,9%), Na₃C₆H₅O₇(trisodium citrate) (Aldrich,99%), HAuCl₄ chloroauric hydrate (99%, Aldrich), PGV-bentonite (99% Aldrich bentonite nanoclay), Deionised water purified by mili-QMT system (Millipore,) and Hydrochloric acid (HCl, 99% Aldrich).

3.4.2 Synthesis of Ag and Au NPs

The AgNPs are generally synthesized from AgNO₃, which is the white crystalline granules powder which acts a metal precursor. To synthesize (AgNPs), wet chemical method was used, and the spherical AgNPs were prepared according to the procedure reported by Awad *et.al*,2015. In this method, AgNPs were synthesized by using trisodium citrate as reducing agent. An aqueous solution of trisodium citrate (2 mM) was added into a 50 ml burette and

then, a 50 ml aqueous solution of AgNO_3 (1 mL, 1 mM) was added into conical flask. The mixture was heated to boil at 70 degrees Celsius. Meanwhile, the reducing agent was added dropwise until the contents turned a light-yellow colour. After 10 s, the suspension changed to a darker yellow after reaction had proceeded for another 20 second amidst mildly boiling conditions extended for 2hrs.

A similar methodology was followed with AuNPs synthesis, where 1 mM of HAuCl_4 precursor was made up in 50 ml container. This solution was allowed to mildly boil, and 0,2 M of trisodium citrate was added drop wise until solution turned light red/pinkish colour. This mixture continued to boil at 90°C for further 1 hour and thereafter cooled.

3.4.3 Synthesis of Ag-Au bimetallic NPs

Co-reduction chemical method was used to synthesis bimetallic NPs. 0,1 mM of both AgNO_3 and HAuCl_4 was mixed made up in 50 ml flask. The mixture was mildly boiled at 90°C and then trisodium citrate was added dropwise until dark maroon/brown colour occurred. This solution was placed to further heat for another hour and allowed to cool.

3.4.4 Preparation of Ag-Au bimetallic functionalized PGV-bentonite nanoclay

Ag-Au PGV-bentonite functionalize nanocomposite was prepared by dispersing 1 g of PGV-bentonite in 100 ml of 1 mM AgNO_3 and HAuCl_4 solutions for 24 h. PGV-bentonite dispersions were centrifuged and dried at 105°C and exchanged Ag-Au PGV-bentonite nanocomposite was reduced by dispersing it in 2 mM of sodium citrate at boiling temperature. This process caused dispersion to colour to change from white to brownish colour (Shameli et.al,2011).

3.4.5 Preparation of modified GCE

The glassy carbon electrode (GCE) was coated at separate times with PGV-bentonite, AgNPs, AuNPs, Ag-Au bimetallic NPs and nanocomposites and throughout, the method that was used to coat was drop-coating method (Fahmy *et.al*,2019). Approximately, 0,5 ml of synthesized AgNPs, AuNPs, Ag-Au bimetallic NPs and PGV-bentonite nanoclay was casted on the bare GCE. The modified GCE was left to dry in open vacuum for 2 hours.

3.4.6 Electrochemical characterization

Cyclic voltametric experiments were performed using an AutoLab PGStat128 (MetrohmAutoLab) equipped with the NOVA 2.1 Software (Metrohm AutoLab). The experimental setting was composed of a conventional three electrodes cell in which a working electrode GCE(with saturated potassium chloride (KCl)) and a platinum wire were used as reference (RE) and counter (CE) electrodes, respectively. A bare glassy carbon (GC) with mono or bimetallic Au and Ag NPs and their nanocomposites was used as working electrode (WE). Before the modification, GC was sequentially polished with diamond powder (0,05, 0,3 and 1 μ m, Sigma Aldrich) cloth and washed with milli-Q water. Cyclic voltammetry was recorded in aqueous solution with 0.1 M HCl as supporting electrolyte.

The CV data presented below was obtained at varying potential ranges against Ag/AgCl (KCl 3 M), which dependent upon the electrooxidation/electro-reduction of each respective material nanoparticle, but same scan rate, 70 mvs/s. Due to electrochemical plausible reversibility of redox couples observed at this scan rate, whilst for voltammograms that represent kinetics they were obtained at scan rate range of 10-90 mV/s.

3.4.7 Infrared spectroscopy & UV/Vis spectroscopy characterization

1 ml approximately of Ag, Au monometallic NPs (1mM) and Ag-Au (1mM) bimetallic NPs were analysed for characteristic absorbance peaks. The instrument that was used is UV-1800-Shimadzu UV spectrophotometer, Advanced African Technology (Scientific division) serial number:127471.

Two quartz cuvettes were used, and one was used as a blank hence contained only the solvent (Millipore water) and was used for baseline and background check. This was done to eradicate noise and interference at the wavelengths of interest.

The cuvettes were both inserted at the sample compartment and with one containing solvent and another respective analyte (NPs). The scan was ran and spectra for each materials were obtained and saved. Meanwhile, 0,5 ml of all NPs and nanocomposites were analysed for characteristic vibrational and stretching bond peaks. The instrument that was used is PerkinElmer FT-IR spectrum Two L1600300 spectrum two LITA, Serial number: 102561.

The sample compartment was cleaned with low concentration alcohol (Isopropanol) and background scan was done to clear noise and interferences. Thereafter, 1 ml of each material was placed on the analysing compartment and the scan was taken sequentially. After few seconds spectrum was obtained and saved.

3.4.8 X-ray diffraction characterization (XRD)

The X-ray diffraction (XRD) studies of the NPs, PGV bentonite and bentonite clay composites was performed by using a Bruker AXS D8 Advance diffractometer with Cu-K α radiation over the scanning range $2\theta = 20^\circ - 90^\circ$ at a voltage of 40 kV and 40 mA. All NPs and clay composites were in typical solid form. Approximately 2 mL of the nanoparticles were dropped on a copper plate and dried.

3.4.9 Scanning electron microscope (SEM)

Scanning electron microscopy (SEM) images were acquired using a Philips-FEI XL30 ESEM-TMP. The powdered samples were first affixed onto adhesive tapes supported on metallic disks and then covered with a thin, electric conductive gold film. Images of metals and bentonite nanocomposite were recorded at different magnifications at an operating voltage of 5.0 kV and 500 μm average particle size range.

3.5 Results and Discussion

Observations during NPs and composite synthesis

The colour changes that were observed for AgNPs, AuNPs and Ag-AuNPs upon addition of trisodium citrate reducing agent changed from colourless solutions to pale yellow, light magenta, and light pink respectively. In contrast, the PGV bentonite solution appeared beige in colour, and Ag-PGV, Au-PGV and Ag-Au-PGV composites colour of solutions after reduction appeared thick brown, salmon pink and thick grey respectively.

3.5.1 UV/Vis spectroscopy

The UV/Vis spectra of the metal NPs is shown in figure 3 (A, B and C). The maximum absorbance wavelength for Ag NPs, Au NPs and Ag-Au NPs were at 436 nm , 512 nm and 414 nm (Ag) and 516 (Au) respectively. The PGV bentonite composites were not examinable using this particular technique as it is only limited to liquid or aqueous solutions and not strong colloidal or suspension solutions.

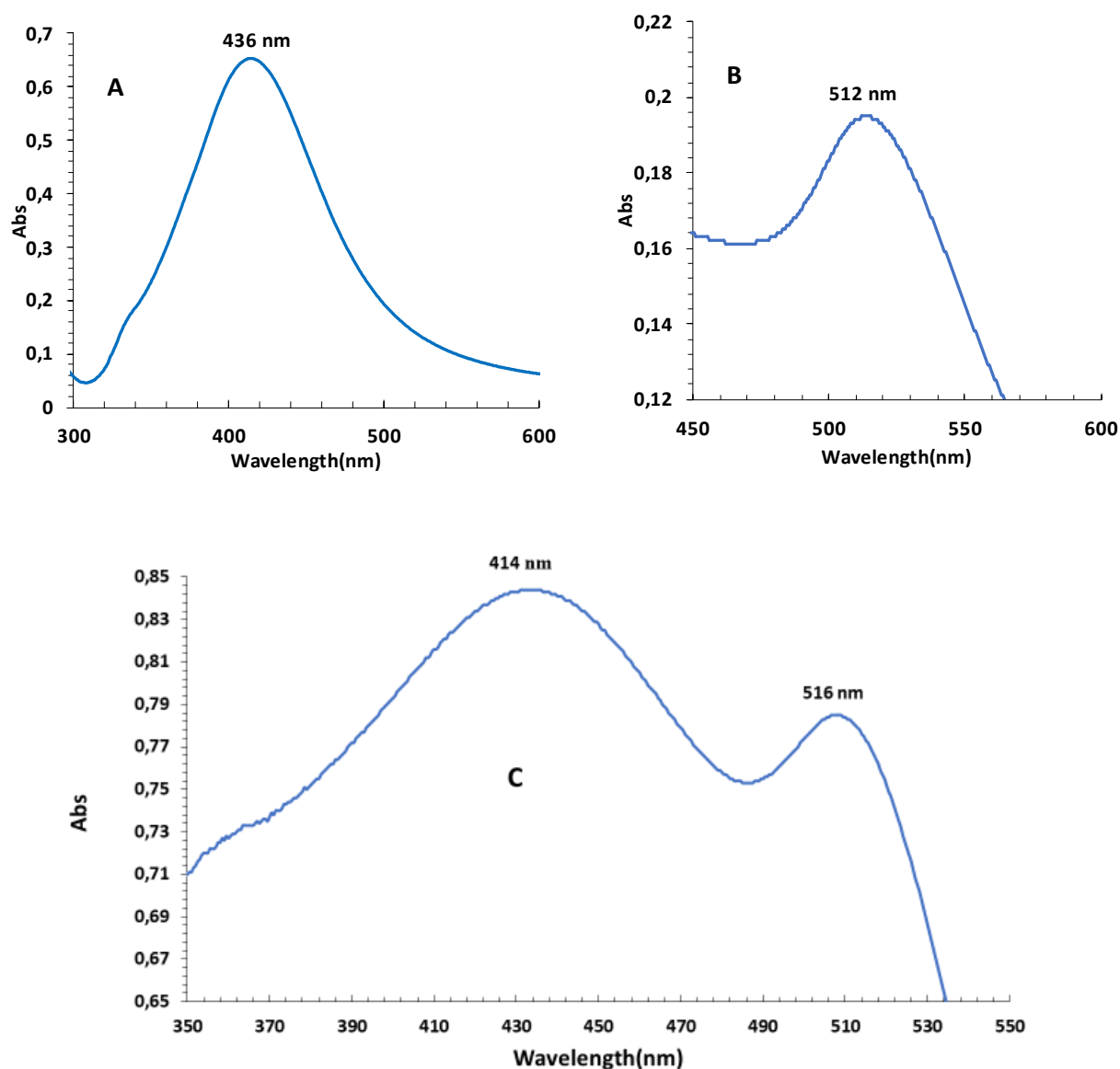


Figure 3-2: UV/Vis spectra of Ag (B), Au (A) and Ag-Au (C) bimetallic NPs.

The peak shape of Ag, as seen in figure 3A is narrow, whilst that of Au was relatively narrow as well. This observation changed as depicted by Ag-Au NPs spectrum, as Ag shape appeared slightly broad and Au shape remained unchanged. This observation was indicative that the size distribution mainly of Ag changed from being relatively small to relatively big, hence the change in the peak shape while Au size distribution was slightly affected hence peak shape was unchanged. This effect was responsible for the clear shift in maximum wavelengths of AgNPs and AuNPs in bimetallic system as AgNPs and AuNPs experienced bathromic and hypsochromic shifts, respectively.

Literature reports that the Ag and Au NPs synthesized via chemical reduction method generally exhibit peak absorbing wavelengths within the range of 450-490 nm for AgNPs and 500-550 nm for AuNPs, respectively (Zhang et.al, 2016). This in the line with what was obtained as respective peak wavelengths of AuNPs and AgNPs appeared to be within ranges suggested by literature. The obtained respective peak wavelengths of Ag and Au within a bimetallic system appeared to be within these reported ranges. According to literature, the peak wavelengths of Au and Ag of Ag-AuNPs are determined particularly by typical formation of Ag-Au cluster. As Ag-Au alloy has reported Ag and Au peak absorption wavelength of 414 nm and 516 nm, respectively (Zhao et.al,2019). This hinted that the typical Ag-Au cluster that was analysed was core-shell alloy which was supported by the similar behaviour of Ag and Au in the bimetallic system analysed as that which was reported particularly for Ag-Au core-shell alloy.

Literature suggests that the general causes of the deviations from peak wavelengths obtained compared to reported wavelengths for monometallic Ag, Au NPs and Ag-AuNPs are due solvent polarity, temperature and pH of the solution analysed (Sahi *et.al*, 2018). However, the data obtained remained consistent with various sources.

3.5.2 Infrared spectroscopy

The FT-IR spectra of AgNPs, AuNPs, Ag-AuNPs and their PGV bentonite composite are presented by figure 3-3. The corresponding table depicting differences in vibrational and stretching wavenumbers of functional groups is displayed below.

As depicted by Ag, Au and Ag-AuNPs spectra the vibrational and stretching frequencies observed were similar for both C=O and OH functional groups. The other notable differences between NPs spectra were the absence of both symmetric and anti-symmetric vibrational bonds

of COO^- for AgNPs and AuNPs, whilst Ag-AuNPs exhibited a symmetric COO^- , which confirmed Ag-AuNPs were better capped by the reducing agent compared to AgNPs and AuNPs, respectively. However, AuNPs and AgNPs were reduced from ionic form to NPs due to $\text{C}=\text{O}$ as has been reported by some studies (Zhang *et.al*, 2016).

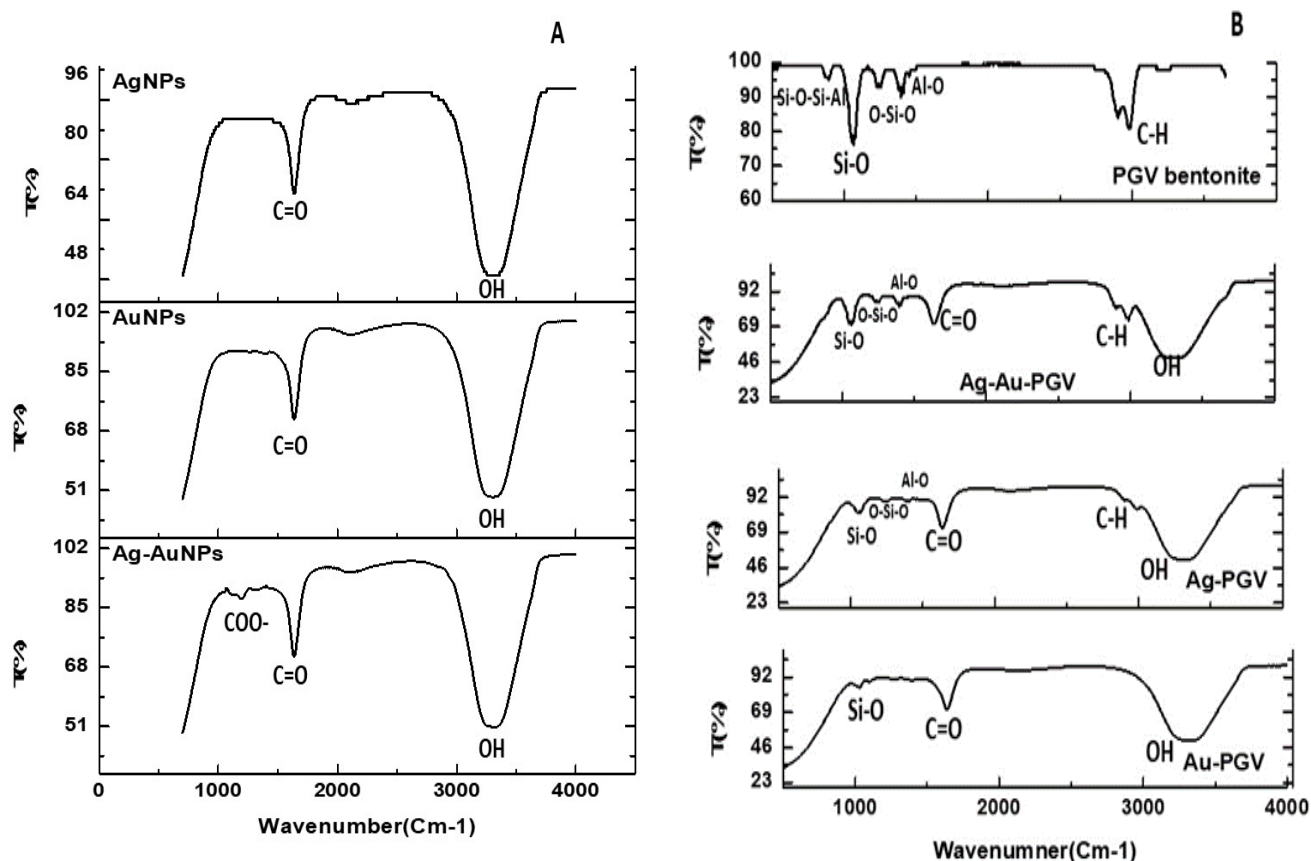


Figure 3-3: Overlaid FT-IR Spectra of metallic NPs films (A) and their respective PGV clay composites (B)

The obtained spectral data; table 3-1 for AgNPs, AuNPs and Ag-Au NPs was largely consistent with several scientific literature as most of spectral peaks exhibited by these NPs were similar to those that had been previously obtained by different of other studies. AgNPs, AuNPs and Ag-AuNPs reported wavenumber ranges for optically active functional groups, where sodium citrate has been used (Zhang *et.al*, 2016).

Table 3-1: Characteristic peak wavelengths ascribed to respective characteristic functional groups. S*(Symmetric) As*(Anti-symmetric)

Nanomaterial	Wavenumber (cm ⁻¹) of Functional groups							
	C=O	OH ⁻	COO ⁻	Si-O	O-Si-O	C-H	Si-O-Si-Al	Al-O
AgNPs	1635	3310	-	-	-	-	-	-
AuNPs	1638	3288	-	-	-	-	-	-
Ag-AuNPs	1636	3302	1346(S)	-	-	-	-	-
PGV bentonite	-	-	-	1095	800	2966	905	1400
Ag-PGV	-	3329	-	1088	820	2902	-	1395
Au-PGV	-	3600	-	1130	-	-	-	-
Ag-Au-PGV	1640	3580	-	1100	1290	2950	-	1410

The PGV bentonite exhibited optical active functional groups and their respective wavenumbers as depicted by the table and spectrum above, which showed the presence of mostly silicates. Iron silicate and magnesium oxide which are amongst the other types of components generally found in bentonite clays was not depicted by the spectrum. Compared to data presented by literature, the silicates found within in bentonite clays are not highly optical active due to the chemical rigidity of clay chemical structures (Reddy *et.al*, 2017). Based on literature, silicates appear within the wavenumber range of 350-900 cm⁻¹, and data obtained was consistent with reported data. However, the difference in wavenumbers of the silicate depicted compared to ones reported by literature is due to preparation methods of clay and pH levels of clay solutions, and the latter is influential in the optical activity of iron silicate, sodium as well as magnesium oxide (Reddy *et.al*,2017).

Some similarity in terms active functional groups for composites compared to AgNPs, AuNPs and Ag-AuNPs films were observed particularly ones due to the activity of Si-O, O-Si-O, C-H and Al-O. However, as depicted by the table and the composites spectra the significant spectral data differences in wavenumbers between these functional groups observed in Ag-PGV, Au-

PGV and Ag-Au-PGV were due to slight differences their synthesis and bentonite clay functionalization.

3.5.3 X-ray diffraction (XRD)

The overlaid XRD patterns depicted below are of Ag, Au and Ag-AuNPs and their respective bentonite clay composites. The XRD patterns observed for Ag,Au and Ag-AuNPs were largely similar due to similarities in plasmonic properties of Au and Ag metals, respectively. Thus, the 2θ diffraction angles obtained were 77.4° , 64.5° , 54.5° , 44.6° , 38.4° , 32.2° , 27.3° and 24.4° . These diffraction angles corresponded to the planes indicated on figure 3-4A. Similar XRD patterns for Ag and Au metals were reported by literature focused on Au and Ag particles XRD patterns in relation to their crystallite sizes (Ogundaraeb *et.al*, 2019).

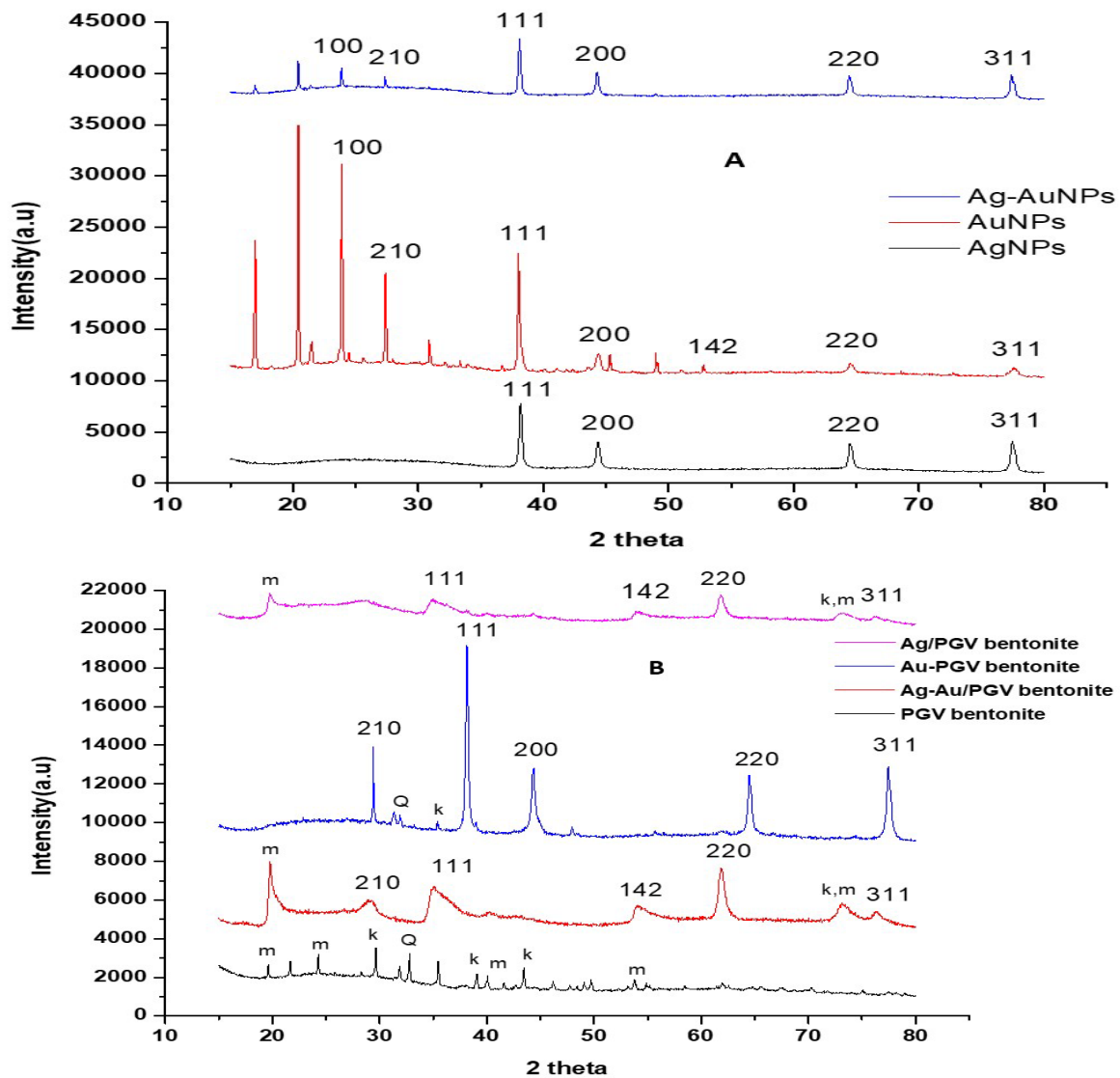


Figure 3-4: An overlay XRD patterns obtained of Ag, Au, Ag-AuNPs (A) and bentonite clay composites (B).

Figure 3-4B exhibiting XRD patterns of clay bentonite composite depicted patterns that were due to Ag, Au and Ag-Au alloy metals, which confirmed the functionalization of bentonite clay. PGV bentonite depicted patterns mainly due to quartz, kaolinites and montmorillonite, which were observed in Ag-PGV bentonite, Au-PGV bentonite and Ag-Au/PGV bentonite clay composites, and recent study reported similar Au-bentonite XRD patterns for determination asernic study (Rastogi *et.al*, 2016).

3.5.4 Scanning electron microscope (SEM)

The SEM images depicted below are that of AgNPs, AuNPs, Ag-AuNPs, PGV bentonite and their respective bentonite composites. The images of metals, particularly the AuNPs and Ag-AuNPs were appeared largely similar with respect to shape and size of particles.

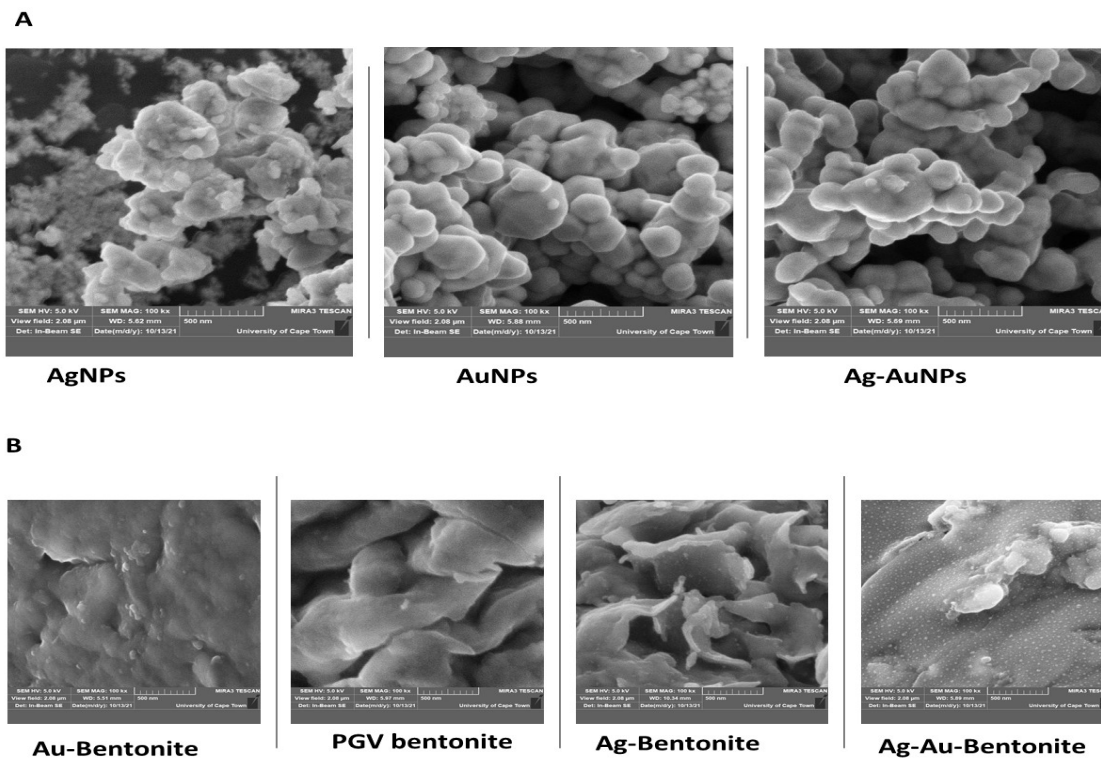


Figure 3-5: SEM data representation of Ag, Au, Ag-AuNPs(A) and bentonite clay composites(B)

AgNPs, AuNPs and Ag-AuNPs depicted crystalline shaped particles which were characteristic of metallic particles. The appearance of particles of AgNPs and AuNPs were very similar, and this was evident in the appearance of particles observed in Ag-AuNPs. AgNPs and AuNPs particles demonstrated least agglomeration compared to Ag-AuNPs, which demonstrated highest agglomeration of particles.

Similar observations have been reported by literature, and agglomeration have been reported to be an advantageous property of bimetallic NPs due to accumulation of particles which form larger clusters thus forming larger particles with increased surface area (Zhao *et.al*, 2018).

In contrast, the effect of PGV bentonite functionalization caused particle size and shape of metal particles to be different compared to metal particles depicted in figure 3-5B. However, slight similarities due to metal particles were observed in composites which confirmed successful functionalization of PGV bentonite. Particles of the composites were bigger in size compared to metal particles due to combinational mass effect caused by PGV bentonite which has relative bigger particles compared to metal particles.

3.5.5 Electrochemical studies

The CVs of the monometallic AgNPs, AuNPs, Ag-Au NPs characterized are presented below by figure 3-6. These voltammograms confirmed electrochemical activity of the monometallic, depicted by redox couples of Ag/Ag⁺ and Au/Au³⁺ respectively.

The chemical half reactions taking place are depicted on relevant voltammograms presented by figure 3-6A and 3-6B and at corresponding peak potentials and peak currents. The corresponding oxidation/reduction peak potential and their respective peak currents that were exhibited by the Ag⁺ and Au³⁺ species are depicted by the table 3.2 below

From figure 3-6C depicting the Ag-Au NPs at a potential range of -0,5 and 1,5V. Similar redox couples peak potentials for both Ag and Au were observed. However, there were slight observable peak potentials differences. The Ag peak potentials (**a** and **a'**) signifying the Ag⁺/Ag redox couples shifted potentials compared to those depicted by figure 3-6A. The oxidation peak (**a**) experienced a very slight potential shift, whilst corresponding reduction

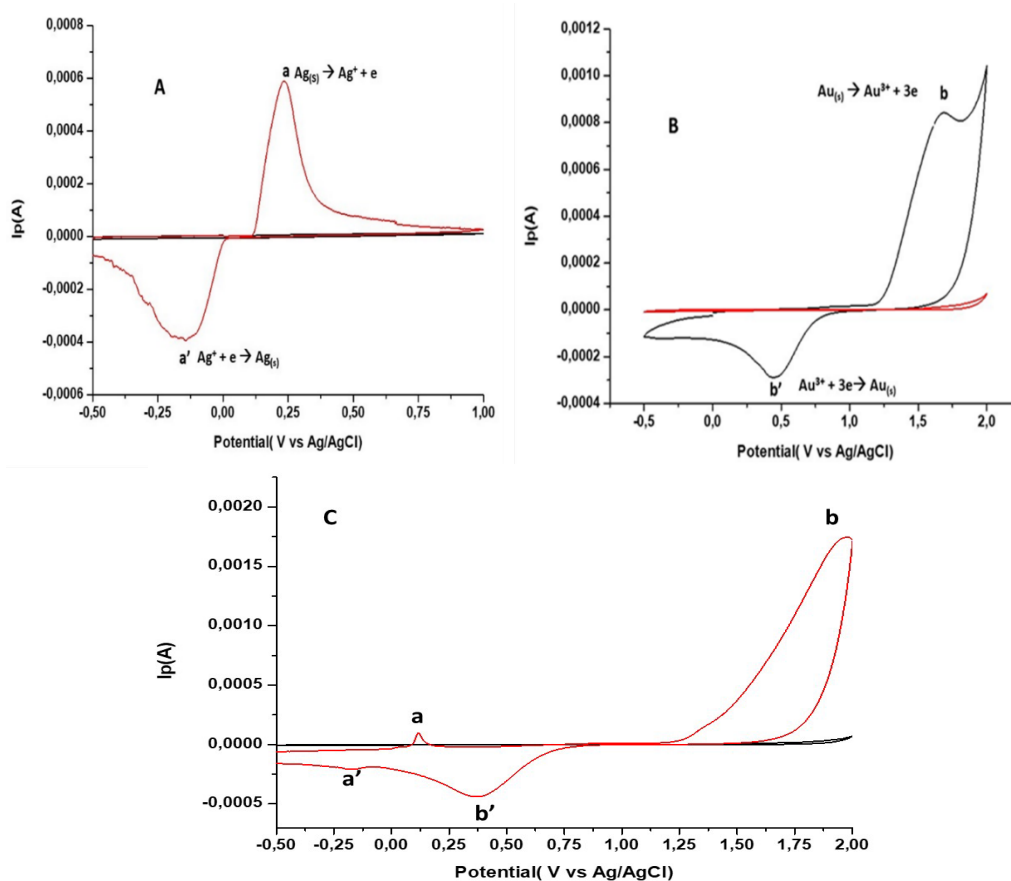


Figure 3-6: Voltammograms of AgNPs(A), AuNPs(B), Ag-Au NPs(C)

peak (**a'**) showed a significant positive shift. The Au peak potentials labelled **b** and **b'** referring to Au^{3+}/Au redox couple, showed a significant potential shift. The oxidation peak potential showed a negative shift whilst the corresponding reduction potential showed a positive potential shift. In addition, the peak currents corresponding to the observed redox couple peak potentials of AgNPs and AuNPs appeared to be higher than those observed for respective metals in the bimetallic system as shown in the table below.

Table 3-2: Electrochemical properties exhibited by NPs

Type of NPs	Ip _c (10 ⁻⁴)	Ipa (10 ⁻⁴)	Ip _c /Ipa	E _p c(V)	E _p a(V)	ΔE _p (mV)
AgNPs	2,20	3,90	0,56	-0,23	0,29	70
AuNPs	2,80	8,50	0,33	0,48	1,58	1100
Au-Ag NPs	0,21 0,13	0,22 0,21	0,97(Ag), 0,64(Au)	0,12 0,94	0,27 1,16	150(Ag), 220(Au)

The electrochemical activity depicted by both AgNPs and AuNPs voltammograms was consistent with various source of literature as the peak potentials at which redox couple activity was observed was within the reported potential range for these active species. The causes of these potential deviations are attributed to differences in types and concentrations of supporting electrolyte used, which also directly affects the pH of the supporting electrolyte (Heakal *et.al*,2018). In addition, according to literature, some potential deviations have been ascribed to different types of reference electrode used, and concentration of chloride ion solution in certain electrochemical reference electrode systems (Aoki *et.al*, 2018).

The difference in peak potentials observed for Ag^+/Ag and Au^{3+}/Au redox couples in monometallic NPs compared to peak potentials observed in Ag-Au bimetallic system is due to cross-hybridization of Ag and Au metals, which brought about electrochemical overlap in overall properties of Ag-Au NPs. In addition, the peak potential shifts observed from these metallic NPs is dependent upon the arrangement of the formed alloy between metals. Thus, the atomic differences between Ag and Au lead to the interstitial formation of this typical alloy, where Au because of the atomic size was the core and the Ag particles formed the shell as they migrated into interstices around the core (Hamidi *et.al*, 2018).

As depicted by table 3-2 it is observed that the peak currents ratio of the Ag/Ag^+ appeared to have deviated from unity (1), which according to Nernstian suggests that it has to occur for electrochemically reversible reactions governed by one electron transfer process (Refer to table 3-2), whilst for AuNPs the ratio appeared to have deviated from 1 more due to a much complex electron transfer process involving three electrons, which Nernst does not account for (Milinska *et.al*, 2019).

However, for Ag-AuNPs the peak ratios for both Ag^+ and Au^{3+} appeared to be closer 1, particularly Ag^+ which confirmed the Nernstian postulation on electrochemical reversible reactions governed by electron transfer processes involving only one electron. Meanwhile, Au^{3+} peak ratio was improved by enhancement of electrochemical properties brought by Ag^+ in the Ag-Au core-shell bimetallic system.

This deviation from unity is also proven by peak -to-peak separation (ΔE_p) values for all NPs which appeared to be greater than 59 mv/0,059 V particularly for reactions that are governed

by electron transfer processes involving one electron, thus Au^{+3} had the greatest separation due to three electron, meanwhile significant reduction in ΔE_p for Ag-Au is ascribed

The electron-transfer process governing particularly AuNPs and AgNPs are semi-infinite diffusion due to significant deviations from ΔE_p 0,059V which remains constant if there is at least switching potential of 0,09V upon E_p obtained for an electrochemical reaction. However, the electrochemical reversibility of indicated mainly by peak ratios indicated that all platforms were electrochemically reversible, although AuNPs did not appear to satisfy Nernstian postulation on electrochemical reversible reactions because it involved three electrons (Milinska *et.al*,2019).

The characterization of the composites was carried out precisely for comparative studies against the Ag, Au and Ag-Au NPs, by so doing the effect caused by the PGV bentonite clay modification was observed, and it is shown by the voltammograms contained in figure 3-7 below.

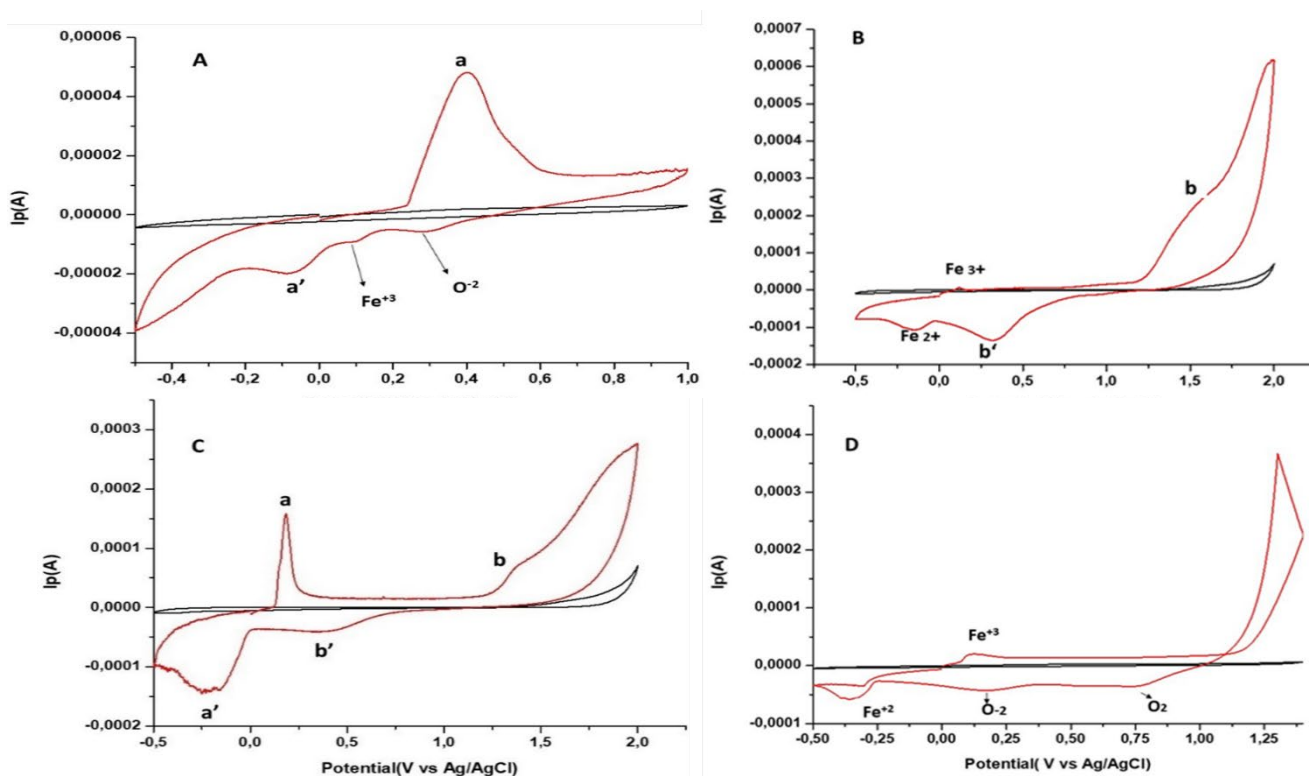


Figure 3-7: Voltammograms of Ag-PGV(A), Au-PGV(B), Ag-Au-PGV(C) and PGV(D)

The effect caused by PGV bentonite was evident, as Ag-PGV and Au-PGV peak current intensities slightly decreased compared to AgNPs and AuNPs as shown by the table below.

Ag-PGV composite exhibited oxidation/reduction peak potentials of differed from those seen for AgNPs, the the oxidation peak potential which was slightly higher than that observed for AgNPs whilst reduction peak potential was significantly lower. The same effect was observed for Au-PGV compared to AuNPs as depicted by the difference in values showed by table 3-2 and 3-3 respectively.

The Ag-Au-PGV composite depicted significantly enhanced peak currents of Ag^+ and Au^{3+} compared to Ag^+ and Au^{3+} peak currents in the Ag-Au bimetallic system as also the oxidation/reduction peak potentials of Ag^+ and Au^{3+} in Ag-Au-PGV composite depicted which were significantly different from those observed for same ions in the Ag-AuNPs as shown by the table below.

Therefore, the PGV bentonite clay functionalization caused the peak potentials deviation and enhanced peak currents from those observed from monometallic Ag, Au and indeed Ag-Au NPs respectively. This was due to the additional electrochemical properties induced by electroactive facets of the PGV bentonite which include ferrous ions other potentially interactive silicates/oxides. In addition, the effect of this was evident in Au-PGV, where oxidation potential peak was recessive, and based on literature the Au displaces the iron which is electrochemically insulated within the clay hindered by silicates and oxides (Gorski *et.al*,2012). This occurred because Au is highly unreactive, thus even more so in electrochemically insulating environment. Thus, the displaced iron is enabled to electrochemically interact with the surroundings, which resulted in $\text{Fe}^{2+}/\text{Fe}^{3+}$ redox couple potential peaks seen in figure 3-7B (Bridge *et.al*,2004).

The causes of the potential peaks observed in PGV bentonite, are due to some electrochemical species, most notably ferrous ions. According to literature, PGV bentonite contains at least three species, one which is electroactive active whilst some have a great potential to be electrochemically active. These have been found to be mostly silicates (MgO , SiO_2 , Al_2O_3 etc.) with ferrous ions concentration being the most electrochemical reactive of them all, thus the potential peak depicted by the voltammogram in figure 3-7D is due to $\text{Fe}^{2+}/\text{Fe}^{3+}$ redox couple (Gorski *et.al*,2012). However, some reported peak potentials of $\text{Fe}^{2+}/\text{Fe}^{3+}$ redox couple from different salts like iron sulphates and ferricyanide complexes are seen at slightly higher peak potentials (Bridge *et.al*,2004). In addition, the additional reduction peak potential observed could be ascribed to oxide stripping(0,39V) and oxygen reduction(0,95V) respectively (Li *et.al*,2020), for which the potentials also depend on fore mentioned conditions.

Table 3-3: Electrochemical properties exhibited by NPs and PGV bentonite based on Nernstian theory on electron-transfer process.

Types of NPs	I _{pc} (10 ⁻⁴)	I _{pa} (10 ⁻⁴)	I _{pc} /I _{pa}	E _{pc}	E _{pa}	ΔE _p (mV)
PGV	0,20	0,55	2,75	-0,15	0,12	270
Ag-PGV	0,98	0,45	0,44	-0,06	0,35	410
Au-PGV	1,25	2,40	0,52	0,35	1,45	1100
Ag-Au-PGV	1,50	1,60	0,94(Ag),	-0,20	0,19	390(Ag),
	0,39	0,67	0,58(Au)	0,42	1,37	950(Au)

In comparison to AgNPs, AuNPs and Ag-Au NPs electrochemical activities and properties discussed, the table below represent the data used to demonstrate the effect of clay functionalization of the NPs electrochemical activities and properties that they had exhibited. The peak ratios of these composites depicted showed a great effect caused by clay functionalization as the ratios were higher than that of AgNPs, AuNPs and Ag-AuNPs, which satisfied Nernstian postulation particularly for electrochemical reactions involving one electron.

In addition, the peak-to-peak separation (ΔE_p) depicted by the table, represented the deviations from 1, and in comparison, Ag, Au and Ag-Au NPs the magnitude of these values was relatively bigger. The potential cause for this is due to clay electrochemical activity which induced additional electrons in each electrochemical system for each composite affecting the electrochemical reversibility and electron-transfer processes (Milinska *et.al*,2019). According to literature, the ΔE_p would ideally produce a 0,059V constant value if 0,09V switching potential is applied upon E_p of the electrochemical reaction thus because of the deviations observed meant that the electron-process governing the electrochemical reactions of the composites is deemed as being semi- infinite diffusion process as was for Ag, Au, Ag-Au NPs, whilst the electrochemical reversibility of the reactions remained unchanged (Milinska *et.al*,2019).

Determination of electrochemical electron-transfer processes involved for Ag, Au, Ag-Ag and their composites.

The electrochemical reactions for NPs and composites films depicted figures 3-6 and 3-7 are governed by distinctly different electrochemical mechanisms. For AgNPs and AuNPs typical electrochemical mechanism expression is depicted below, denoted by an E.



In contrast, Ag-Au NPs electrochemical mechanism much more complex than those depicted for AgNPs and AuNPs, respectively. The Ag-Au NPs electrochemical mechanism accounts for both Ag and Au NPs in the same electrochemical instance. The expression for such is denoted by EE and is depicted below.



Through observation, composites demonstrated similar chemical reversibility as was observed for Ag, Au and Ag-Au NPs as the voltammograms depicted by figure 3-6. Thus, this proved that clay functionalization did not significantly deter the electrochemical behaviour of these NPs. Moreover, these chemical expressions suggested that the reactions are chemically reversible, which is also confirmed by voltammograms and corresponding electrochemical equations. Meanwhile, the PGV bentonite exhibited a similar electrochemical mechanism, which depicted Fe^{2+}/Fe^{3+} as being chemically reversible. In addition, although this expression did not determine the electrochemical reversibility of the reactions, but it did highlight and hint at the typical degree of reversibility of the reactions.

To confirm the electrochemical reversibility of these NPs, the theory of Matsuda, Aybe and Nicholson who introduce dimensionless parameter(A), and the relation between standard rate constant K_0 and mass transport (M_{trans}) one can obtain and estimate the transition between reversible and irreversible electrochemical reactions or determine the electron-transfer mechanism (Aristov,2015). This equation can be mathematically manipulated to determine any

of the variables contained, thus these can be used and compared with standard values in determining the electron-transfer process.

$$\Lambda = \frac{K_0}{m_{trans} \times (n \times \pi \times F \times D \times v)} / (R \times T)^{1/2} = \frac{K_0}{(0,035v)^{1/2}} \quad \text{Eq.3.7}$$

$$\Lambda = \frac{\Delta E p}{mv} \quad \text{Eq.3.8}$$

For AgNPs: For AgNPs: $\Lambda = \frac{300 - (-,210)}{50} = 10,20$

$$K_0 = \Lambda \times (0,035v^{1/2})$$

$$K_0 = 10,20 \times (0,035(0,05)^{1/2}) = 0,079$$

Table 3-4: An exhibition of dimensionless parameter(Λ) and standard rate(K_0) for all NPs and PGV bentonite composites based on Nicholson theory on electron-transfer process.

Type of NPs/ composites	Λ	K_0 (cm/s)
AgNPs	10,20	0,08
AuNPs	22,00	0,17
Au-Ag NPs	3,00(Ag), 4,40(Au)	0,02(Ag), 0,03(Au)
PGV	5,40	0,04
Ag-PGV	8,2	0,06
Au-PGV	22	0,17
Au-Ag PGV	7,80(Ag), 19(Au)	0,06(Ag), 0,15(Au)

According to such a theory, the electron-transfer process is confirmed, and is determined by the variables presented by the table above. The AuNPs and AgNPs electron-transfer processes which was depicted by respective electrochemical mechanisms which demonstrated chemical reversibility. The electrochemical reversibility shown by Au and Ag redox couple is further proved by magnitude of Λ and K_0 respectively. As shown by the table, both Λ values of Ag

and Au monometallic were significantly higher than 10 with, which is the threshold that is suggested by the Nicholson postulated mathematical expression, $\Lambda > 10$.

In addition, the K_0 which is the standard rate constant was determined after the deduction of dimensionless parameters for respective Ag and Au electron-transfer processes. The data exhibited by the table showed that both Ag and Au NPs exhibited values which were almost equal by AuNPs being slightly higher, potentially due to number of electrons involved during the transfer process compared to AgNPs. However, for both monometallic NPs, K_0 were also higher than the Nicholson postulated mathematical expression, $K_0 > 0,035v^{1/2}$. This affirmed that the chemical reversibility of AgNPs and AuNPs redox couples were indeed also electrochemically reversible. These results confirmed the electrochemical reversibility of both platforms as was initially suggested or hinted by their electrochemical mechanism.

Contrary, the bimetallic Ag-Au NPs, Λ and K_0 reported for both monometallic NPs within a bimetallic system decreased notably, with both Λ values obtained lower than 10 whilst values of K_0 remained relatively within threshold set by $K_0 > 0,035v^{1/2}$. These findings confirmed that the monometallic NPs had maintained their electrochemical reversibility within a bimetallic system. However, the notable decrease in Λ values obtained for each monometallic NPs, could ascribed to the hybridization of electrochemical properties, and typical formation of bimetallic NPs which effected the overall electrochemical activity of each monometallic NPs.

Furthermore, the presumed electrochemical reversibility of all the composites was maintained and proved mainly by magnitude of Λ and K_0 respectively as was done for AgNPs, AuNPs and Ag-AuNPs. In comparison with AgNPs, AuNPs and Ag-Au NPs, the Λ values of Ag-PGV and Au-PGV were satisfactory ($\Lambda > 10$), however AgNPs values experienced a slight decrease.

Ag-Au-PGV composite showed the Λ value for Au^{3+} to be increased significantly compared to Λ of Au^{3+} within Ag-Au NPs system, whilst Λ for Ag^+ of the composite was relatively bigger than that Ag-AuNPs bimetallic system.

In addition, the value of K_0 , which was also determined after the deduction of the dimensionless parameters for respective Ag-PGV, Au-PGV and Ag-Au- PGV electron-transfer processes. The data exhibited by the table above showed that both Ag^+ and Au^{3+} of a composite showed higher values than Ag-Au bimetallic system. Furthermore, Ag-PGV and Au-PGV composites expressed significantly higher K_0 values than both Ag^+ and Au^{3+} from monometallic NPs as well as an alloy in Ag-AuNPs system. This affirmed that the chemical reversibility of Ag and

Au redox couples were indeed also electrochemically reversible and were not affected by PGV bentonite functionalization; rather, they were enhanced electrochemically.

Effect of scan rates on peak currents, potentials, and electrochemical reversibility/electron transfer processes of NPs

The investigation of varying scan rates on current peak densities, potentials, as well as electron-transfer processes was done. The voltametric data depicting that data is shown below by figure 3-8 for Ag, Au and Ag-Au NPs.

Based on observations depicted by figure 3-5, peak potential and current shifts changed as scan rates increased; this observation was consistent for all NPs. For AgNPs and AuNPs, the anodic potential (E_{pa}) shifted slightly positive as the scan rates increased, whilst the cathodic potential (E_{pc}) shifted slightly negative as the scan rate increased. In addition, the peak currents for both platforms increased linearly with the increasing scan rates.

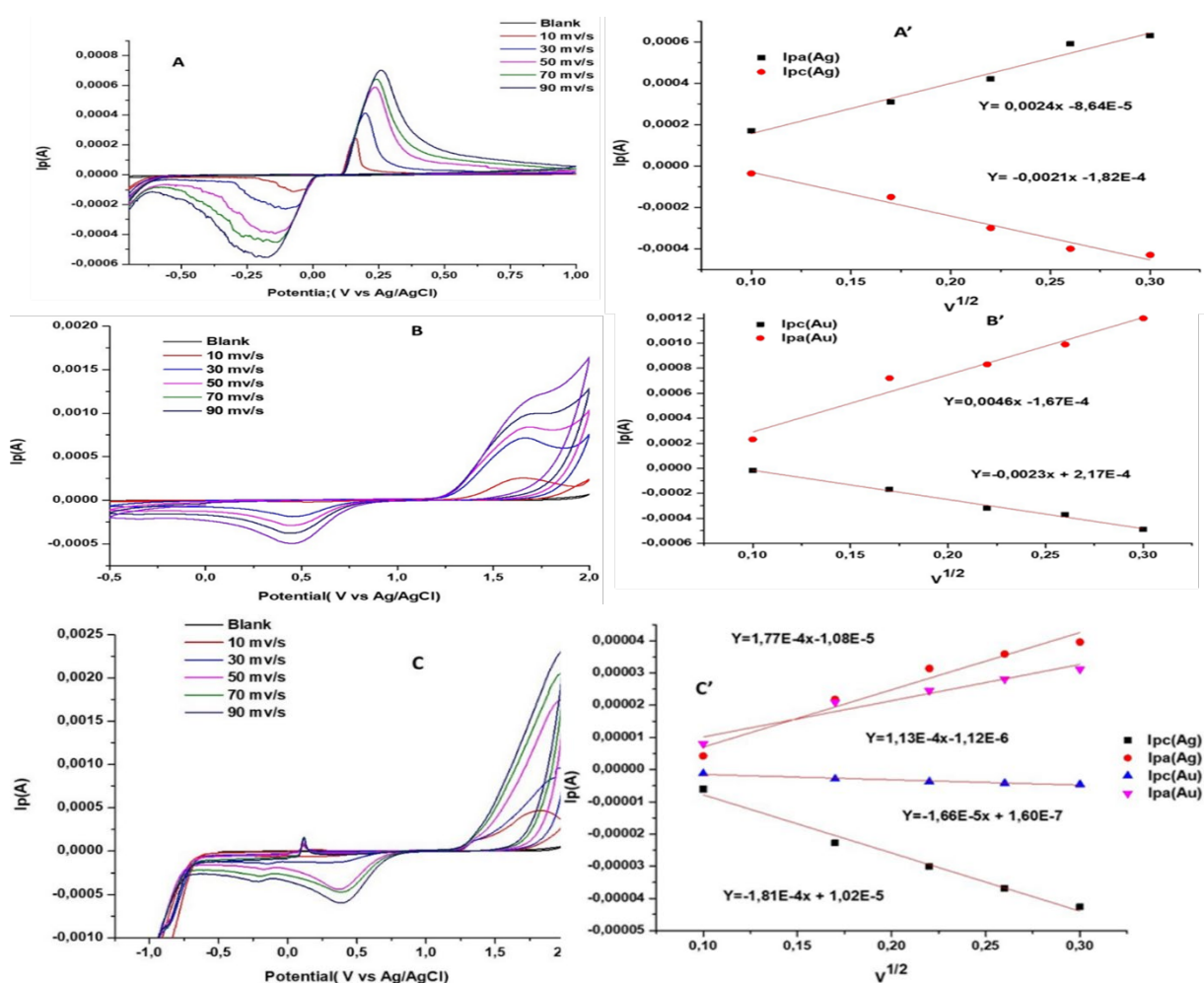


Figure 3-8: Voltammograms and linear dependence plots of AgNPs(A&A'), AuNPs(B&B') and Ag-AuNPs(C&C')

Based on literature, the peak potential shifts that were observed were due to reduction in diffusion layer between electroactive species and GCE interface. This phenomenon meant that the potential at which the metallic NPs and composites alike oxidized/reduced changed correspondingly as more ions of NPs and composites were getting closer to the interface due to the reduction of diffusing of the layer (Chanfreau et.al,2007). Thus, across all NPs and composites that were examined, the greatest effects were observed at the scan rate of 90 mV/s.

The electrochemical reversibility of the chemical reactions responsible for peak potentials is demonstrated by the minute or no changes in peak potentials upon changes in scan rates (Aristov, 2015). Thus, the observations depicted for monometallic and bimetallic NPs proved that the scan rates did not affect the electrochemical reversibility of the chemical reactions involved. The changes in increasing peak currents are due to faster diffusion of electroactive species to and from the electrode interface, whilst the other part of it is largely non-faradaic but is induced incrementally to the whole electrochemical system from increasing scan rates (Elgrishi,2018)

The dependence plots of $I_p(A)$ vs $V^{1/2}$ for NPs were done to examine the changes caused kinetically by the increasing scan rate on typical electron-transfer processes that were initially exhibited by Ag, Au and Ag-Au NPs. As such, the $I_p(A)$ vs $V^{1/2}$ slopes (I_{pc} and I_{pa}) were lower than 0,5 which demonstrated that the typical electron-transfer process that all NPs exhibited was diffusion-controlled to and from the electrode interface even after the electrochemical systems were subjected to increasing of scan rates.

The effect of varying scan rates on composites was studied comparatively against Ag, Au and Ag-Au NPs to mainly monitor changes in peak potential, currents and electron-transfer processes and or electrochemical reversibility of chemical reactions relative to varying changes of scan rates. Thus, the figure below represents the voltammograms of Ag-PGV, Au-PGV and Ag-Au-PGV composites at various scan rates. Correspondingly, the electron transfer and electrochemical reversibility studies are reflected by data plots adjacent to each respective voltammogram of each composite.

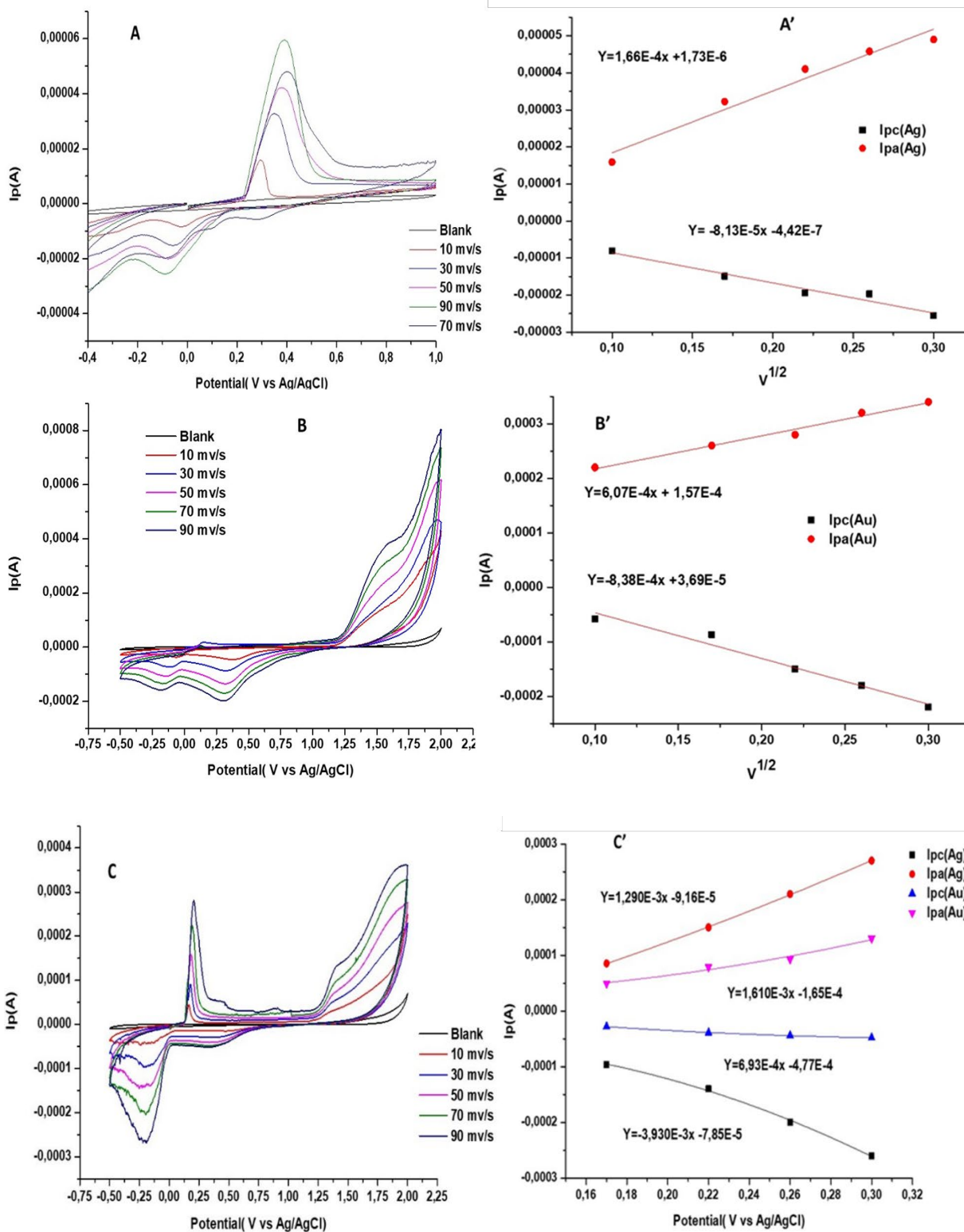


Figure 3-9: Voltammograms and linear dependence plots of Au-PGV(A&A'), Ag-PGV(B&B') and Ag-Au-PGV(C&C')

Ag-PGV composite, similar to AgNPs increasing scan rates caused increasing peak intensities, whilst the potential shifts were slightly affected. This observation concluded that the scan rates

only had maximum effect on peak intensities and minimal for potential shifts. Meanwhile, Au-PGV depicted similar effect caused by varying of scan rates, as the peak currents of both Au^{3+} and $\text{Fe}^{2+}/\text{Fe}^{3+}$ had increased proportionally with increasing scan rates, although Epa of Au-PGV were significantly affected by the varying of scan rates compared to AuNPs, this is depicted clearly by their voltammograms as seen in figure 3-9B and 3-9A respectively.

The Au-PGV voltammogram depicted similar peak potentials that were observed for PGV bentonite clay, and this concluded that PGV bentonite clay $\text{Fe}^{2+}/\text{Fe}^{3+}$ component which was electroactive was visibly prominent and compared to Ag-PGV. This ferrous redox couple demonstrated similar behaviour as Au^{3+}/Au couple upon changes in the scan rates.

Ag-Au-PGV behaviour at various scan rates demonstrated similar electrochemical behaviour to that of Ag-AuNPs. As the peak potentials of both Ag^+ and Au^{3+} within the composite was slightly affected by scan rates, however the peak currents of both redox couples continued to increase linearly with varying of scan rates.

The effect of varying scan rates on the composites was demonstrated through their linear dependence plots for their electron-transfer processes and electrochemical reversibility, which reported insignificant difference from those which were obtained for Ag, Au and Ag-Au NPs.

As Ag-PGV and Au-PGV both confirmed unchanged electron- transfer processes, which was diffusion controlled due to their $\text{Ip}(\text{A})$ vs V slopes that were below 0,5, and the electrochemical reversibility of these composites indicated by the degree of correlation between $\text{Ip}(\text{A})$ vs $V^{1/2}$ indicated sufficient electrochemical reversibility of active redox couples, although the correlation factor of both AgNPs and AuNPs were slightly higher than those of Ag-PGV and Au-PGV as depicted by R^2 values shown in table 3.9. This fact could be ascribed to PGV bentonite functionalization, which induced electrochemical complexities on AgNPs and AuNPs respectively.

The effects on electron-transfer process and electrochemical reversibility that were observed for Ag-Au-PGV were similar to that observed for Ag-Au NPs although there were differences in the respective slopes observed. The slopes observed from the $\text{Ip}(\text{A})$ vs $V^{1/2}$ plots for Ag-Au-PGV were all below 0,5, which demonstrated that the electron transfer mode of transportation to and from electrode interface was diffusion-controlled. The correlation factor values of Ag-Au-PGV were all close to unity as was the case for Ag-Au, which demonstrated the electrochemical reversibility of redox couples was maintained.

Determination of electroactive surface area, electrochemical properties and kinetic parameters of AgNPs, AuNPs, Ag-AuNPs and their composites

The surface area can be determined mathematically using Randles-Sevcik (Eq 3-4). The electroactive surface area for AgNPs was determined below, and all the other electroactive active surfaces involving all NPs and composites were determined in a similar method. Moreover, the I_p value that was used in each case was that which was obtained from scan rate of 90 mV/s, as it was the one that showed both higher electrochemical reversibility and increased peak intensities.

$$3,90 \times 10^{-4} = \frac{(0,65)^2 \times (96,850)^2}{4(8,314)(298)} \times (0,07) \times (0,09) \times \Gamma$$

$$\Gamma = 0,06 \text{ cm}^2 \text{ for AgNPs}$$

Table 3-5: Presentation of obtained Randles-Sevcik properties for all NPs and PGV composites

Type of NPs	n	D (cm ² /s) x 10 ⁻¹⁰	Γ (cm ²)	R ² (average)
AgNPs	1	44,5	0,06	0,98
AuNPs	2	8,10	0,01	0,98
Ag-Au NPs	1(Ag), 2(Au)	187	0,07	0,97
Ag/PGV	1	2210	0,12	0,96
Au/PGV	2	27600	0,90	0,98
Ag-Au/PGV	1(Ag),2(Au)	2290	2,16	0,97

Therefore, the tabulated results present a summary of Randles properties and variables of the data obtained for both NPs and their respective composites. The diffusion coefficient(D) obtained from $I_p(A)$ vs $V^{1/2}$ slope of NPs were significantly higher than that of those of shown by composites. This suggested that the NPs diffuse from and to the electrode interface faster from higher concentration bulk solution towards GCE interface compared to composites (Bucker *et.al*,2018).

Some of the reason that may have affected the differences in D between NPs and composites as reflected by the table above include, but not limited to temperature and solvent density. The temperature, according to literature controls particles movement, as it is known that higher temperatures effect fast particle movement while lower impose slower particle movement (Manhoudi *et.al*,2019). In addition, composites and NPs were not necessarily analysed on the same day, thus the temperature may have been different in the solvent, which affected the solvent density as well resulting in apparent differences in D values between composites and NPs.

The table also depicted differences in active surfaces areas or surface coverage(A), AgNPs depicted the highest surface area of all NPs and the composites. In contrast, Ag-Au-PGV composite showed the highest surface coverage of all composites. Based on data presented by the table, D of NPs was higher thus higher concentrations of these NPs were able to sufficiently be reduced at the surface of the electrode. Thus, the surface coverages of these NPs appeared to be higher than the composites. However, Ag-Au-PGV appeared to have relatively higher D than some NPs and composites, thus exhibited high surface coverage.

The literature suggested that causes that affect the changes in the electroactive areas are particle size, shape and diffusion coefficient (Bucker *et.al*,2018). Based on current data, D may have influenced the electroactive area particularly that of Ag-AuNPs compared to both Ag and AuNPs, which were higher and thus higher corresponding electroactive areas of Ag and Au NPs respectively (Chanfreau *et.al*,2007). The effect of particle size has been seen as a catalyst in the discussion of electroactive areas. Thus, although the concentrations of these NPs were mostly equal or symmetrical in the case of Ag-AuNPs. The particles sizes and shapes of formed NPs were not necessarily similar. Thus, based on the data presented, AgNPs particle sizes were larger than AuNPs and Ag-AuNPs hence higher electroactive areas as was the case for Ag-Au-PGV compared to both Ag-PGV and Au-PGV respectively.

Electron-transfer kinetic parameters

To deduce the kinetic parameters, such as electron transfer coefficient and the heterogeneous electron transfer rate. Confirmation of the kinetic influence on the overall electrochemical response of Ag, Au, Ag-Au NPs and their respective composites were obtained by application

of the Nicholson Shain method derived from laviron's equation, where k_s is the apparent rate of electron transfer, R is the standard gas constant, T is temperature, F is Faraday's constant, D is the rate of diffusion as determined using, and ΔE_p is the difference in value of the E_{pa} and E_{pc} , taken at various values of v . The equation below used to deduce the electron rate constants of NPs and composites forementioned. In addition, based on laviron's postulations $n\alpha$ is derived from E_p vs $\ln v$ slope, whilst K_s can be derived from the intercept

$$\log_{10}K_s (\sqrt{\frac{RT}{nFvD}}) = 0,294(\frac{nF}{RT}\Delta E_p - 2,218)^{-1} - 0,0803 - 0,108(\frac{nF}{RT}\Delta E_p - 2,218) \text{ Eq. 3-5}$$

$$\log_{10}K_s \frac{2,16}{11,65}$$

$$K_s = -\log(0,1854) = 0,732 \text{ Ag-PGV}$$

$$K_s = 1,79(\text{Ag} + \text{Au}) \text{ Ag-Au PGV}$$

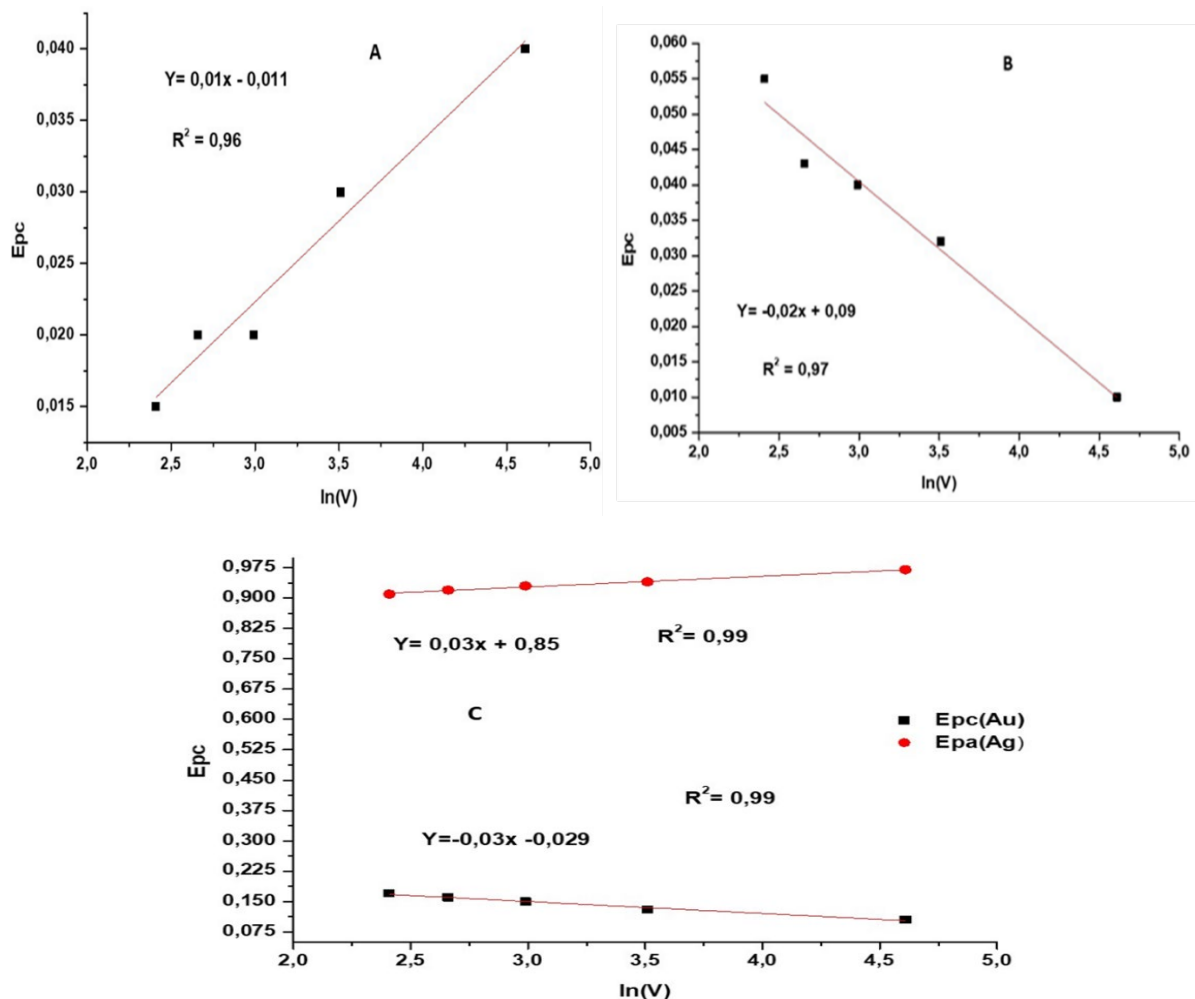


Figure 3-9: Electron transfer coefficient plot, AgNPs (A) and AuNPs (B) Ag-AuNP

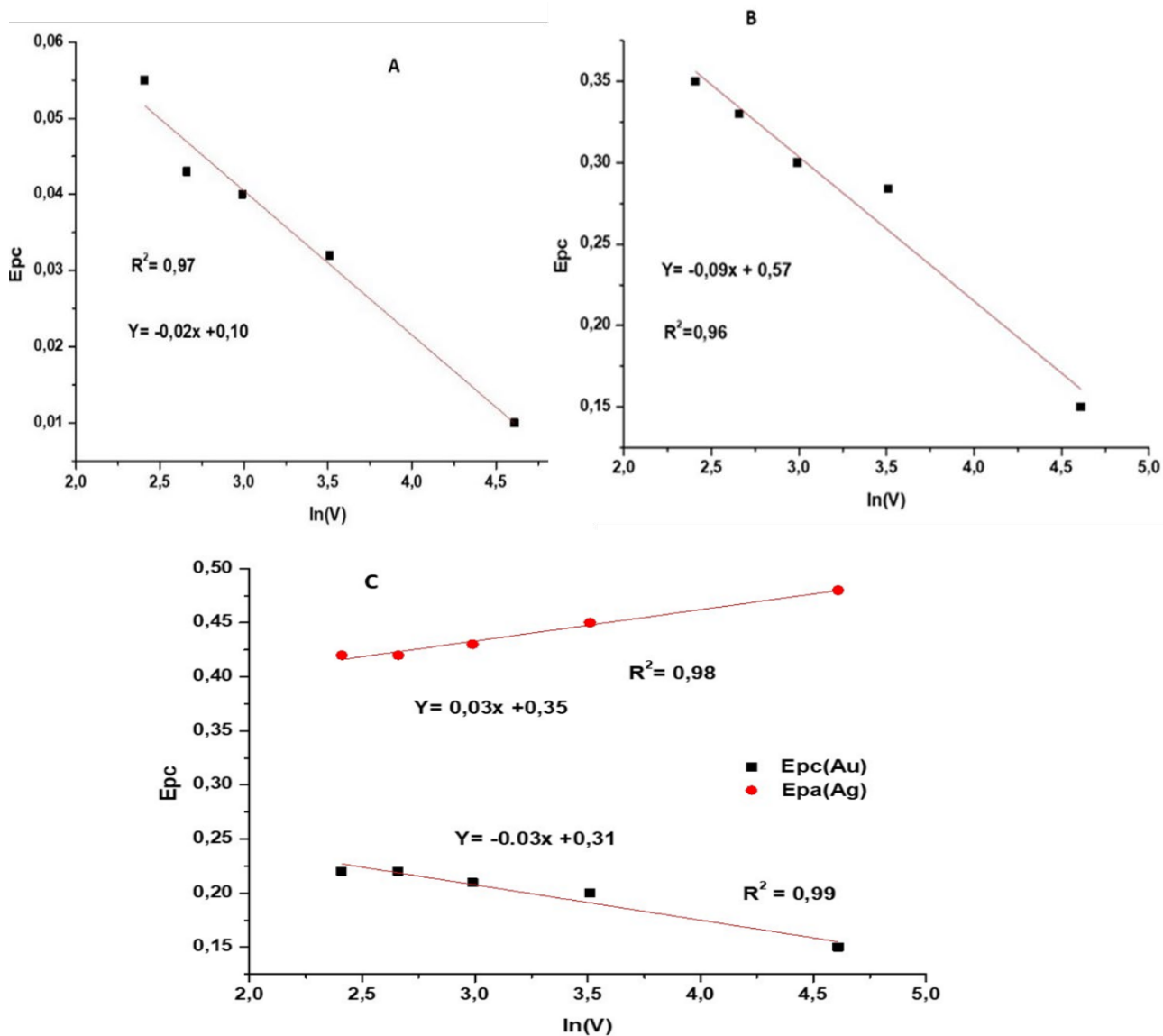


Figure 3-10: Electron transfer coefficient plot, Ag-PGV(A) and Au-PGV(B) Ag-Au-PGV(C)

Table 3-6: Electron transfer-rate constant and electron-transfer coefficient obtained through Shain Nicholson and Lavirons equation and plot for all NPs and PGV composites

Types of NPs	K_s	αn
Ag	0,68	0,01
Au	0,01	0,06
Ag-Au	1,31	0,09
Ag-PGV	0,94	0,02
Au-PGV	0,06	0,08
Ag-Au-PGV	1,79	0,07

The rate constant thus gave an indication of the speed of electron transfer between Ag and Au ions relative to electrode interface and thus the overall nanocomposite electron rate constant capacity (Homna et.al,2015). The data obtained using an equation above indicated that the nanocomposites were superior to NPs based on the magnitude of K_s . This was because the exchange of electrons between interface of and composites was greatly increased by clay functionalization, which increased electron circulation within the electrochemical system.

The total transfer rate constant of bimetallic was the summation of both Ag^+ and Au^{3+} rate constants, which exhibited a considerably increase in transfer rate constant of a bimetallic NPs compared to monometallic NPs as shown the table 3.10, whilst the transfer rate constant of AgNPs was significantly greater than that of AuNPs which that the due to the difference in transfer of electrons involved, Ag transfer single electron whilst Au transfers three, which is more complex.

Furthermore, the individual electron coefficients (αn) of Ag, Au, Ag-Au NPs and composites are indicated by the slopes in figure 3.7 & 3.8 respectively. Based on data depicted table 3.10, Au NPs and Au composites showed greater electron coefficient compared to AgNPs and Ag composite. This signified that there was increasingly low free energy barrier between the bulk ions and the electrode interface functionalized with AuNPs and Au composite (Guidelli et.al,2014). In addition, the Ag-Au NPs and Ag-Au-PGV showed similar electron coefficient in magnitude. However, the combinational effect of both electron rate constant and electron coefficient of Ag-Au/PGV demonstrated a superior overall electrochemical performance of Ag-Au-PGV compared to other composites and indeed NPs.

3.6 Conclusion

The objectives set for the synthesis of monometallic, bimetallic NPs and PGV bentonite functionalized nanocomposites were successfully met, and their spectroscopic characterization was successfully achieved through FT-IR and UV/vis techniques. In addition, the spectroscopic data obtained was corresponding to what the most literature studies suggested.

The electrochemical studies of synthesized NPs (Ag, Au and Ag-Au NPs) and their respective PGV composites were successfully done in line with objectives outlined. And based on current

data obtained, the electrochemical properties of AgNPs, AuNPs and Ag-Au NPs were indicative of what is reported in the literature. In contrast, electrochemical characterization of PGV composites and PGV itself produced a bit complex voltammograms, although most of them were interpretable with aid of literature findings.

Moreover, based on the effect of scan rate studies, other PGV bentonite functionalized NPs demonstrated significant enhancements in electrochemical activity according to Nicholson postulated equation on electron-transfer processes compared to unfunctionalized PGV bentonite NPs. This was later confirmed by Randles-Sevcik postulated equation across all scan rates but particularly at 90 mV/s. In addition, continued study using Randles-Sevcik equation proved that the PGV composites were found to have better surface attributes that influence the kinetics of electron transfer on the GCE with significant surface coverages determined in each case. From these results, Ag/PGV bentonite exhibited a slightly bigger electroactive surface coverage than Ag-Au/PGV bentonite but the latter exhibited an overall superior electrochemical activity.

As a result of comparable electrochemical properties of Ag/PGV and Ag-AuNPs/PGV, Nicholson and Shain equation helped to determine the overall electrochemical efficiency of these sensing nanofilms. Ag-Au NPs/PGV had a significantly higher electron transfer rate constant compared to all NPs and composites, although the electron coefficient was slightly less than that of Au-PGV, Ag-Au/PGV was chosen to further the studies due to overall electrochemical performance and efficiency.

3.7 References

Ahmed, S. and Ikram, S., 2016. Biosynthesis of gold nanoparticles: a green approach. *Journal of Photochemistry and Photobiology B: Biology*, 161, pp.141-153

Ajitha, B., Reddy, Y.A.K. and Reddy, P.S., 2015. Green synthesis and characterization of silver nanoparticles using *Lantana camara* leaf extract. *Materials science and engineering: C*, 49, pp.373-381.

Awad, M.A., Hendi, A.A., Ortashi, K.M., Alotaibi, R.A. and Sharafeldin, M.S., 2016. Characterization of silver nanoparticles prepared by wet chemical method and their antibacterial and cytotoxicity activities. *Tropical Journal of Pharmaceutical Research*, 15(4), pp.679-685.

Arshad, N., Aamir, M. and Sher, M., 2017. Electrochemical investigations of some newly synthesized arylazapyrazole derivatives. *Monatshefte für Chemie-Chemical Monthly*, 148(2), pp.245-255.

Aristov, N. and Habekost, A., 2015. Cyclic voltammetry-A versatile electrochemical method investigating electron transfer processes. *World J. Chem. Educ*, 3(5), pp.115-119

Aoki, K.J. and Chen, J., 2018. Tips of Voltammetry. In *Voltammetry*. IntechOpen.

Begum, R., Farooqi, Z.H., Naseem, K., Ali, F., Batool, M., Xiao, J. and Irfan, A., 2018. Applications of UV/Vis spectroscopy in characterization and catalytic activity of noble metal nanoparticles fabricated in responsive polymer microgels: a review. *Critical reviews in analytical chemistry*, 48(6), pp.503-516.

Bücker, M., Orozco, A.F. and Kemna, A., 2018. Electrochemical polarization around metallic particles—Part 1: The role of diffuse-layer and volume-diffusion relaxation. *Geophysics*, 83(4), pp.E203-E217.

Chanfreau, S., Cognet, P., Camy, S. and Condoret, J.S., 2007. Electrochemical determination of ferrocene diffusion coefficient in liquid media under high CO₂ pressure: Application to DMF–CO₂ mixtures. *Journal of Electroanalytical Chemistry*, 604(1), pp.33-40.

Chen, D.H., Chen, C.J. 2002. Formation and characterization of Au-Ag bimetallic nanoparticles in water-in-oil microemulsions. *J. Mater. Chem.*, 12: 1557-1562.

Dzimitrowicz, A., Jamróz, P., Sergiel, I., Kozlecki, T. and Pohl, P., 2019. Preparation and characterization of gold nanoparticles prepared with aqueous extracts of Lamiaceae plants and the effect of follow-up treatment with atmospheric pressure glow microdischarge. *Arabian Journal of Chemistry*, 12(8), pp.4118-4130.

Elemike, E.E., Onwudiwe, D.C., Fayemi, O.E. and Botha, T.L., 2019. Green synthesis and electrochemistry of Ag, Au, and Ag–Au bimetallic nanoparticles using golden rod (*Solidago canadensis*) leaf extract. *Applied Physics A*, 125(1), p.42.

Elgrishi, N., Rountree, K.J., McCarthy, B.D., Rountree, E.S., Eisenhart, T.T. and Dempsey, J.L., 2018. A practical beginner's guide to cyclic voltammetry. *Journal of chemical education*, 95(2), pp.197-206.

El-Naggar M.E., Shaheen, T.I., Fouda, M.M. and Hebeish, A.A., 2016. Eco-friendly microwave-assisted green and rapid synthesis of well-stabilized gold and core-shell silver-gold nanoparticles. *Carbohydrate polymers*, 136, pp.1128-1136.

Erk, M. and Raspor, B., 2000. Advantages and disadvantages of voltammetric method in studying cadmium-metlothionein interactions.

Fahmy, H.M., Mosleh, A.M., Abd Elghany, A., Shams-Eldin, E., Serea, E.S.A., Ali, S.A. and Shalan, A.E., 2019. Coated silver nanoparticles: Synthesis, cytotoxicity, and optical properties. *RSC advances*, 9(35), pp.20118-20136.

Feng, L., Gao, G., Huang, P., Wang, K., Wang, X., Luo, T., Zhang, C. 2010. Optical properties and catalytic activity of bimetallic gold-silver nanoparticles. *Nano Biomed. Eng.*, 2: 258-267.

Feng, L., Sun, X., Yao, S., Liu, C., Xing, W. and Zhang, J., 2014. Electrocatalysts and catalyst layers for oxygen reduction reaction. In *Rotating electrode methods and oxygen reduction electrocatalysts* (pp. 67-132). Elsevier.

Ferrando, R., Jellinek, J. and Johnston, R.L. 2008. Nanoalloys: from theory to applications of alloy clusters and nanoparticles. *Chem. Rev.*, 108: 845-910.

Frost, M.S., Dempsey, M.J. and Whitehead, D.E., 2017. The response of citrate functionalised gold and silver nanoparticles to the addition of heavy metal ions. *Colloids and Surfaces A: Physicochemical and Engineering Aspects*, 518, pp.15-24.

Galicia, M., Li, X. and Castaneda, H., 2014. Interfacial Characterization of Single-and Multi-Walled CNT-Doped Chitosan Scaffolds under Two Flow Conditions. *Journal of The Electrochemical Society*, 161(12), p.H751.

G. Gangahara , U. Maheshwarib and S. Guptac. 2014. ‘Application of nanomaterials for the removal of pollutants from effluent streams.’ *Nanoscience Asia*. Vol. (2). 140-150.

García-Miranda Ferrari, A., Foster, C.W., Kelly, P.J., Brownson, D.A. and Banks, C.E., 2018. Determination of the electrochemical area of screen-printed electrochemical sensing platforms. *Biosensors*, 8(2), p.53.

Garg, S., Rong, H., Miller, C.J. and Waite, T.D., 2016. Oxidative dissolution of silver nanoparticles by chlorine: Implications to silver nanoparticle fate and toxicity. *Environmental science & technology*, 50(7), pp.3890-3896.

Garrido-Ramírez, E.G., Marco, J.F., Escalona, N. and Ureta-Zañartu, M.S., 2016. Preparation and characterization of bimetallic Fe–Cu allophane nanoclays and their activity in the phenol oxidation by heterogeneous electro-Fenton reaction. *Microporous and Mesoporous Materials*, 225, pp.303-311.

Guidelli, R., Compton, R.G., Feliu, J.M., Gileadi, E., Lipkowsky, J., Schmickler, W. and Trasatti, S., 2014. Defining the transfer coefficient in electrochemistry: An assessment (IUPAC Technical Report). *Pure and Applied Chemistry*, 86(2), pp.245-258.

Gurunathand S, Z.Lui , W. Shen and X. Zhang. 2016. ‘Silver Nanoparticles: Synthesis, Characterization, Properties, Applications, and Therapeutic Approaches’. *International journal of molecular sciences*. 17(9). 1534.

Gritsch, L., Meng, D. and Boccaccini, A.R., 2017. Nanostructured biocomposites for tissue engineering scaffolds. *Biomedical composites*, pp.501-542.

Hamidi-Asl, E., Dardenne, F., Pilehvar, S., Blust, R. and De Wael, K., 2016. Unique properties of core shell Ag@ Au nanoparticles for the aptasensing of bacterial cells. *Chemosensors*, 4(3), p.16.

Huang, W., Yan, M., Duan, H., Bi, Y., Cheng, X. and Yu, H., 2020. Synergistic antifungal activity of green synthesized silver nanoparticles and epoxiconazole against *Setosphaeria turcica*. *Journal of Nanomaterials*, 2020.

Honma, K. and Clemmer, D.E., 1995. The Importance of Electron Transfer Mechanism in Reactions of Neutral Transition Metal Atoms. *Laser Chemistry*, 15(2-4), pp.209-220

Iravani, S., Korbekandi, H., Mirmohammadi, S.V. and Zolfaghari, B., 2014. Synthesis of silver nanoparticles: chemical, physical and biological methods. *Research in pharmaceutical sciences*, 9(6), p.385.

Ke, J., Zhu, Y., Zhang, J., Yang, J., Guo, H., Zhao, W., Wen, C. and Zhang, L., 2019. Size-Dependent Uptake and Distribution of AgNPs by Silkworms. *ACS Sustainable Chemistry & Engineering*, 8(1), pp.460-468

Landry, A.M., 2016. Bimetallic Nanoparticles: Synthesis, Characterization, and Applications in Catalysis (Doctoral dissertation, UC Berkeley).

Li, J., Xu, J., Li, B., He, L., Lin, H., Li, H.W. and Shao, H., 2018. Advanced sem and tem techniques applied in Mg-based hydrogen storage research. *Scanning*, 2018.

- Li, S. and Thomas, A., 2020. Emerged carbon nanomaterials from metal-organic precursors for electrochemical catalysis in energy conversion. In *Advanced Nanomaterials for Electrochemical-Based Energy Conversion and Storage* (pp. 393-423). Elsevier.
- Łukowiec, D. and Radoń, A., 2020. Self-organization of silver nanoparticles during synthesis of Ag–Au nanoalloy by UV irradiation method. *Journal of Materials Science*, 55(7), pp.2796-2801.
- Liu, C., Cai, X., Wang, J., Liu, J., Riese, A., Chen, Z., Sun, X. and Wang, S.D., 2016. One-step synthesis of AuPd alloy nanoparticles on graphene as a stable catalyst for ethanol electro-oxidation. *international journal of hydrogen energy*, 41(31), pp.13476-13484
- Mahmoudi, S., Jafari, A. and Javadian, S., 2019. Temperature effect on performance of nanoparticle/surfactant flooding in enhanced heavy oil recovery. *Petroleum Science*, 16(6), pp.1387-1402.
- Malińska, D., Więckowski, M.R., Michalska, B., Drabik, K., Prill, M., Patalas-Krawczyk, P., Walczak, J., Szymański, J., Mathis, C., Van der Toorn, M. and Luetlich, K., 2019. Mitochondria as a possible target for nicotine action. *Journal of bioenergetics and biomembranes*, 51(4), pp.259-276.
- Mohamed, A.M.O., Rodrigues, V.G. and Paleologos, K.E., 2021. Pollution assessment of nanomaterials. In *Pollution Assessment for Sustainable Practices in Applied Sciences and Engineering* (pp. 921-973). Butterworth-Heinemann.
- Nasrullah, M., Gul, F.Z., Hanif, S., Mannan, A., Naz, S., Ali, J.S. and Zia, M., 2020. Green and chemical syntheses of CdO NPs: a comparative study for yield attributes, biological characteristics, and toxicity concerns. *ACS omega*, 5(11), pp.5739-5747.
- Nedyalkov, N., Koleva, M.E., Nikov, R., Stankova, N.E., Iordanova, E., Yankov, G., Aleksandrov, L. and Iordanova, R., 2019. Tuning optical properties of noble metal nanoparticle-composed glasses by laser radiation. *Applied Surface Science*, 463, pp.968-975.
- Özkar, S. and Finke, R.G., 2019. Nanoparticle formation kinetics and mechanistic studies important to mechanism-based particle-size control: evidence for ligand-based slowing of the autocatalytic surface growth step plus postulated mechanisms. *The Journal of Physical Chemistry C*, 123(22), pp.14047-14057

- Patil, M.M., Shetti, N.P., Malode, S.J., Nayak, D.S. and Chakklabbi, T.R., 2019. Electroanalysis of paracetamol at nanoclay modified graphite electrode. *Materials Today: Proceedings*, 18, pp.986-993.
- Rajput, N., 2015. Methods of preparation of nanoparticles-a review. *International Journal of Advances in Engineering & Technology*, 7(6), p.1806
- Reddy, T.R., Kaneko, S., Endo, T. and Reddy, S.L., 2017. Spectroscopic characterization of bentonite. *J. Laser Opt. Photonics*, 4, p.171.
- Sahi, S., Magill, S., Ma, L., Xie, J., Chen, W., Jones, B. and Nygren, D., 2018. Wavelength-shifting properties of luminescence nanoparticles for high energy particle detection and specific physics process observation. *Scientific reports*, 8(1), pp.1-9.
- Sajid, M., 2018. Bentonite-modified electrochemical sensors: a brief overview of features and applications. *Ionics*, 24(1), pp.19-32.
- Sharma, G., Kumar, A., Sharma, S., Naushad, M., Dwivedi, R.P., AlOthman, Z.A. and Mola, G.T., 2019. Novel development of nanoparticles to bimetallic nanoparticles and their composites: a review. *Journal of King Saud University-Science*, 31(2), pp.257-269.
- Sibiya, P.N. and Moloto, M.J., 2014. EFFECT OF PRECURSOR CONCENTRATION AND pH ON THE SHAPE AND SIZE OF STARCH CAPPED SILVER SELENIDE (Ag_2Se) NANOPARTICLES. *Chalcogenide letters*, 11(11).
- Thapliyal, N Chimunze T and Karpoormath R. 2016. Research progress in electroanalytical techniques for determination of antimalarial drugs in pharmaceutical and biological samples. *Royal society of chemistry*. 62(57580-57602).
- Zhang, X.F., Liu, Z.G., Shen, W. and Gurunathan, S., 2016. Silver nanoparticles: synthesis, characterization, properties, applications, and therapeutic approaches. *International journal of molecular sciences*, 17(9), p.1534.
- Zhao, G. and Liu, G., 2019. Electrochemical deposition of gold nanoparticles on reduced graphene oxide by fast scan cyclic voltammetry for the sensitive determination of As (III). *Nanomaterials*, 9(1), p.41.
- Zhao, L., Wang, Y., Zhao, X., Deng, Y., Li, Q. and Xia, Y., 2018. Green preparation of Ag-Au bimetallic nanoparticles supported on graphene with alginate for non-enzymatic hydrogen peroxide detection. *Nanomaterials*, 8(7), p.507.

Chapter 4: Efavirenz method development

Chapter 4: Summary

The EFV method development mainly discussed the optimum workable conditions for EFV analysis both experimentally and detection technique parameters of the method. Fabrication optimization depicted drop-coating as the most optimum sensor fabricating method. Henceforth, other experimental conditions including concentrations of supporting electrolyte, Huma serum albumin (HSA) as well as type of supporting electrolyte were all determined.

DPV technique was determined as best working technique, and parameters governing the technique such as step-potential and pulse amplitude were determined. Thus, optimum conditions obtained from experimental conditions and technique parameters were used to construct EFV calibration curve and conduct subsequent EFV analysis in real samples.

The EFV method developed displayed plausible sensitivity in the detection of EFV particularly in real samples as content obtained in EFV capsule was close to that specified by EFV formulation manufacturer, and overall results of EFV in spiking studies, reproducibility and stability studies were statistically plausible through respective RSD values obtained. Thus, the method developed was successfully validated.

4.1 Development and application of an electrochemical Efavirenz sensor

This chapter explores potential electrochemical application of Ag-Au-PGV/HSA on various EFV aqueous media. There has been a number of reported applications of electrochemical sensing platforms comprised of metallic NPs in determination of EFV and other ARV drugs, thus this study explores an enhanced alternative to those previously reported.

The application of modified electrodes of such nature has come with much appreciated success in various scientific platforms. However, there has been a few challenges that have been encountered in their application which include but not limited to inadequate sensitivity in some instances, and electrode fouling because of attachment of biological and organic molecules (Pournara *et.al*,2019, Abraham *et.al*, 2020). Consequently, to mitigate such shortcomings an establishment of better sensing materials with greater sensitivity and stability for analysis of

ARVs drugs such as EFV is necessary, and this study proposes an alternative by detailing metallic and bimetallic composites, particularly silver (Ag) and gold bimetallic (Ag) composites electrode modification systems as potential detection and quantitation method for EFV.

The metallic NPs unlike other types of electrode modifiers, exhibits greater activity through cluster of atoms which possesses free valence electrons which aid with electrical conductivity (Khan *et.al*,2019). In addition, the metallic NPs have total atomic volume which has exceptional surface area-to volume ratio through which enables them to exhibit excellent catalytic activity (Khan *et.al*, 2019, Malekzad *et.al* ,2020). Other attributes of metallic NPs include excellent chemical stability and surface tenability which generally improve the sensory materials applied in fabrication of chemical and biosensors. Furthermore, metallic NPs that have been used to fabricate a typical electrochemical sensor include Ag, Fe and sometimes even metal oxides like ZrO and ZnO (Chavali *et.al*,2019, Li *et.al*, 2020). As such a recent study confirmed a successful application of ZnO sensing material to detect lamiduvine in ART formulations, which indicated the excellent capability of metallic oxide NPs material of carry out electrochemical analysis of determining drug type, concentration and/or activity (Bowen *et.al*, 2020)

ZnO is one of few metal oxides NPs that has been used to functionalize sensors of various kinds and for different applications. Metal oxides are not as conductive as metallic NPs but do offer better surface area, and thus able to exhibit better catalytic effect compared to that which is generally exhibited by bare surfaces.

However, the application of monometallic NPs like AgNPs and AuNPs in modification of bare electrode for drug analysis has been a success along with metal oxide and unmodified electrodes alike. However, some of the main disadvantages associated with monometallic NPs application have been slower response, surface fouling predominantly with bare electrode surfaces, noise, unstable signals, and lower dynamic range as well as lower sensitivity compared to application of bimetallic NPs (BMNPs) (Romero-Nunez *et.al*, 2019, Khan *et.al*,2019). Hence, the modification of electrode using BMNPs has gained prevalence in various scientific applications particularly in development of electrochemical sensors.

The properties of BMNPs are reportedly superior to those of monometallic NPs mainly because of hydrid effect which is brought about by an overlap of chemical and physical properties of two metals or sometimes metal oxides and/or metal and an oxide combination (Paszkievicz

et.al, 2016). According to various sources, in bimetallic catalysts the electronic effect plays an important role which describes the charge transfer and thus enabling them to effect much desired catalytic action (Gowthaman *et.al*, 2016). Alloying of the constituting elements can result in the structural changes of the bimetallic nanoparticles, and from monometallic to bimetallic nanoparticles, an extra degree of freedom is introduced (Sharma *et.al* ,2019). Different methods and correlations have been developed with the help of physical and spectroscopic measurements. The preparation conditions determine the structure and miscibility of the two metals in BMNPs.

There is minimal application of Ag-Au NPs BMNPs in drug analysis particularly EFV. However, this study aims to explore the capacity of a BMNPs consisting of these metals as potential sensing material for drug an ARV drug analysis. In addition, apart from ARVs analysis Ag-Au NPs has been used to detect drugs of different kinds, organic and inorganic analytes. Recent study was testament to this as Ag-Au NPs were successfully used to modify bare electrode to detect Anthracene, an important hydrocarbon in dyes (Mailu *et.al*,2010).The same study further indicated the use of them in formation of a bimetallic nanocomposite which enhanced their catalytic properties, thus increasing the sensitivity of the sensor and BMNPs stability (Mailu *et.al*,2010).

The application of BMNPs has however seen some shortcomings in different scientific fields but particularly in nanotechnology, thus the nanocomposites of BMNPs have been prepared by supporting them on the organic or inorganic counterparts. BMNPs nanocomposites have improved properties as compared to those of BMNPs (Sharma *et.al*,2019). Due to reduction in size and increase in surface area, these are prominently used as catalysts. In addition, these have also been inherently synthesized to overcome disadvantages observed with BMNPs like tendency to agglomerate caused by degree of instability amongst few more others (Hynh *et.al*, 2020).

In this work, bentonite (MMT) nanoclay was used to overcome such instability. This type of nanoclay like many other types of nanoclay naturally exhibit minimal electroactivity, however there has been reported electrochemical studies involving application of MMT bentonite in detection and determination of drugs, dyes and organic substances with plausible sensitivity (Shetti *et.al*, 2017). Thus, this study through Ag-AuNPs nanoclay functionalized composite, fabricated a sensing platform by so doing developed an electrochemical sensor to conduct EFV electrochemical analysis.

A series of experimental analysis were carried out to enhance the conditions to exhibit plausible EFV signal response. After the optimum fabrication method for sensor developed was obtained, the type of supporting electrolytes, concentrations of elected supporting electrolyte, effect of HSA were all investigated as part of optimization of experimental conditions.

The technique detection parameters optimization evaluated the optimum detecting technique, thereby determining effect step-potential (scan rates) and pulse amplitude were investigated as part of EFV kinetic studies. The data established from experimental conditions and technique parameters optimization was used to carry out calibration curve studies.

Using DPV under optimized conditions and parameters, interferences and stability studies were done and discussed. Furthermore, the proposed method was applied in human urine and pharmaceutical capsules during real sample analysis of EFV. The electroanalytical method proposed produced reliable, plausible, and sensitive detection and determination of EFV using sensing platform Ag-Au-PGV/HSA

4.2 Experimental

4.2.1 Material, reagents, and instruments

Sodium hydroxide (NaOH) and Hydrochloric acid (HCl) supporting electrolyte were prepared from laboratory standards. Efavirenz (200 mg/ml) reference standard was purchased at Sigma-Alrich. PBS (Phosphate buffer saline) of pH 7.2 was made from sodium hydrogen phosphate (NaHPO_4), Dihydrogen potassium phosphate (KH_2PO_4), sodium chloride (NaCl) and potassium chloride (KCl) all purchased from Sigma-Alrich. 1g Human serum Albumin (HSA) powder purchased from Merck, all working standards of HSA were made from 0,5 g.

Cyclic voltametric and differential pulse voltammetry experiments were performed using an AutoLab PGStat 128 (MetrohmAutoLab) equipped with the NOVA 2.1 Software (Metrohm AutoLab). The experimental setting was composed of a conventional three electrodes cell in which a saturated potassium chloride (KCl) electrode and a platinum wire were used as reference (RE) and counter (CE) electrodes, respectively. The electroactivity of EFV was determined under potential range of 0.8V to 1,4V at 30mvs.

4.2.2 GC and GC electrode modified preparation

GCE was polished repeatedly with 1, 0.3 and 0.05 μm alumina slurries. After each polishing, electrode cleaning adopted was as follows; successive 5 minutes rinsing with doubly distilled water, ultrasonication in ethanol and finally with another doubly distilled water to remove any adsorbed substances on the electrode surface. The reference electrode, Ag/AgCl (3 M NaCl) was rinsed thoroughly with distilled water and used. The counter electrode, platinum (Pt) wire was cleaned by burning in a gas flame.

The preparation of film modification of GCE followed for drop-coating method used the outlined methodology in chapter 3 section 3.4.5

4.2.3 Optimization of experimental conditions methodology

The 200 μM EFV standard that used in the optimization of detection method and was prepared from EFV reference standard (200 mg). 0,01 g of EFV reference standard was weighed and diluted in 100 ml absolute ethanol to produce a working standard of 316,8 μM . 63 ml of 316,8 μM was pipetted into another 100 ml volumetric, which was made up to the mark with absolute ethanol. 200 μM working standard resulted from that dilution and was used as working standard for optimization of detection method.

The optimization of sensor fabrication method used 200 μM EFV working standard. Human serum Albumin (HSA) was used as powder form, as provided by supplier. 0,01g HSA was weighed and diluted with 1 ml to make primary HSA concentration. All other HSA concentrations were made by diluting 0,01g/ml HSA primary standard. Ag-Au/PGV film volumes were casted on the electrode and dried over 30 min-45 min in very humid fume hood. HSA film concentration were casted upon dried Ag-Au/PGV films, thereby forming GCE/Ag-Au-PGV-HSA platforms which was were immediately.

Hydrochloric acid (HCl) working supporting electrolyte was made from 10.2M analytical grade standard solution. 5×10^{-3} ml of 10.2M was pipetted into 50 ml distilled water to make 1 M working standard from which 0,025 ml was pipetted into 25 ml distilled water making 0,001M HCl working standard which was used. Sodium hydroxide (NaOH) supporting electrolyte was made from weighing 0,19 g pallets into 50 ml distilled water, which resulted in 0,1M NaOH. 0,25 ml of 0,1M NaOH standard was pipetted into 25 ml volumetric flask and

made to the mark with distilled water making 0,001M NaOH working standard which was used as supporting electrolyte.

Phosphate buffer saline (PBS) was made using Disodium phosphate (Na_2HPO_4) and Sodium dihydrogen phosphate (NaH_2PO_4). To make 1 M primary stock of PBS, 20,214g of Na_2HPO_4 and 3,394 g of NaH_2PO_4 were quantitatively weighed and transferred into 100 ml volumetric flask, and flask was made up to the mark with distilled water. The adjustment of pH of the PBS was adjusted to pH 7,2 using 0,1M HCl. All other concentrations of PBS supporting electrolytes were made from quantitative dilutions 1M primary supporting electrolyte.

4.2.4 Preparation EFV working standards for calibration curve

Primary EFV working stock solution was prepared by quantitatively weighing 0,011g of EFV reference standard in 100 ml, which was made up to the mark using absolute ethanol. The primary stock concentration resulted was 350 μM , and all subsequent EFV working standards used in construction of curve were made from quantitative dilutions of 350 μM primary working standard.

All the stock solutions were kept in the refrigerator. The ratio of voltage versus current (slope of calibration curve) was used to measure EFV sensitivity while detection limit was measured from the (3 x standard deviation of blank) in the linear dynamic range of calibration plot.

4.2.5 Method validation methodology

Interferences, reproducibility and stability studies were all conducted using one of EFV standards made from calibration. Meanwhile, recovery studies were conducted using human urine, which mimicked composition of a real sample. 10ml and 2,5ml urine aliquots was diluted using distilled water in two separate 20ml and 10 ml volumetric flask and spiked using one of the EFV standards used in the calibration curve.

4.2.6 Determination of EFV in pharmaceutical capsules methodology

Three capsules of 200 mg capsules were quantitatively weighed, and produced masses of 0.451g ,0.405g and 0,401 g respectively. These masses were quantitatively transferred into 50ml separate volumetric flask and diluted with absolute ethanol to the mark. 1 ml from each was pipetted and mixed with 3 ml of 1M PBS supporting electrolytes in a cell and analysis were conducted from resulting solutions.

4.3 Results and discussion

4.3.1 Electrochemical identification of Efavirenz at bare GCE and GCE/Ag-Au/PGV bentonite/HSA

The investigation of the electrochemical behaviour of EFV was conducted on different electrode surfaces. Differential pulse voltammetry (DPV) was used as a technique to conduct analysis of EFV on bare and modified surface under same experimental condition

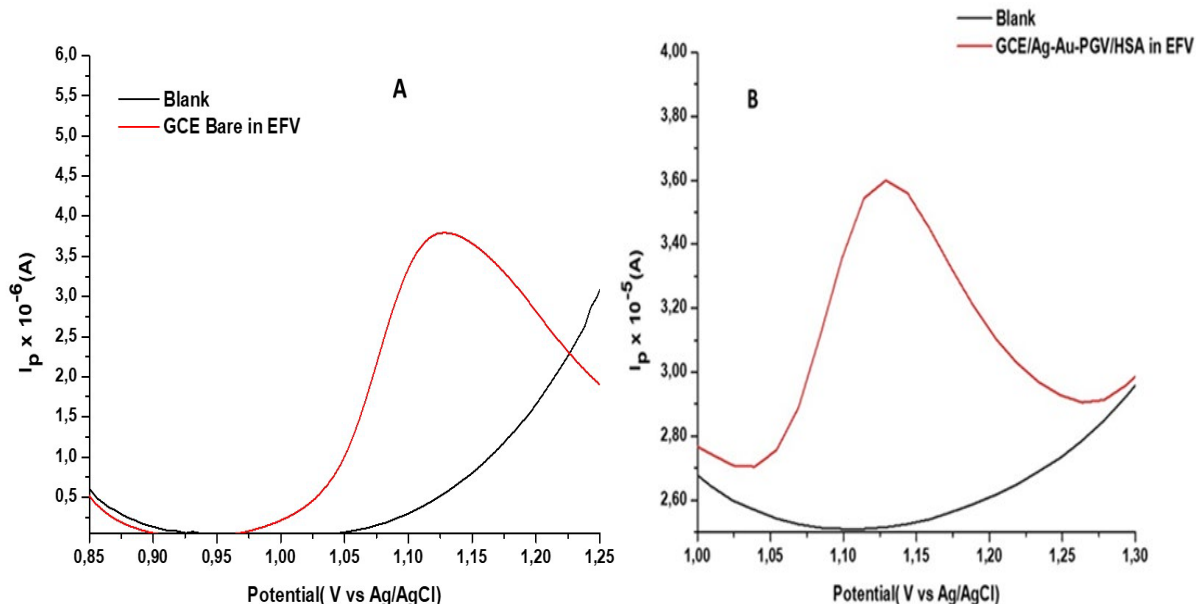


Figure 4-1:EFV electrochemical identification of 200 uM EFV on bare GCE (A and B) and Ag-Au-PGV/HSA platform at 30 mvs and differential pulse voltammetry in 0,5M PBS pH 7.2 supporting electrolyte.

Electrochemical activity of EFV on bare GCE and modified surface as shown in figure A and B depicts electrochemical activity within potential window of 1 to 1.4V DPV through a single irreversible peak potential. However, EFV activity was observed at 1,15V for bare GCE, whilst for modified surface exhibited slightly lower oxidation potential at 1,14V. The corresponding peak current of EFV was observed to be significantly higher for modified surface compared to peak current of EFV exhibited by bare surface.

The cause of significantly enhanced peak currents of EFV exhibited by Ag-Au-PGV/HSA platform are due to greater surface area providing more electroactive sites for EFV electrochemical interaction compared to bare GCE surface. The electroactive active sites synergistically evolve more electrons between EFV and platform surface, which increased the rate at which the EFV electrochemical reaction occurred (Wang, *et.al*,2018).

The low potential shifts observed in EFV electrochemical reaction with platform compared to bare GCE are mainly due to metals (Ag and Au) electrochemical participation, particularly Au which intrinsically exhibit high oxidation potential. The overall electrochemical effect subsequently affected the potential at which EFV oxidizes. The complex formation due to sensing film could be another cause of low detection potential of EFV observed (Schneider *et.al*, 2018).

4.4 Optimization of experimental conditions

4.4.1 EFV detection technique

the EFV voltammograms depicted were obtained using DPV and SWV electrochemical detection techniques, respectively. This was done to ascertain the electrochemical technique at which EFV could be detected with optimum efficiency and sensitivity.

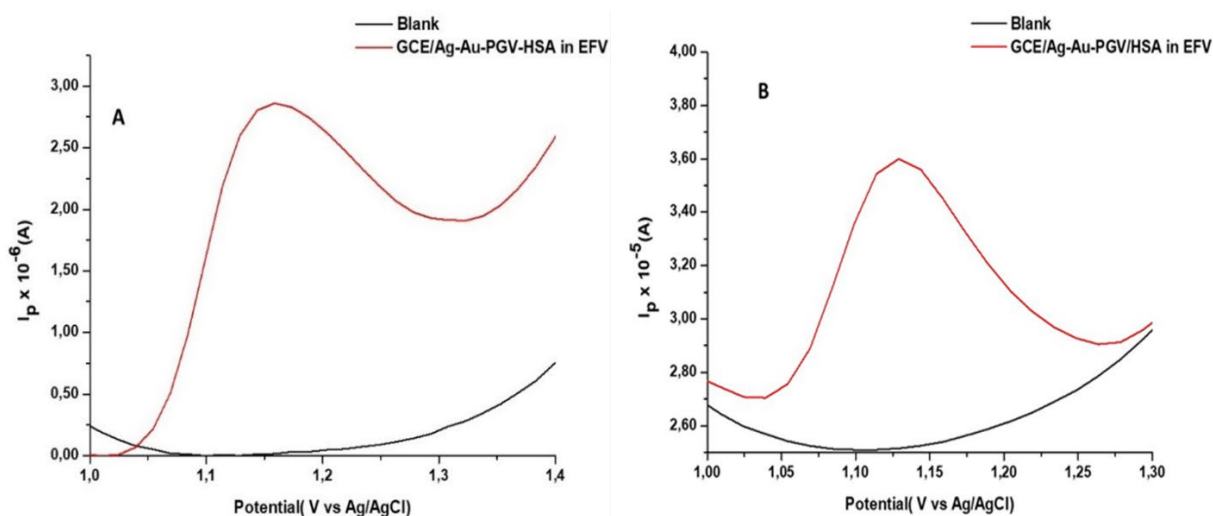


Figure 4-2: Electroactivity of 200 uM EFV under different electrochemical detection techniques, DPV(B) and SWV(A).

As depicted by the voltammograms, the through shape and size the voltammograms were very similar. Peak potential and peak current of EFV electroactivity depicted by both techniques were appeared similar the peak resolution depicted by DPV was significantly enhanced compared to SWV. Thus, findings concluded that DPV gave better optimum condition for the detection of EFV, although SWV exhibited greater peak current but comparable sensitivity.

4.4.2 Optimization of sensor fabrication method

The voltammograms shown below depict the electrochemical difference exhibited by two sensor fabrication methods for EFV detection.

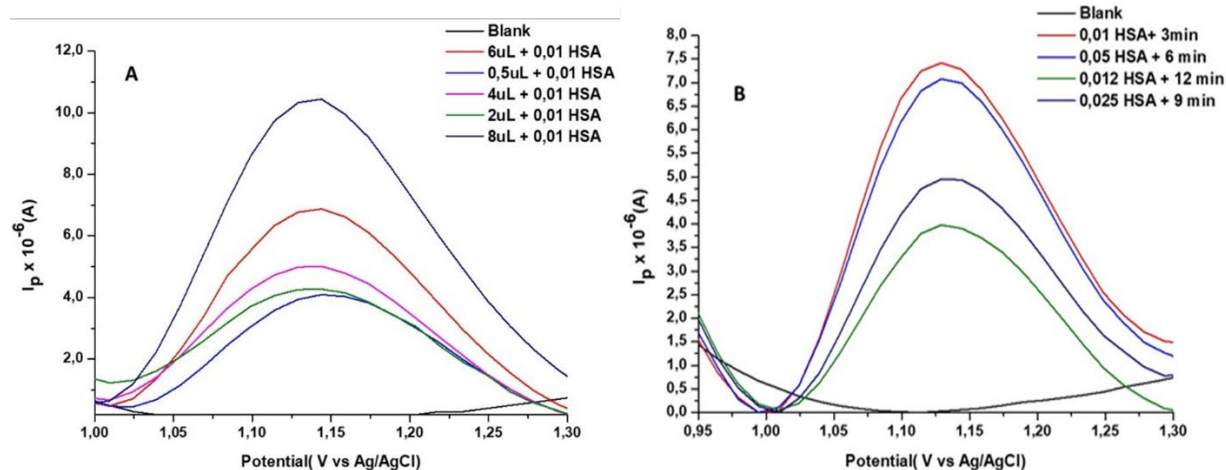


Figure 4-3: Voltammograms depicting effect caused by drop-coating method (A) and immersion method (B) in detection of EFV

Figure 4-3A which represented drop coating method showed that as volumes of composite films used to coat increased whilst HSA volume was constant the peak current of EFV electroactivity increased linearly. This indicated the effect caused by the amount of volume of composite as drying time and HSA volume were kept constant.

The cause of this observations was due to increased concentration of composite as number of participating particles increased as volume of film increased. This increased the participating electroactive sites of composite whilst the electrochemical effect was that the rate of electrochemical reaction increased as more electrons were evolved causing interaction between film interface and EFV to increase. This caused the enhancement of detection of EFV which

was observed mainly through an increase in peak current as peak potential exhibited minute negative shifts, which indicated complex formation.

Comparatively, immersion method investigated mainly the effect of HSA concentration and time being the changing variable whilst the volume of composite film was kept constant. As was observed with drop coating method, HSA did not exhibit electrochemical effect on the electroactivity of EFV as the peak potential change was extremely minute. However, the peak current of EFV increased linearly as concentration of HSA increased with least amount of time spent under immersion. The most dilute HSA exhibited lowest peak current whilst the most concentrated contributed to higher EFV peak current as shown by the voltammogram.

However, the increase observed was not due to electrochemical activity of HSA but was caused largely by adsorption of some content from HSA unto the surface of composite film. The time of immersion thus did not affect HSA adsorption rate but its concentration did. This was evident as more time film spent under HSA immersion peak current of EFV decreased linearly.

Based on data presented by both methods, electrochemically drop coating method exhibited peak potential of EFV with enhanced peak resolution compared to immersion method. The data also proved that HSA immersion method exhibited no positive electrochemical enhancement in the EFV detection even after varying HSA concentrations as the peak current increase was due to adsorption of HSA constituents, which possessed no electrochemical properties.

4.4.3 Choice of supporting electrolyte

The voltammograms depicted below showed the effect of type of supporting electrolyte in the electrochemical detection of EFV under similar experimental conditions. The supporting electrolyte used ranged from basic, neutral to acidic chemical environment.

The DPV demonstrated visible electrochemical activity of EFV in NaOH and PBS as supporting electrolytes although PBS exhibited greater peak current and well resolved EFV peak potential compared to NaOH. The electrochemical activity of EFV in HCl was not present, and this observation demonstrated EFV pH sensitivity, particularly in highly acidic media. The effect causing and contributing to this observation is HCl, which is largely enzymic and pH dependent as it denatures in drastically low and high pH levels with exceptions to those pH levels close to neutrality.

Although both NaOH and HCl exhibited a greater electrochemical activity on EFV compared to PBS buffer due to significantly greater ionic strength. The reason behind this claim is attributed to smaller ionic sizes of H^+ , Cl^- , OH^- and Na^+ compared to phosphate ions, thus causing these ions to have greater ionic strength and more conductivity as a solution than PBS (Zhang et.al,2017 and Krol *et.al*, 2020). However, the electroactivity of EFV as a biological

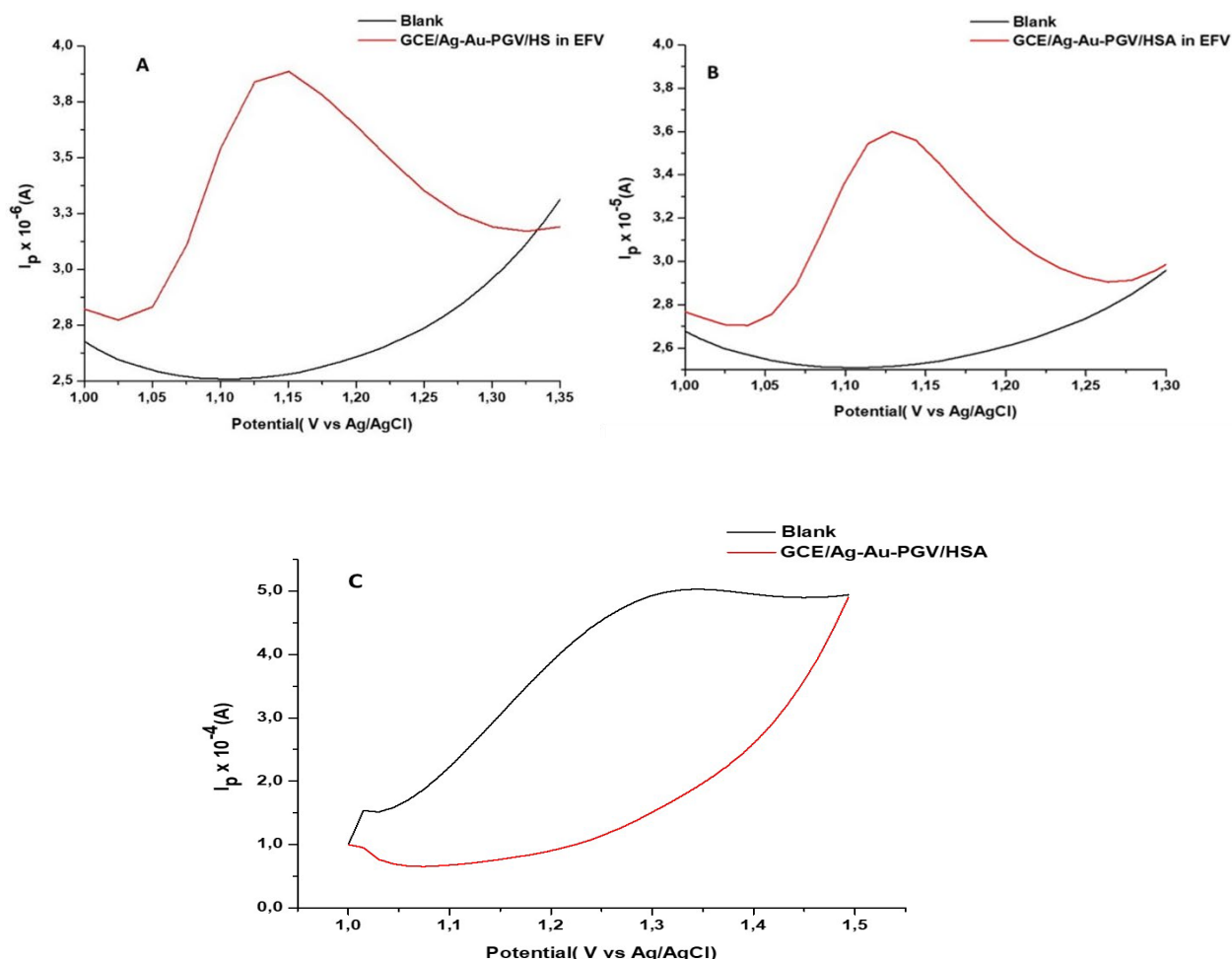


Figure 4-4: DPV exhibition of electrochemical behaviour of EFV at 30 mvs in 0.001M concentration of different type of supporting electrolytes of PSB (B), NaOH (A) and HCl (C).

drug is detectable in highly conductive chemical environment but is pH sensitive as well as the HSA modified platform that was used to detect it, as it contained a protein which is pH sensitive.

Consequently, this study opted for the continued use of PBS buffer as supporting electrolyte compared mainly with NaOH due to pH dependency of detecting platform and EFV drug itself as well as electrochemically better and efficient detection of EFV demonstrated by excellent EFV resolved peak under the application of PBS.

4.4.4 Effect of PBS concentrations

The voltammogram showed below the effect of PBS concentration on the electrochemical activity of EFV. The peak current of EFV increased linearly with increasing PBS concentration, whilst the peak potential shifted positively.

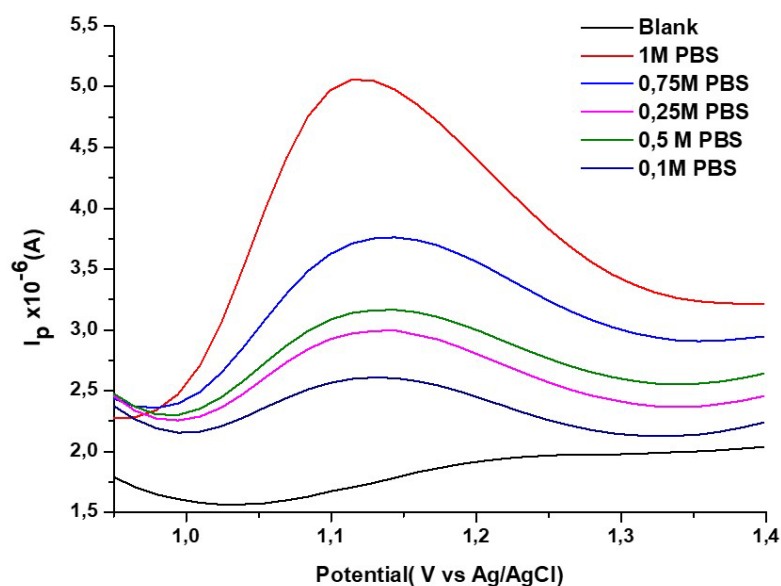


Figure 4-5: Effect of PBS concentration on EFV electroactivity

This cause for the increase in peak current was due to the increase ionic strength of PBS at high concentrations, which caused the overall conductivity of the electrolyte to increase (Chaparro *et.al*, 2016). This increase in the conductivity of the electrolyte facilitated for fast electrochemical reaction between EFV and surface interface of the platform as the reaction solution was experiencing low electrical resistance. Conversely, at low PBS concentration as depicted by the voltammogram small electroactivity of EFV was observed due to high resistance within the electrolyte which caused the electrochemical interaction between EFV and interface of the platform to occur at significantly low rate (Purwidyantri *et.al*,2021). Therefore, 1 M PBS was chosen as optimum concentration condition for the detection of EFV based on electrochemical activity exhibited by voltammogram.

4.5 Optimization of detection parameters

4.5.1 Effect of step potential and pulse amplitude

The step potential depicted by diagram 4-6A, which is also regarded as scan rate depicted 0,015V/s or 30 mV/s as the step potential for the detection of EFV due to a well defined and resolved potential peak obtained for EFV at varying step-potential.

The the effect on varying pulse amplitude and peak current on electrooxidation of EFV depicted by diagram 4-6B was determined. This was determined over a potential range of 0,8 to 1,4V. The data obtained depicted that pulse amplitude increased linearly with peak current, however the maximum pulse amplitude was reached at 0,085 Vs⁻¹ and from that point peak current began to change slightly . This result implied that the optimum pulse amplitude was 0.085Vs⁻¹ which also produced a greatest resolved electrochemical peak due to EFV, thus the electrooxidation reaction of EFV was optimum at 0,085 pulse amplitude.

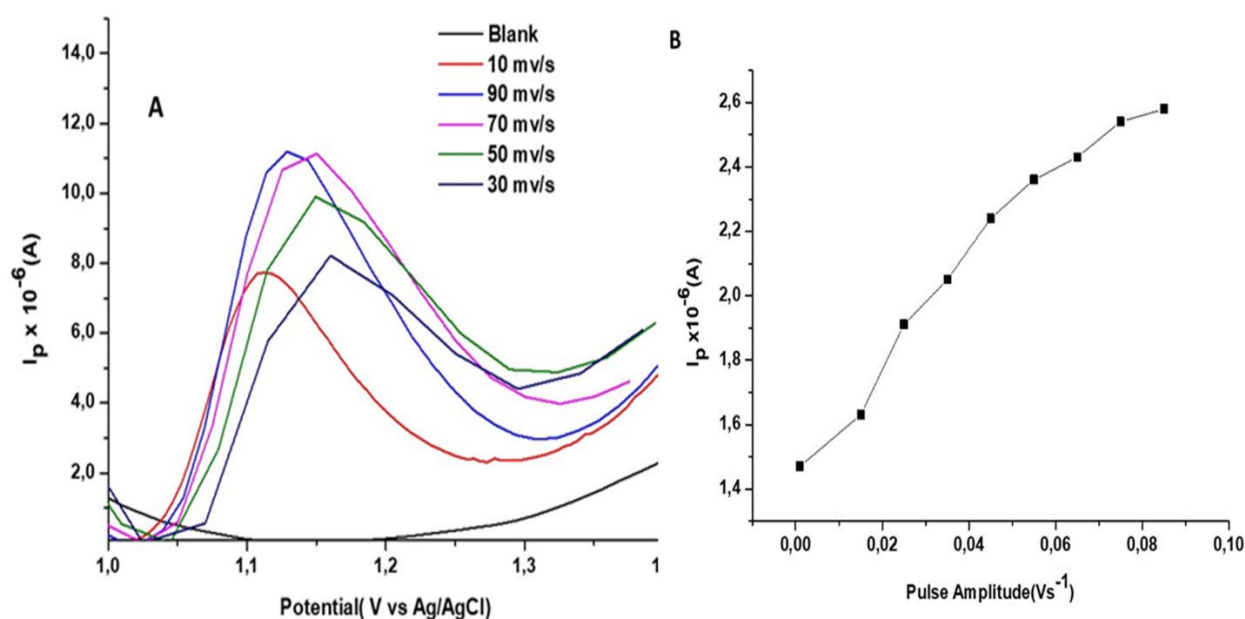


Figure 4-6: Effect caused by step-potential (A) and pulse amplitude (B) on electroactivity of 200 uM EFV in 1M PBS.

4.5.2 Determination of electron-kinetic parameters

The step-potential, which is the conventional equivalence of scan rate depicted change in peak current with respect to increasing step-potential. This relationship was used to study the electrochemical kinetics of EFV with respect to the sensing platform. Randles sevcik equation (Refer to Eq. 3-4) and Lavirons equation (Eq. 3-5) was used determine kinetic parameters for an irreversible kinetic reaction between Ag-Au-PGV/HSA platform and EFV.

Table 4-1: Electrochemical properties obtained from Randles Sevcick plots and laviron equation for 200 uM EFV

Parameters	Ag-Au-PGV/HSA
n	1
E°	1,15
K _s (S ⁻¹)	1,11
Γ	0,2
D (cm ² S ⁻¹ x 10 ⁻⁹)	2,76

The electrochemical electron-charge transfer obtained from lavirons plot depicted by the table indicated that the analyte-sensor electrochemical interaction was governed by an electrocatalytic mechanism oxidation of EFV. The heterogenous rate constant was high and positive in magnitude, which was indicative of great speed at which the electrons moved from the platform to EFV interchangeably. This was the cause for the fast observed electrochemical reaction between the platform and EFV.

4.5.3 Calibration studies of EFV

A EFV stock standard solution of 300 uM was used to conduct calibration analysis, and subsequent calibration curve. The concentration range used to construct the curve ranged from 1-300 uM in 1 M PBS solution. The voltammogram and plot shown below depicted that as concentration of EFV increased the anodic potential peak of EFV increased linearly, thus a linear relationship between peak current and concentrations of EFV was established.

Under optimized condition, EFV limit of detection (LOD), limit of quantitation (LOQ) and concentration linearity range were determined using equation $LOD = 3.3\sigma/S$ and $LOQ = 10\sigma/S$, respectively. The standard deviation is represented by σ whilst S represented the slope.

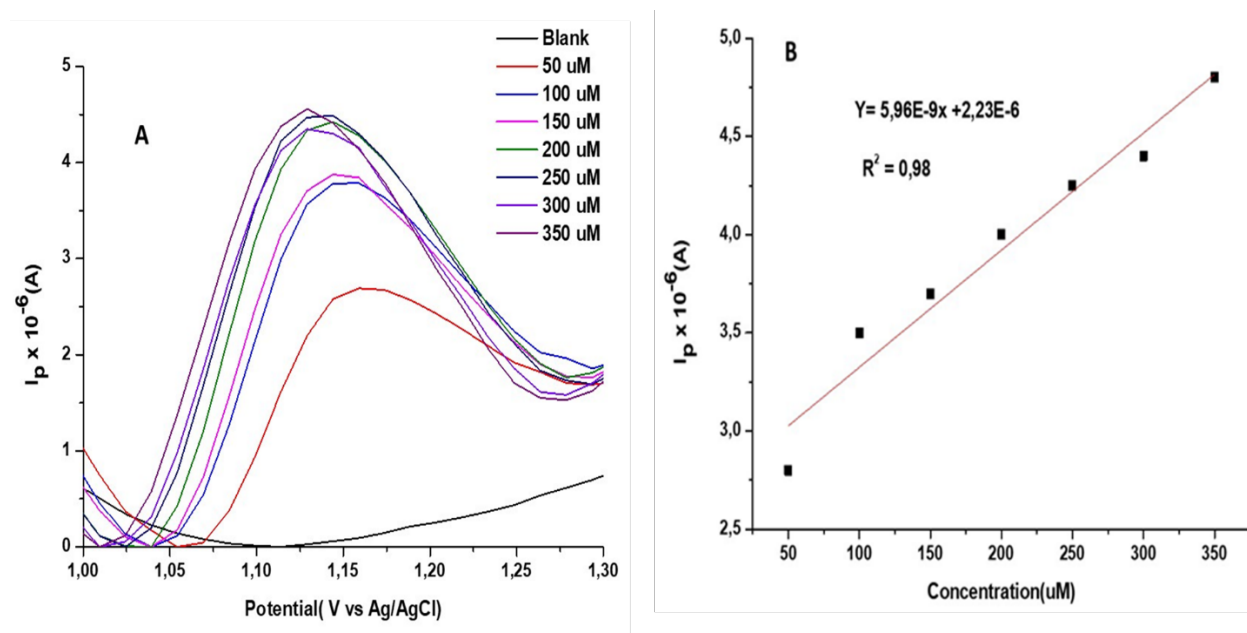


Figure 4-7: Calibration graph of EFV and corresponding plot at optimum working conditions.

Table 4-2: Characteristics and parameters of EFV calibration plot using DPV at GCE/Ag-Au-PGV-HSA platform

Parameters	Efavirenz oxidation
Regression coefficient(n= 7)	0,99
LOD(uM)	0,31
LOQ(uM)	0,94
Sensitivity($\mu A \mu M^{-1} cm^{-2}$)	$5,96 \times 10^{-9}$
Peak potential at 30 mvs	1,18V

Table 4-3: Summary of studies depicting sensitivities of electrochemical sensors used for detection of various ARVs and pharmaceuticals in various media.

Detection method	Sensor	LOD ^a /LOQ ^b	Sample	References
Adsv	Hg-film electrode	1.0 ppb ^a 0,01 ppm ^b	Pharmaceutical formulations	Castro. A <i>et.al</i> ,2011
DPV	GCE	0.05 uM ^a	Human serum	Zhang. F <i>et.al</i> ,2013
CV	GCE/NiO-ZrO	1.36 uM ^b	Pharmaceutical formulations Urine samples	Thapliyal. N <i>et.al</i> ,2015
DPV	GCE	0.0025mg/L ^a and 0.025 mg/L ^b	Pharmaceutical formulations	Leandro. C <i>et.al</i> ,2010
DPV	GCE/Ag-Au-PGV/HSA	0,31uM ^a and 0,94uM ^b	Pharmaceutical capsules	This study
CV	MMT/CPE	1,01 nM ^a and 3.37 nM ^b	Nimesulide (NIM)	Shetti, <i>et.al</i> ,2020
CV	MMT/CPE	1,01nM ^a	Azo food dye	Shetti, <i>et.al</i> , 2018

The low sensitivity of Ag-Au-PGV/HSA platform demonstrated through low values of LOD and LOQ confirmed the method as plausible for detection and determination of EFV. In comparison to the sensitivity exhibited by electrochemical sensors summarized in the table above demonstrate that the current work is competitive and enhanced in terms of efficiency and sensitivity using DPV as a detection technique.

4.6 EFV electrochemical sensor method validation

4.6.1 Interference studies

Under optimized conditions, the influence of three different types of interferants on activity and detection of EFV were studied. The study used these interferents based of their common high content in basic supplements and food consumed by most HIV-1 patients.

Glucose(C₆H₁₂O₆), Ascorbic acid(C₆H₈O₆) and sodium chloride (NaCl) were used as 3-fold concentration of EFV, and the results depicted glucose with greatest hindrance on the detection of EFV due to lowest return of EFV and sodium chloride exhibited the least chemical hindrance

in the detection of EFV. This effect was indicated by the peak current of EFV observed within both glucose and sodium chloride interferents compared to EFV spiked concentration peak current without interferents.

Table 4-4: Summary of EFV recoveries observed under the influence of each interferents.

Interferent (mole ratio)	Ascorbic acid (3:1)	Glucose (3:1)	Sodium chloride (3:1)
EFV (uM)	50 uM	50 uM	50 uM
Recovered(uM)	33,65 uM	33,08 uM	34,62 uM
Recovered (%)	67	66	69

The table above depicted the recoveries obtained from each interferent after equal EFV concentration was spiked. As shown by the voltammograms, the table proved EFV to have been recovered the most when NaCl was used whilst EFV was recovered the least when glucose was used. This observation and finding was due to the difference in the molecular size of the interferents. As glucose molecules are significantly bigger than sodium and chloride ions in solution (Gao *et.al*, 2021, Bleiholder *et.al*, 2017). As a result, glucose molecules exerted greater impedance in the mobility of EFV molecules in solution whilst also decreasing the conductivity of the solution, thus decreasing the electrochemical activity of EFV (Witkowska *et.al*, 2016).

In contrary, Sodium and chloride ions are significantly smaller in size compared to EFV and thus exerted smaller impedance on EFV mobility, whilst also sodium and chloride ions significantly increased the conductivity of the solution thus increasing the EFV electrochemical activity, which translated into higher EFV recovery compared to glucose and ascorbic acid, respectively.

4.6.2 Determination of EFV in urine samples

To verify the efficiency and accuracy of method developed, the GCE/Ag-Au-PGV/HAS platform was used to detect and determined EFV content in Equi-spiked urine samples of varying urine concentration. This analysis was done to evaluate the effect of urine

concentration of EFV electrochemical activity as well as the workability of the platform on real biological sample matrix.

Table 4-5: Summary of EFV recoveries obtained from two different concentration of urine samples.

Urine sample	EFV Concentration uM or mg	Recovered (%)	Recovered(mg)	RSD (%)
2x diluted urine	300 uM / 175 mg	94	164,5	3,22
4x diluted urine	300 uM/ 175 mg	115	201,25	2,09

The results summarized from the table above indicated percentage recoveries of EFV in two urine samples. The recoveries were determined by comparing the peak current of 300 uM observed in calibration curve with those obtained for EFV in two urine samples. The most diluted sample of urine exhibited more EFV content compared to least diluted. The cause of this was due to matrix effect which was prominent in least diluted sample due to strong interactions between interferants found in urine and EFV, which caused least EFV recovery compared to most diluted urine sample.

However, it was observed that the EFV percentage recoveries obtained ranged between 90% - 115%, which was within the acceptable range analytical application for the method proposed. In addition, statistically the results obtained for EFV content recovery in both urine samples were acceptable as this was indicated by low RSD values, which were below threshold of 5%.

4.6.3 Reproducibility and stability studies

The reproducibility, repeatability studies of the platform were done to investigate changes in responses of EFV standard solution signal between set time intervals for EFV signal acquisition. One solution of EFV of known concentration was used to determined repeatability, while reproducibility five separate solutions of EFV with equal concentrations were used. Stability studies were done on one solution with constant EFV concentration on over a period of 4 days.

After five successive EFV signal acquisition from one EFV standard solution, the RSD value obtained from the data was 3.21%. Meanwhile, the data acquired for EFV of signal responses in five equi-molar EFV standard solutions produced RSD value 4.90%. The stability of the Ag-Au-PGV/HSA platform analysed after GCE/Ag-Au-PGV/HSA was stored for three days at room temperature. The results obtained showed 90% recovered of EFV from the initially measured EFV signal in terms of peak current three days prior the storage.

Stability performance of Ag-Au-PGV/HSA platform was also done on EFV capsule with known concentration. This was done over period of three days, and the results obtained show a 20% deterioration rate in terms of EFV concentration current signal that was obtained in comparison to the one originally obtained three days prior, thus 80% stability performance was exhibited by a GCE/Ag-Au-PGV/HSA platform.

4.6.4 Determination of EFV in pharmaceutical commercial capsules

The applicability of sensor developed was carried out of commercial EFV capsule. The 200 mg capsule powder was dissolved in water. The resulting solution was filtered and mixed with absolute ethanol for complete dissolution of EFV. The solution was quantitatively transferred into 100 ml volumetric flask. The voltammograms depicted below showed the activity of EFV in three respective EFV commercial capsules.

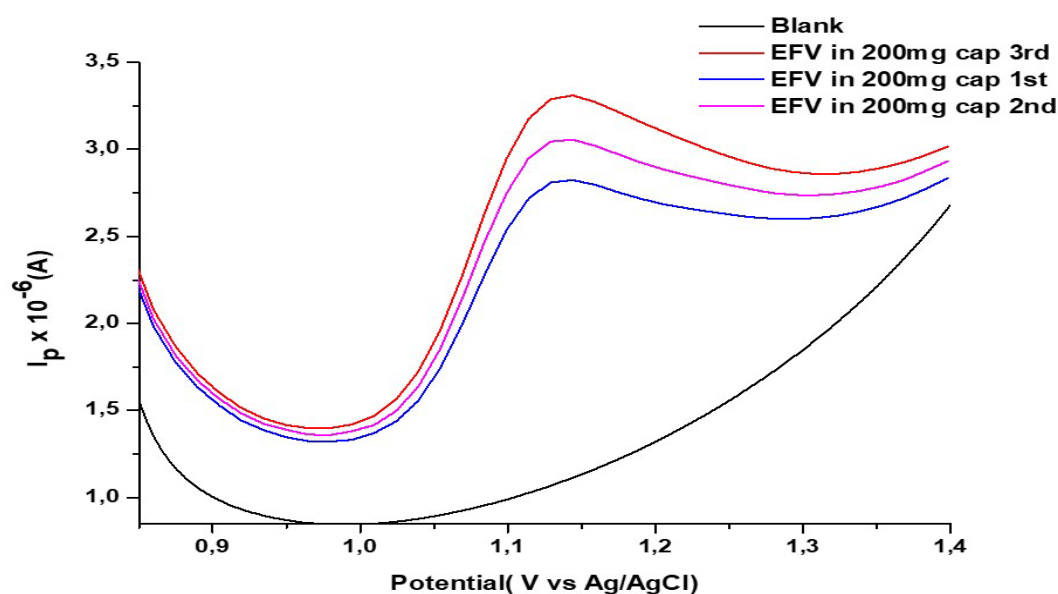


Figure 4-9: Depiction of influence of Ascorbic acid (**Red**), Glucose (**Pink**), and Sodium chloride (**Blue**) interferences on EFV electrochemical activity.

The overlaid voltammogram above depicting EFV electrochemical quantitation in three separate 200 mg EFV capsules, where each capsule is represented by its colour-coded voltammogram. Thus, the EFV mass concentrations for three commercial capsules calculated experimentally averaged to 192,02 mg EFV, which is very comparable to 200 mg EFV specified by manufacturer of commercial capsules.

The precision of the method is depicted by closeness of the experimentally obtained EFV contents from triplicate EFV signals demonstrated the precision of the proposed method and technique applied using the electrochemical modified sensor for detection and quantitation of EFV. Meanwhile, the average EFV or mean EFV content (192,02 mg) proximity of the specified EFV value demonstrated the accuracy of the method and technique proposed for EFV electrochemical analysis.

The RSD that was calculated from 192,02 mg EFV mean average was 4,69% which was slightly high but statistically acceptable as it was below the threshold value of 5%. Therefore, this confirmed the reliability of the proposed method and technique used for the electrochemical detection and quantitation of EFV in commercial and analytical samples.

4.7 Conclusion

A voltametric sensor based on Ag-Au-PGV/HSA sensing platform was successfully developed for EFV detection and determination. Based on data obtained from analysis, the platform demonstrated enhanced electron-transfer rate, sensitivity, efficiency, and catalytic detection of EFV compared to bare GCE electrochemical performance.

Optimization of experimental working conditions depicted DPV as the best working technique whilst the drop-coating method as optimum sensor fabrication method for detection of EFV. HAS protein effect investigation demonstrated minimal effect because of absence inherent electroactive species within its composition. Choice of supporting electrolyte showed PBS as most electrochemically effective electrolyte and subsequent PBS concentration studies depicted that 1M was the optimum concentration within which EFV electrooxidation studies could be conducted.

Optimization of detection parameter for EFV exhibited a step potential and pulse amplitude of 0,015V/s and 0,085V/s as optimum parameters, respectively. Under optimized working and

analytical conditions, Ag-Au-PGV/HSA platform demonstrated excellent electrochemical properties and characteristic, which included, low detection limit, limit of quantitation and sensitivity. Method validation which included interference, repeatability, reproducibility and stability studies were all carried under optimized conditions and exhibited feasible data

As such, the overall data presented showed a great potential for wide applicability of Ag-Au-PGV/HSA platform particularly for novel analysis. As the sensor produced plausible data in analysis of EFV in commercial capsules which yielded experimentally comparable EFV content to that specified by commercial products with plausible statistical limit given by RSD, which was less than 5%

4.8 References

Abraham, P., Renjini, S., Vijayan, P., Nisha, V., Sreevalsan, K. and Anithakumary, V., 2020. Review on the progress in electrochemical detection of morphine based on different modified electrodes. *Journal of The Electrochemical Society*, 167(3), p.037559.

Balkourani, G., Damartzis, T., Brouzgou, A. and Tsiakaras, P., 2022. Cost Effective Synthesis of Graphene Nanomaterials for Non-Enzymatic Electrochemical Sensors for Glucose: A Comprehensive Review. *Sensors*, 22(1), p.355.

Blanco, J.R., Alejos, B. and Moreno, S., 2018. Impact of dolutegravir and efavirenz on immune recovery markers: results from a randomized clinical trial. *Clinical Microbiology and Infection*, 24(8), pp.900-907.

Bleiholder, C. and Bowers, M.T., 2017. The solution assembly of biological molecules using ion mobility methods: from amino acids to amyloid β -protein. *Annual Review of Analytical Chemistry*, 10, pp.365-386.

Bowen, A., Sweeney, E.E. and Fernandes, R., 2020. Nanoparticle-Based Immunoengineered Approaches for Combating HIV. *Frontiers in Immunology*, 11, p.789.

Bozal, B., Uslu, B. and Özkan, S.A., 2011. A review of electroanalytical techniques for determination of anti-HIV drugs. *International Journal of Electrochemistry*, 2011.

Chaparro, C.V., Herrera, L.V., Meléndez, A.M. and Miranda, D.A., 2016, February. Considerations on electrical impedance measurements of electrolyte solutions in a four-

electrode cell. In *Journal of Physics: Conference Series* (Vol. 687, No. 1, p. 012101). IOP Publishing.

Chavali, M.S. and Nikolova, M.P., 2019. Metal oxide nanoparticles and their applications in nanotechnology. *SN Applied Sciences*, 1(6), pp.1-30

Clark, K.J., Sarr, A.B., Grant, P.G., Phillips, T.D. and Woode, G.N., 1998. In vitro studies on the use of clay, clay minerals and charcoal to adsorb bovine rotavirus and bovine coronavirus. *Veterinary microbiology*, 63(2-4), pp.137-146.

Couto, R.A.S., Lima, J.L.F.C. and Quinaz, M.B., 2016. Recent developments, characteristics, and potential applications of screen-printed electrodes in pharmaceutical and biological analysis. *Talanta*, 146, pp.801-814.

Devrukhakar, P.S., Borkar, R., Shastri, N. and Surendranath, K.V., 2013. A validated stability-indicating RP-HPLC method for the simultaneous determination of tenofovir, emtricitabine, and efavirenz and statistical approach to determine the effect of variables. *International Scholarly Research Notices*, 2013.

Djobet, M.N., Singhe, D., Lohoue, J., Kuaban, C., Ngogang, J. and Tambo, E., 2017. Antiretroviral therapy supply chain quality control and assurance in improving people living with HIV therapeutic outcomes in Cameroon. *AIDS research and therapy*, 14(1), pp.1-8

Fortunak, J.M., de Souza, R.O., Kulkarni, A.A., King, C.L., Ellison, T. and Miranda, L.S., 2014. Active pharmaceutical ingredients for antiretroviral treatment in low-and middle-income countries: a survey. *Antiviral therapy*, 19(0 3), p.15.

Gao, J., He, S. and Nag, A., 2021. Electrochemical Detection of Glucose Molecules Using Laser-Induced Graphene Sensors: A Review. *Sensors*, 21(8), p.2818.

Gowthaman, N.S.K., Sinduja, B. and John, S.A., 2016. Tuning the composition of gold–silver bimetallic nanoparticles for the electrochemical reduction of hydrogen peroxide and nitrobenzene. *RSC advances*, 6(68), pp.63433-63444.

Huynh, K.H., Pham, X.H., Kim, J., Lee, S.H., Chang, H., Rho, W.Y. and Jun, B.H., 2020. Synthesis, Properties, and Biological Applications of Metallic Alloy Nanoparticles. *International Journal of Molecular Sciences*, 21(14), p.5174.

- Kassa, A. and Amare, M., 2019. Electrochemical determination of paracetamol, rutin and sulfonamide in pharmaceutical formulations by using glassy carbon electrode—A Review. *Cogent Chemistry*, 5(1), p.1681607.
- Khan, I., Saeed, K. and Khan, I., 2019. Nanoparticles: Properties, applications and toxicities. *Arabian journal of chemistry*, 12(7), pp.908-931.
- Krol, A., Mizerna, K. and Bożym, M., 2020. An assessment of pH-dependent release and mobility of heavy metals from metallurgical slag. *Journal of hazardous materials*, 384, p.121502.
- Makoni, P.A., Khamanga, S.M., Wa Kasongo, K. and Walker, R.B., 2018. The use of experimental design for the development and validation of an HPLC-ECD method for the quantitation of efavirenz. *Die Pharmazie-An International Journal of Pharmaceutical Sciences*, 73(10), pp.570-578.
- Malekzad, H., Zangabad, P.S., Mirshekari, H., Karimi, M. and Hamblin, M.R., 2017. Noble metal nanoparticles in biosensors: recent studies and applications. *Nanotechnology reviews*, 6(3), pp.301-329.
- Mailu, S.N., Waryo, T.T., Ndangili, P.M., Ngece, F.R., Baleg, A.A., Baker, P.G. and Iwuoha, E.I., 2010. Determination of anthracene on Ag-Au alloy nanoparticles/overoxidized-polypyrrole composite modified glassy carbon electrodes. *Sensors*, 10(10), pp.9449-9465.
- More, S., Tandulwadkar, S., Nikam, A., Rathore, A., Sathiyarayanan, L. and Mahadik, K., 2013. Separation and determination of lamivudine, tenofovir disoproxil fumarate and efavirenz in tablet dosage form by thin-layer chromatographic-densitometric method. *JPC-Journal of Planar Chromatography-Modern TLC*, 26(1), pp.78-85.
- Moosavi, S.M. and Ghassabian, S., 2018. Linearity of calibration curves for analytical methods: A review of criteria for assessment of method reliability. *Calibration and Validation of Analytical Methods: A Sampling of Current Approaches; IntechOpen Limited: London, UK*, pp.109-127.
- Li, J., Wang, H., Li, Z., Su, Z. and Zhu, Y., 2020. Preparation and application of metal nanoparticles elaborated fiber sensors. *Sensors*, 20(18), p.5155.

Paszkiwicz, M., Gołębiewska, A., Rajski, Ł., Kowal, E., Sajdak, A. and Zaleska-Medynska, A., 2016. Synthesis and characterization of monometallic (Ag, Cu) and bimetallic Ag-Cu particles for antibacterial and antifungal applications. *Journal of Nanomaterials*, 2016.

Pournara, A.D., Tarlas, G.D., Papaefstathiou, G.S. and Manos, M.J., 2019. Chemically modified electrodes with MOFs for the determination of inorganic and organic analytes via voltammetric techniques: a critical review. *Inorganic Chemistry Frontiers*, 6(12), pp.3440-3455.

Romero-Núñez, A., González, G., Romero-Ibarra, J.E., Vega-González, A., Cruz-Jiménez, G., Hernández-Cristóbal, O., Zárraga-Núñez, R.A., Obregón-Herrera, A., López-Romero, E., Pedraza-Reyes, M. and Cuéllar-Cruz, M., 2019. Synthesis of Bimetallic Nanoparticles of Cd₄HgS₅ by Candida Species. *Crystals*, 9(2), p.61.

Rossi, S., Yaksh, T., Bentley, H., van den Brande, G., Grant, I. and Ellis, R., 2006. Characterization of interference with 6 commercial Δ^9 -tetrahydrocannabinol immunoassays by efavirenz (glucuronide) in urine. *Clinical chemistry*, 52(5), pp.896-897.

Sharma, G., Kumar, A., Sharma, S., Naushad, M., Dwivedi, R.P., AlOthman, Z.A. and Mola, G.T., 2019. Novel development of nanoparticles to bimetallic nanoparticles and their composites: a review. *Journal of King Saud University-Science*, 31(2), pp.257-269.

Teich-McGoldrick, S.L., Greathouse, J.A., Jove-Colon, C.F. and Cygan, R.T., 2015. Swelling properties of montmorillonite and beidellite clay minerals from molecular simulation: comparison of temperature, interlayer cation, and charge location effects. *The Journal of Physical Chemistry C*, 119(36), pp.20880-20891.

Thakre, D., Rayalu, S., Kawade, R., Meshram, S., Subrt, J. and Labhsetwar, N., 2010. Magnesium incorporated bentonite clay for defluoridation of drinking water. *Journal of Hazardous Materials*, 180(1-3), pp.122-130.

Thapliyal, N., Osman, N.S., Patel, H., Karpoormath, R., Goyal, R.N., Moyo, T. and Patel, R., 2015. NiO-ZrO₂ nanocomposite modified electrode for the sensitive and selective determination of efavirenz, an anti-HIV drug. *RSC Advances*, 5(50), pp.40057-40064.

Thomas, T., Mascarenhas, R.J., Swamy, B.K., Martis, P., Mekhalif, Z. and Sherigara, B.S., 2013. Multi-walled carbon nanotube/poly (glycine) modified carbon paste electrode for the

determination of dopamine in biological fluids and pharmaceuticals. *Colloids and Surfaces B: Biointerfaces*, 110, pp.458-465.

Uslu, B. and Ozkan, S.A., 2007. Electroanalytical application of carbon-based electrodes to the pharmaceuticals. *Analytical Letters*, 40(5), pp.817-853

Uslu, B. and Ozkan, S.A., 2011. Electroanalytical methods for the determination of pharmaceuticals: a review of recent trends and developments. *Analytical letters*, 44(16), pp.2644-2702

Wang, P., Sheng, Y., Wang, F. and Yu, H., 2018. Synergistic effect of electron-transfer mediator and interfacial catalytic active-site for the enhanced H₂-evolution performance: A case study of CdS-Au photocatalyst. *Applied Catalysis B: Environmental*, 220, pp.561-569.

Witkowska Nery, E., Kundys, M., Jelen, P.S. and Jönsson-Niedziółka, M., 2016. Electrochemical glucose sensing: is there still room for improvement?

World Health Organization, 2019. *Policy brief: update of recommendations on first-and second-line antiretroviral regimens* (No. WHO/CDS/HIV/19.15). World Health Organization.

Schneider, S., Janssen, C., Klindtworth, E., Mergel, O., Möller, M. and Plamper, F., 2018. Influence of polycation composition on electrochemical film formation. *Polymers*, 10(4), p.429.

Shetti, N.P., Nayak, D.S., Malode, S.J. and Kulkarni, R.M., 2018. Fabrication of MWCNTs and Ru doped TiO₂ nanoparticles composite carbon sensor for biomedical application. *ECS Journal of Solid State Science and Technology*, 7(7), p.Q3070.

Zhang, H., Hwang, S., Wang, M., Feng, Z., Karakalos, S., Luo, L., Qiao, Z., Xie, X., Wang, C., Su, D. and Shao, Y., 2017. Single atomic iron catalysts for oxygen reduction in acidic media: particle size control and thermal activation. *Journal of the American Chemical Society*, 139(40), pp.14143-14149.

Chapter 5: Conclusion and recommendations

Chapter summary

This chapter mainly outlines the key conclusive findings obtained from the results of the application studies of Ag-Au-PGV/HSA platform in detection and determination of EFV. Thus, it also outlines and suggests recommendation formulated from conclusive findings of the study and its limitations. This chapter also evaluates results obtained from spectroscopic and electrochemical characterization and synthesis of sensing films.

5.1 Conclusion

The spectroscopic data obtained and detailed in chapter 3 indicated the differences in between monometallic and bimetallic NPs, and differences between metallic NPS and PGV-bentonite modified composites. UV-Visible spectroscopy data indicated a core-shell typical formation of bimetallic NPS, which confirmed a seeded growth method that was used to its synthesis, Au formed a core whilst Ag a shell. Moreover, both FT-IR and UV/Visible spectroscopic data confirmed the synthesis of both metallic NPs and their respective composites.

Morphological data showed enhanced average particle size of composites compared to metallic NPS. XRD data depicted similarities between Ag and Au metals, which has been vastly reported on by various literature in Ag and Au nanomaterials. The corresponding Ag and Au composites depicted similarities as was with the metallic NPs of both Ag and Au. XRD and SEM confirmed the enhanced electrochemical performance of metallic composites compared to metallic NPs because of improved electrochemical active sites through increased average particle size of composites.

The data exhibited by electrochemical studies exhibited the electrochemical activity of both metallic and composites. The electrochemical activity of Ag and Au exhibited slight shifts in terms of potential in a bimetallic system as well as in composites, moreover the potentials reported of metallic NPs and composites affirmed those in reported literature. As was observed with morphological properties composites, particularly Ag-Au-PGV having greater average particle size and thus more electrochemical active sites. Thus, increased electron-transfer rate and enhanced diffusion coefficient as well as electron transfer coefficient. This finding was

affirmed by electrochemical studies as Ag-Au-PGV composite demonstrated more enhanced electrochemical properties thus was used to fabricate an electrochemical platform.

The applicability of the method developed using Ag-Au-PGV/HSA platform through a voltametric method, DPV which provided most sensitive EFV detection signals compared to other techniques was optimized. The experimental conditions and detection parameters were optimized, however optimization of detection parameters demonstrated enhanced electrooxidation of EFV. As such, low LOD, LOQ and high sensitivity were achieved from calibration curve. These properties combined were indicative of the sensitivity of the platform to the detection and determination of EFV, which was more enhanced than sensitivity exhibited by mainly chromatographic and spectroscopic techniques as reported in literature.

The applicability of method developed was evaluated on real samples analysis under optimized conditions, which included human urine and pharmaceutical HIV-1 tablets. The method was applied on both samples and demonstrated plausible EFV content recoveries, while interference studies was conducted to assess method robustness and selectivity levels. Ascorbic acid, glucose, sodium chloride was all used as interferents, based on results they had minimal effect in the determination of EFV. This further proved the efficiency and sensitive of the method proposed by this study for EFV detection.

Reproducibility, repeatability, and stability studies were done to monitor the deterioration rate of the sensing platform and its effect on sensitivity. Based on results obtained, reproducibility and repeatability of EFV detection signals were achieved with plausible statistical RSD values, while the stability of the platformed exhibited 10% deterioration rate over 3 days, which was good compared to other conventional techniques. Moreover, the proposed method demonstrated ease of application, rapidity and low cost of application and high sensitivity for EFV in pharmaceutical drugs and biological samples.

5.2 Recommendations

- Morphological studies for metallic NPs and composites synthesized from metallic NPs, are best morphologically characterized by use of both SEM and TEM, as well as EDX. As these will deduce the effect of average particle size of metallic NPs and metal composites on their elemental content and vice versa.

- For synthesis of metallic NPs, particularly bimetallic NPs could be done together with kinetics using UV/Visible spectroscopy to determine typical particle formation, whether core-shell or alloy.
- Electrochemical impedance studies (EIS) are an essential part of metallic NPs in an electrochemical system, and thus could be used to deduce electron-charge on particles as well as the resistance/conductivity of the supporting electrolyte which is essential for sensory application.
- The applicability of the Ag-Au-PGV/HSA platform is not limited to novel studies of HIV drugs but could be other oxidizable pharmaceuticals and other oxidizable substances. This potential could be explored and expanded upon by various future electrochemical studies.